Title
Functional Brain Connectivity during Emotion Regulation and Applications to Bipolar Disorder

Author
Torrisi, Salvatore John

Publication Date
2013

Peer reviewed|Thesis/dissertation

UNIVERSITY OF CALIFORNIA

Los Angeles

Functional Brain Connectivity during Emotion Regulation and Applications to Bipolar Disorder

A dissertation submitted in partial satisfaction of the requirements for the degree Doctor of Philosophy in Neuroscience

by

Salvatore John Torrisi

2013

ABSTRACT OF THE DISSERTATION

Functional Brain Connectivity during Emotion Regulation

and Applications to Bipolar Disorder

by

Salvatore John Torrisi

Doctor of Philosophy in Neuroscience

University of California, Los Angeles, 2013

Professor Lori Altshuler, Chair

Emotion regulation is a complex cognitive ability wherein conscious or non-conscious processes in an individual result in a change of experienced affect. The work in this dissertation involves advanced fMRI analyses to elucidate the connectivity of the neurobiological mechanisms of emotion regulation. We investigate the temporality of activation and functional connectivity in a form of explicit emotion regulation (cognitive reappraisal), as well as the effective connectivity of a form of implicit emotion regulation (affect labeling). We also investigate resting state functional connectivity in a subset of the emotion regulation network. Finally, these approaches are applied to euthymic individuals with bipolar disorder, a serious psychiatric illness in which the ability to regulate emotion is a cyclical and fundamental difficulty. The aim of this work is to identify system-level biomarkers to someday assist the diagnostic process and the tracking and treatment of therapeutic interventions.

The dissertation of Salvatore John Torrisi is approved.

Susan Y. Bookheimer

Edythe D. London

Martin M. Monti

John D. Van Horn

Lori L. Altshuler, Committee Chair

University of California, Los Angeles

2013

TABLE OF CONTENTS

LIST OF FIGURES

Chapter 6

LIST OF TABLES

ACKNOWLEDGMENTS

I am so fortunate and spoiled to have had this UCLA NSIDP experience. What great minds and resources all around me and what opportunities for freedom of exploration and learning. In the largest part this was enabled by my advisor, Lori Altshuler, whose calm and positive presence always put me at ease and whose understanding of my temperament and abilities allowed me to pursue the avenues I was compelled to travel in. Without her shrewd balance of clinical judgment, encouragement, guidance and allowing me to be independent, I would never have become the scientist I have.

And yet becoming a scientist takes so long (I am still working on it), and there were others who helped along the way. Besides Lori, the person that stands out more than anyone else is Susan Bookheimer, whose many meetings taught me to consider my questions and approaches more deeply and carefully, and whose technical wisdom turned at some point into a deep mentorship. I am grateful for the time she gave me, and the way she embraced me and my work as if I was one of her own students.

I have also been spoiled by the rest of my “all-star” dissertation committee, with which each and every one I share special memories: rotating in Edythe London’s laboratory, collaborating with Martin Monti on the mediation analysis in chapter 6 and TAing Jack Van Horn’s neuroanatomy class. These experiences were milestones.

Unfortunately as I run out of room here I’m forced to simply list the names of others who helped me in a number of technical and intellectual capacities, so please believe me when I say I could have written a glowing paragraph about each of them as well. Thank you, thank you: Elliot Berkman, Jeffrey Fischer, Lara Foland-Ross, Dara Ghahremani, Edward Lau, Matthew Lieberman, Christopher McKinlay, Kateri McRae, Donald McLaren, Teena Moody, Alfonso

Nieto-Castañón, Elizabeth Pierce, Jeffrey Rudie, Jennifer Townsend, Nathalie Vizueta and the rest of the Mood Disorders Research Program crew! Thank you also Grants, such as those from the NIMH: 5R21MH075944, 1K24MH001848, 1R01MH084955, from NIDA (a NITP fellowship): 1T90DA022768 and the Swift and Nancy Furlotti Family foundations. Last but not least I thank my reason for being here, my family, whose love and acceptance for me has no boundary: Thank you Mom, Dad and Nedelle. This work is dedicated to you.

VITA

05 / 2001	**BA**	Interdisciplinary Arts and Performance • Arizona State University, West
2001 - 2003		Lulu May & Richard Von Hagen Scholarship
12 / 2003	**MFA**	Music Composition/New Media • California Institute of the Arts
04 / 2007	**MA**	Applied Linguistics • University of California, Los Angeles
Spring, 2009		UCLA QGE special course funding, FSL/FreeSurfer class (SF)
Winter, 2010		UCLA QGE special course funding, SPM Connectivity (Boston)
Spring, 2010		UCLA QGE special course funding, Clinical Imaging with SPM (Boston)
07 / 2010		NITP Advanced Neuroimaging Summer School, UCLA
12 / 2010		Fellowship to *New Horizons in Human Brain Imaging* (Oahu, HI)
2011- 2012		UCLA Neuroimaging Training Program Fellowship (NIH T90)
06 / 2011		Brain Connectivity Workshop. (Montréal, Canada)
02 / 2012		SPM Course. (Zurich, Switzerland)
Fall, 2012		Teaching Assistant. Neuroanatomy (NS102)
Summer, 2013	**PhD**	(projected) Neuroscience • University of California, Los Angeles
08 / 2013	**Postdoc**	(projected) M. Ernst & C. Grillon • National Institute of Mental Health

ACADEMIC PUBLICATIONS

K Cross, **S Torrisi**, ER Losin, M Iacoboni. (2013) *Controlling automatic imitative tendencies: Interactions between mirror neuron and cognitive control systems*. NeuroImage. 83, 493–504

S Torrisi, MD Lieberman, SY Bookheimer, LL Altshuler. (2013) *Advancing understanding of affect labeling with dynamic causal modeling*. NeuroImage 82, 481–488

PK Douglas, EP Lau, I Rodriguez-Pinto, A Anderson, **S Torrisi**, MS Cohen. *A State Space Model of Basal Ganglia LFP Oscillations Consistent with Two Movement Disorders*. (under review)

S Torrisi, T Moody, M Thomason, N Vizueta, MM Monti, JD Townsend, J Fischer, SY Bookheimer, LL Altshuler. (2013) *Differences in resting corticolimbic functional connectivity in bipolar I euthymia*. Bipolar Disorders 15(2) 156-166.

JD Townsend, **S Torrisi,** MD Lieberman, CA Sugar, SY Bookheimer, LL Altshuler. (2013) *Frontal-Amygdala Connectivity Alterations During Emotion Downregulation in Bipolar I Disorder*. Biological Psychiatry, 73(2): 127-135.

N Vizueta, JD Rudie, JD Townsend, **S Torrisi**, TD Moody, SY Bookheimer, LL Altshuler. (2012) *Regional fMRI Hypoactivation and Altered Functional Connectivity During Emotion Processing in Nonmedicated Depressed Patients with Bipolar II Disorder*. Am J Psychiatry. 2012; 169(8):831-40.

LC Foland-Ross, S Bookheimer, MD Lieberman, J Townsend, J Fischer, **S Torrisi**, C Penfold, SK Madsen, PM Thompson, L Altshuler. (2011) *Normal amygdala activation but deficient ventrolateral prefrontal activation in adults with bipolar disorder during euthymia*. NeuroImage. 2012; 59(1):738-44. Epub 2011 Aug 10.

S Torrisi. (2010). Social Regulation in Frontotemporal Dementia: A Case Study. In A. Mates, L. Mikesell, & M. Smith (Eds.) *Language, Interaction and Frontotemporal Dementia: Reverse Engineering the Social Mind*. London: Equinox Publishing

I. Teramitsu, A. Poopatanapong, **S. Torrisi**, S.A. White. (2010) *Striatal FoxP2 Is Actively Regulated during Songbird Sensorimotor Learning*. PLoS One. 5(1) e8548

MUSIC PUBLICATIONS

S Torrisi. *F_0 r Woody*, 2013 solo for clarinet and recording
Frog Peak Experimental Music Collective, Lebanon, NH

S Torrisi. *acute trio*, 2004 computer-aided clarinet duet
Frog Peak Experimental Music Collective, Lebanon, NH

POSTER PRESENTATIONS

S. Torrisi, K. McRae, N. Vizueta, S. Bookheimer, L.L. Altshuler. *Hypoactivity in left vlPFC during reappraisal in bipolar disorder euthymia.* Presented at the 19th annual meeting of the Organization of Human Brain Mapping. June 16-20, 2013, Seattle, WA.

S. Torrisi, N. Vizueta, J. Townsend, E. Lau, S. Bookheimer, L.L. Altshuler. *Effective Connectivity Network Differences During Incidental Emotion Regulation in Euthymic Bipolar Disorder.* Presented at the 67th Society of Biological Psychiatry annual meeting. May 3-5, 2012, Philadelphia, PA.

S. Torrisi, N. Vizueta, E. Berkman, L. Foland-Ross, J.D. Townsend, T.D. Moody, J. Fischer, S.Y. Bookheimer, L.L. Altshuler. *Differences in Amygdala to VLPFC Resting State Functional Connectivity in Bipolar I Euthymia.* Presented at the 17th Annual Organization for Human Brain Mapping meeting. June 26-30, 2011, Québec City, Canada.

S. Torrisi, J.D. Townsend, N. Vizueta, A. Aquino, J. Fischer, S.Y. Bookheimer, L.L. Altshuler *Dysfunction of Frontal and Subcortical Connectivity During a Task of Emotion Regulation in Bipolar II Disorder Depression* presented at New Horizons in Human Brain Imaging: A Focus on Brain Networks and Connectivity, December 1, 2010. Oahu, HI.

S. Torrisi, N. Vizueta, E. Berkman, L. Foland-Ross, J.D. Townsend, T.D. Moody, J. Fischer, S.Y. Bookheimer, L.L. Altshuler. *Fronto-limbic Functional Connectivity in Bipolar II Depression during Emotion Labeling.* Presented at the 4th Annual Meeting of the Social & Affective Neuroscience Society. September 18, 2010. Chicago, I

CHAPTER 1: INTRODUCTION

Principles of brain function

One prominent conceptual distinction in neuroscience of the principles of neural organization is between brain segregation and brain integration. This can be described as a view of the brain composed of many specialized and segregated information-processing regions and a view that many regions serve multiple processing abilities that are only understandable when observing their integration within a broader functional context. It is for both empirical and historical reasons that such a distinction arose, and it is largely for empirical and historical reasons that both views are more recently seen as critical and convergent (Friston and C. J. Price, 2011). And yet despite their increasingly recognized complementarities, the neuroimaging tools we currently possess are generally built to provide evidence for one or the other perspective. Therefore today's neuroimager, realizing that the brain possesses both segregated *and* integrated properties, must themselves integrate multiple kinds of neuroscientific findings to address his or her scientific questions. The present dissertation is one attempt to do so.

As with efforts to understand any complex phenomenon, the manner in which one conceptualizes the brain often dictates the lens through which we measure and model it. The majority of data presented here were derived from the technologically astounding and yet now quite common functional magnetic resonance imaging (fMRI) machinery. Data that fMRI provides are rich, multidimensional and can be analyzed in a number of ways, each offering a particular window into brain function. The most commonly employed method is to measure Blood-Oxygen-Level-Dependent (BOLD) signal changes that occur throughout the brain under a psychological task by creating spatial maps of statistical significance using the general linear model (GLM) (Friston et al., 1995). These maps demonstrate brain regions that activate to a

greater or lesser extent between various conditions within or across groups of individuals. This standard fMRI approach lends itself naturally to the “segregation” perspective, and has offered many profound and robust indications of where in our neuroanatomy sensory and higher cognitive functions are represented. There exist, however, a number of psychological and statistical assumptions that underlie this approach, and many prominent users of the technique have self-referentially examined its limitations (Friston et al., 1996; Monti, 2011; Poline and Brett, 2012).

One way to evade some of these limitations is through a more integrated or connected perspective of the brain. There are currently many methods one can use to investigate brain connectivity. One can, for example, examine the BOLD signal for correlations across regional time series. A strong positive or negative correlation between two regions indicates a functional coupling between them. Often one chooses a region of interest (ROI) and observes significant correlations to multiple other regions across the entire brain. In that manner one can begin to build an understanding of the broader communication of that ROI within networks tapped by a particular sensory or psychological process. This “functional connectivity” approach, however, does not yield very simple interpretations as to which regional couplings are specifically modulated by a task condition. Therefore, a somewhat similar way to analyze fMRI data is to look for an interaction between psychological and physiological variables, i.e. a psychophysiological interaction (PPI), which reveals task-induced changes in coupling between an ROI and other regions across the brain (Friston et al., 1997). These partially data-driven approaches bring us closer to describing the actual dynamics of cognition. However, like all techniques, they have their limitations. These include the testing of regional couplings from only one ROI and the weak inferences one can make about the influence a region may have on another.

These issues have been recognized and, therefore, approaches to measure "effective connectivity" have been developed (Ramnani et al., 2004). Effective connectivity methods are generally more hypothesis-driven than functional connectivity methods and allow an investigator to model direct and causal effects between a finite number of *a priori* regions of interest. Dynamic causal modeling (DCM) is one form of this approach, and specifically encourages comparison between causal models that themselves have been evaluated in relation to one's empirical data (Friston et al., 2003; Penny et al., 2010). Metaphorically, DCM permits one to draw 'arrows' between regions instead of simply 'lines', and additionally estimates how these connection strengths are modulated under task conditions.

Finally, there is a burgeoning field within the fMRI neuroimaging community of investigating connectivity in the brain while it is "at rest" (Fox and Raichle, 2007). Resting state data benefits from being relatively easy to acquire, which expands its applicability, and the analyses reveal intrinsically and functionally connected networks that appear to underlie many cognitive processes (Smith et al., 2009). For mostly technical reasons, however, researchers do not yet in general apply effective connectivity analyses to these data and for this and other reasons interpretations of resting state analyses can be difficult (Cole et al., 2010). Nonetheless, the much slower signal fluctuations that one correlates with resting state data seem to be a valuable, and until recently underappreciated, dimension to where the majority of the brain's metabolic activity is allocated (Raichle, 2011).

Each of these analytic methods provides a unique window into brain function that was entirely unprecedented only a couple decades ago. They were generally built by and for methods researchers with non-methodological scientific concerns as well. In this dissertation three of these techniques are applied to a particular cognitive process, emotion regulation, and then to bipolar disorder, a psychiatric population in which this cognitive processes is deficient.

Before discussing these translational efforts, however, let us first discuss what healthy network-level emotion regulation looks like in the brain, and a number of different tasks that engage it.

Emotion Regulation

There is no escaping that everyday existence provides ample opportunities for a variety of emotional responses. Our capacity to exert control over these reactions, and transform them into (usually) more desirable responses, is called emotion regulation. Some years ago, psychologist James Gross developed a "process model" for how we may consider emotion regulation in a broadly defined context involving an individual's attentional and cognitive alterations within an emotion-generating situation. Types of control implemented at various stages in the process were outlined, and hypotheses made as to which type of control, implemented when, would have what effect on generated emotions (Gross, 1998). Although his framework has influenced a broad range of research and applied domains, many neuroscientists and brain-oriented psychologists have also compared and contrasted the neural underpinnings of different kinds of emotion regulation, such as cognitive reappraisal or expressive suppression (Mcrae et al., 2009; Ochsner et al., 2004), demonstrating their differential efficacy in an individual's emotion generating brain regions, physiological responses and self-reported experiences.

Implicit and explicit forms of emotion regulation

Although Gross's model established an influential precedent for thinking about emotion regulation as a conscious, intentional and reportable process, recent theory and empirical work has brought about an additional distinction within emotion regulation research (Gyurak et al., 2011). Partly due to the window into non-reportable processes that neuroimaging offers, one can now speak not only of explicit forms of emotion regulation but additionally *implicit* forms that are more automatic, can run to completion without monitoring, and are less effortful and

conscious. By observing the downregulation of emotion and reward-generating subcortical regions by prefrontal cortical regions, researchers have shown that forms of implicit emotion regulation occur while an individual is simply labeling affect with words (Lieberman et al., 2007), during conflict regulation (Egner et al., 2008) or even when considering the attractiveness of an alternate partner while in a romantic and committed relationship (Meyer et al., 2011).

This explicit/implicit dichotomy frames implicit emotion regulation as a valuable area of research in itself, and yet most psychologists who study both forms of regulation do not see them as fully separate (Berkman and Lieberman, 2009; Gyurak et al., 2011). For example, some explicit forms can *become* implicit (e.g., when conscious pain suppression becomes implicit in chronic patients who must perform this form of regulation constantly), and some implicit forms can become explicit (e.g., as with the technique of "noting" as one trains in Vipassana meditation). As further evidence for their relation, forms of implicit emotion regulation have been shown to activate neural control regions that overlap with those recruited during explicit emotion regulation (Payer et al., 2012), and they also have similar dampening effects upon emotion generating regions. It seems, therefore, that while some psychological subprocesses differ among emotion regulation subtypes, they also share crucial neurobiological substrates.

Anatomical substrates of emotion regulation

Both human and animal research has shown that there exist structural (axonal) projections between the amygdala, an emotion generating region, and the prefrontal cortex. These connections largely connect the medial and orbital zones of prefrontal cortex (PFC) and the basolateral nucleus of the amygdala (Ghashghaei and Barbas, 2002; J. L. Price and Drevets, 2009). Specifically, glutamatergic prefrontal efferents synapse on amygdala GABAergic interneurons to provide inhibitory input (Amaral, 1992). In animals, lesions or

inactivation of the PFC have been shown to prompt abnormal affective behaviors, whereas stimulation of the PFC suppresses these (Morgan and LeDoux, 1995). Neurological patients with lesions or atrophy to orbital PFC characteristically display inadequate regulation of affective behaviors, including loss of social empathy and high emotional impulsivity (Anderson et al., 1999; Wittenberg et al., 2008). This suggests the amygdala and orbital PFC are critical nodes in a network involved in the perception and regulation of emotional experience.

Other important regions involved in emotion regulation depend in part on the psychological context of the regulation and the nature of the processes employed. For example, despite their shared recruitment of the ventrolateral PFC (vlPFC) (Payer et al., 2012), more regions are significantly activated during the cognitive reappraisal of emotion than for the labeling of affect. Regions consistently recruited during reappraisal include the dorsolateral PFC (dlPFC), dorsomedial PFC (dmPFC), anterior cingulate cortex (ACC), and posterior parietal lobes (Buhle et al., 2013; Ochsner et al., 2012), whereas regions involved in labeling affect recruit proportionately less of these and more regions relevant to language processing (Lieberman et al., 2007; Torrisi et al., 2013). Active areas of research across the different kinds of emotion regulation processes include what constitute primary emotion regulation regions, whether there is actually a single "core" region and the interactions of these (or this) core region(s) with other networks critical to more tangential higher cognitive functions.

Emotion regulation connectivity

One way to probe these interactions is by testing brain connectivity. Psychologists using experimental paradigms with healthy humans have evaluated functional brain connectivity during implicit and explicit forms of emotion regulation. Ahmad Hariri and colleagues designed the now commonly-used task where subjects simply choose one of two labels to describe an emotional face (Hariri et al., 2000). They then used the left amygdala as a seed region for a PPI

analysis and observed negative connectivity between it and right vlPFC (BA 47). This was interpreted as the prefrontal region exhibiting inhibitory (dampening) control over the amygdala. Subsequently, other researchers have found inverse relationships between the activities of amygdala and ventrolateral PFC during explicit emotion regulation using functional connectivity analyses (Banks et al., 2007; Townsend et al., 2013). Finally, a handful of researchers have applied functional connectivity metrics to resting state data by exploring low frequency coupling among regions known to be involved in emotion regulation. Interestingly, many of these studies that focused on emotion-relevant regions also studied a clinical population (see table 1 of Chapter 6). Few studies have focused on *a priori* designated emotion regions in healthy individuals only, although there are some notable exceptions (Roy et al., 2009).

Several studies have also examined effective connectivity among brain regions involved in emotional experiences and regulation. Most focus on the perception of emotional faces (Dima et al., 2011; Li et al., 2010; Stein et al., 2007). Some, however, have assessed labeling emotional faces (Almeida et al., 2009a; 2009b), and one group performed an analysis that demonstrated that activity in prefrontal and subcortical regions mediated successful self-reported cognitive reappraisal (Wager et al., 2008). Although a complete description of the functional anatomic circuits involved in emotion regulation has not yet emerged, these studies each add something valuable and enable further research based on or in relation to them.

A major reason for these research efforts is their potential to identify highly descriptive neurological or psychiatric *biomarkers*. Connectivity analyses, rather than standard GLM analyses, offer a more fine-grained mechanistic description of the networks involved in complex mental processes such as emotion regulation. By identifying the specific manner in which brain networks functionally connect and are modulated when cognitively engaged, we will have a reference for locating when and where pathophysiology occurs in brain diseases (Greicius, 2008; Rowe, 2010). This systems-level approach is immensely suited to bipolar disorder.

Application to Bipolar disorder

Bipolar disorder type I is a severe psychiatric disease characterized by cyclical, dramatic mood swings that range from feelings of euphoria, expansiveness and overconfidence (mania), to lethargy, hopelessness and suicidal ideation (depression). Epidemiologically, it effects men and women equally, has a lifetime prevalence of approximately 1% of the population and has an average age of onset between the late teens and early twenties (Kessler et al., 2005; Merikangas et al., 2011). Unfortunately, people with bipolar disorder are often clinically misdiagnosed as having unipolar depression when the first clinical presentation of the illness is the depressed state (that is, before any episodes of mania have emerged). Treatment of the disorder can therefore be problematic, as medication suited for unipolar depression misallocated to an individual with bipolar disorder will put the latter at risk for switches into hypomania or mania (Altshuler et al., 1995; Wehr and Goodwin, 1987). Many researchers conceptualize bipolar disorder as a genetically-influenced brain disorder (Strakowski, 2012), and so there is hope that improved diagnoses and treatment tracking will someday incorporate descriptions of functional patterns in brain networks that distinguish healthy from bipolar disordered individuals, and will distinguish bipolar from other mood and anxiety disorders (Zorumski and Rubin, 2011). The network which engages emotion regulation processes holds particular promise for critical descriptions of dysfunction in bipolar disorder.

Why study emotion regulation in BP

A reason for studying emotion regulation in bipolar disorder, considered a disorder of mood and emotion, is that it is possibly the best lead we currently posess. Although the phenotype of bipolar includes disturbances in other domains such as sleep, energy, ‘cold cognition’ and even sociality, the majority of structural and functional findings throughout the short history of bipolar neuroimaging have strongly implicated regions involved in emotion

processing and regulation. Emotion regulation should therefore figure prominently into a full description of the pathophysiology of bipolar. We know, for example, that emotion regulation is a component of successful therapies and more specifically, cognitive reappraisal is a component of cognitive behavioral therapy (Leahy et al., 2011). Cognitive behavioral therapy in turn has proved to be an important component, in conjunction with medication, to better health and welfare outcomes in bipolar disorder (Lam et al., 2005).

Previous GLM and connectivity findings in BP

This dissertation examines the network mechanisms underlying emotion regulation, and its application to bipolar disorder. Such an investigation, however, is built upon research already conducted by our group which elucidates regional differences in the functioning bipolar brain. Using standard GLM analyses, the UCLA Mood Disorders Research Program has observed in the manic state hyperactivation of amygdala and hypoactivation of vlPFC (Altshuler et al., 2005a; Foland-Ross et al., 2008), in the depressed state hypoactivation of both amygdala and vlPFC (Altshuler et al., 2008) and in euthymia no significant change in amygdala but hypoactivation in vlPFC (Foland-Ross et al., 2012). These findings implicate state-related changes in amygdala but trait-related abnormalities in vlPFC. Remaining questions center on the extent to which other regions mediate the communication between amygdala and vlPFC, the nature of that coupling, and how that coupling is altered in bipolar disorder.

Summary of Chapters to follow

In the chapters that follow I address some of these questions using the tools and psychological paradigms outlined above. I apply a functional connectivity method to an explicit emotion regulation task, an effective connectivity method to an implicit emotion regulation task and functional connectivity techniques to resting state fMRI of a subset of the emotion regulation

network. I also apply these approaches to a euthymic cohort of individuals with bipolar disorder, type I. Because the application of these connectivity techniques in the task-based studies was novel, I further divided the larger bipolar projects into two smaller projects: the first addressing connectivity in these paradigms in healthy subjects and the second applying these analyses to the bipolar population. This sequential strategy allowed me to become more familiar with the psychology of emotion regulation and to consider more deeply how it relates to the disorder.

Chapter 2 presents our study of the activation dynamics and functional connectivity of the cognitive reappraisal of emotion in healthy subjects. We used a novel GLM-based procedure to elucidate the temporally-changing dynamics across the reapraisal period in early and late epochs. We then applied a psychophysiological interaction analysis across these epochs to observe changing connectivity between the vlPFC and other task-modulated regions across the brain. This study is currently in preparation for publication. For this chapter and the following chapters (3-6), figures and tables are provided at the end of each.

Chapter 3 presents our application of the novel GLM-based procedure to reappraisal to a matched cohort of euthymic bipolar subjects. This study is also in preparation for publication.

Chapter 4 presents our study of the effective connectivity of affect labeling in healthy subjects. We applied Dynamic Causal Modeling to a four node network to elucidate changes in directional coupling during affect labeling. The chapter is a version of a publication, reproduced here with permission: Torrisi, S.J., Lieberman, M.D., Bookheimer, S.Y., Altshuler, L.L., 2013. Advancing understanding of affect labeling with dynamic causal modeling. NeuroImage 82, 481–488.

Chapter 5 presents our application of this DCM analysis to a matched cohort of euthymic bipolar subjects. A report on this study is currently in preparation for publication.

Chapter 6 presents our study of the euthymic bipolar brain during resting state. We took a focused ROI-based approach to assess bilateral functional connectivity between key regions involved in emotion regulation. We then further explored the results with a mediation analysis. The chapter is a version of this publication, reproduced here with permission: Torrisi, S.J., Moody, T.D., Vizueta, N., Thomason, M.E., Monti, M.M., Townsend, J.D., Bookheimer, S.Y., Altshuler, L.L., 2013. Differences in resting corticolimbic functional connectivity in bipolar I euthymia. Bipolar Disorders 15, 156–166.

Chapter 7 consists of a summary, relating of findings, discussion and a consideration of both limitations and future directions for the field of fMRI-based brain connectivity research and its application to psychiatric populations.

CHAPTER 2: Uncovering early and late stage activity during the cognitive reappraisal of emotion

Salvatore Torrisi[a], Kateri McRae[b],

Nathalie Vizueta[a], Susan Y. Bookheimer[c], Lori L. Altshuler[a]

Semel Institute for Neuroscience & Human Behavior, Dept. of Psychiatry, UCLA[a];
Dept. of Psychology, University of Denver[b]; Center for Cognitive Neuroscience, UCLA[c]

Introduction

The cognitive reappraisal of emotion, an explicit emotion regulation strategy, involves re-conceptualizing a stimulus in a way that alters one's affective response, such as by reframing something negative more positively. This complex operation involves a number of subcomponent processes including the selection, maintenance and monitoring of goal representations which interact with generated emotions (Ochsner et al., 2012). Reappraisal has been studied for decades (Lazarus, 1991), often in the context of a well-known psychological "process model" that provides a useful framework for a broad sequence of emotion regulation operations (Gross, 1998; Sheppes and Gross, 2011; Urry, 2009). Psychologically characterizing the process in this manner has important implications for both basic and translational sciences, so neuroimaging researchers have also become interested in characterizing the neural mechanisms involved. Recent meta-analyses of reappraisal have shown across many studies that particularly areas of the medial, ventrolateral and dorsolateral prefrontal brain are strongly recruited with amygdala activations usually dampened (Buhle et al., 2013; Diekhof et al., 2011). Despite this focus on brain areas involved in and effected by reappraisal, few studies have empirically acknowledged the complex temporality of the process by testing models that elucidate its dynamics.

A notable exception can be found with the work of Raffael Kalisch, who postulated an implementation-maintenance model (IMMO) of reappraisal which he and his colleagues supported with a meta-analysis of reappraisal studies (Kalisch, 2009) and empirical work (Kalisch et al., 2006; Ochsner et al., 2012; Paret et al., 2011). Their hypothesis is that throughout the course of an episode of reappraisal, in general, initial increases in brain activity occur in left posterior regions and then spread into right anterior regions. They tested this using general linear model (GLM) designs with linearly increasing or linearly decreasing regressors. This model effectively captured an important property of the dynamics of reappraisal, namely that activity in certain right and anterior prefrontal regions gradually increases throughout the course of reappraisal. However, reappraisal is a highly dynamic and complex process whose neural instantiation is thought to be additionally influenced by the tactic an individual deploys during the process (Lazarus, 1991; Mcrae et al., 2012). Alternative models of reappraisal may, therefore, uniquely reveal complementary features of its dynamics.

In the first part of this paper, we elaborate a feature of the IMMO to parse neural activations specific to separate *early* and *late* phases of the cognitive reappraisal of emotion. Consistent with the IMMO, we hypothesized that we would observe distinct recruitment and attenuation of activations during each phase of reappraisal, namely recruitment of primarily left and posterior brain regions during the *early* stage, and recruitment of primarily right and anterior regions during the *late* stage. We further hypothesized that some components of these neural patterns would only appear statistically significant when the early or late periods were tested separately and would not be present during a third (and standard) analysis where reappraisal was modeled in *full*. In other words, by dividing the reappraisal epoch we also hypothesized we would uncover regional activations that the *full* model normally dilutes, obtaining greater specificity as to which brain regions are instrumental in which phase of the process.

Dividing the *full* epoch into shorter *early* and *late* epochs would further enable us to explore brain connectivity as it changed throughout the reappraisal process. In the second part of this paper we use a psychophysiological interaction (PPI) (Friston et al., 1997; Gross, 1998; Sheppes and Gross, 2011; Urry, 2009) analysis to assess task-induced changes in functional coupling. We chose a seed region for which we had *a priori* interest (the ventrolateral prefrontal cortex (vlPFC)) and performed separate *early* and *late* PPI analyses. This allowed us to ask where across the brain does task-induced modulation of connectivity with this seed 'pivot' across the period of reappraisal.

Materials and Methods

Participants

Fifty one healthy subjects were recruited as part of a larger study of emotion regulation in bipolar disorder by advertisement in local newspapers and campus flyers. Participants provided written informed,consent in accordance with the Institutional Review Board at the University of California, Los Angeles (UCLA). Participants completed the Structured Clinical Interview for DSM-IV Structured Clinical Interview for DSM-IV Axis I Disorders (SCIDI/P; (Buhle et al., 2013; Diekhof et al., 2011; First, 2002)). Exclusion criteria included any current or past psychiatric diagnosis (including history of substance abuse), neurological illness, metal implants, left-handedness, a history of head trauma with loss of consciousness greater than 5 minutes, or currently taking any medications with psychotropic effects. Four participants were excluded from data analysis due to excessive head motion, resulting in 47 participants for analysis (mean age = 38.9, *SD* = 12; 27 male).

Experimental design

We used a well-validated task of cognitive reappraisal of emotion (Kalisch, 2009; Minkel et al., 2012). Participants viewed 45 color photographs (30 negative, 15 neutral) selected from the International Affective Picture System set (IAPS; (Lang et al., 1997)). Fifteen negative pictures were presented in each condition (*look*, *decrease*) with 15 neutral images presented in the look neutral condition. Based on normative affective ratings, the negative pictures were highly unpleasant and arousing, with mean ratings of valence=2.13 and arousal=6.38 (where 1-point represented most unpleasant and lowest arousal and 9-point represented most pleasant and highest arousal). Neutral photographs had mean normative ratings of valence=5.16 and arousal=3.03.

Each photograph was preceded by a 2-second instruction presented on a colored background: either the word “LOOK” (a nonregulation condition; green background) or the word “DECREASE” (the reappraisal condition; blue background). We presented neutral pictures in the look condition for a neutral baseline. Stimuli were then presented for 7-seconds, during which a border, colored as stated, surrounded each photograph to remind the participant of the instructions for that trial. Following this, a 4-second rating scale asked them to indicate by button press how distressed they felt at that moment from 1 (not at all) to 4 (very much). Lastly, a screen that read “Rest” was presented for a randomized duration of 1 or 3 seconds at the end of each trial (Figure 1A). Fifteen trials of each of the three conditions (*look negative, look neutral, decrease negative*) were presented.

To ensure task comprehension, participants completed a pre-scan training session including 8 example photographs to allow participants to rehearse the instructional conditions. In the *decrease* condition, they were instructed to change the way they thought about the photo in order to decrease the intensity of the emotion they felt. To ensure that strategies used were

consistent with cognitive reappraisal (cf. Gross, 1998b) different regulation strategies were discussed. After generating a working reappraisal participants were told that "…once you come up with something just mentally repeat it to yourself and try to convince yourself it's true for the rest of the short time the picture is up." Incorrect methods of regulation were illustrated as thinking of things unrelated to the picture, focusing only on parts of it, looking away, or generating unrelated emotions.

Behavioral data

We tested for a significant change in self-reported negative affect following the *look negative* and *decrease negative* trials by performing two-sample t tests between the ratings. We hypothesized that a significant change would occur in the form of a reduction of negative affect following *decrease* trials.

Image acquisition

All subjects were scanned on a 3T Siemens Trio scanner. A high resolution structural T1 MPRAGE was acquired with parameters of TR=1.9 seconds, TE=2.26 ms, Flip-Angle = 9°, Matrix = 256×256, FOV=250mm, voxel size 1mm isotropic, and total sequence time 6 minutes and 50 seconds. The fMRI scan was acquired using a T2*-weighted EPI gradient-echo pulse sequence with IPAT, with TR=2 seconds, TE = 25 ms, Flip-Angle = 78°, Matrix=64×64, FOV=192mm, in-plane voxel size 3x3 mm, slice thickness 3mm, 0.75mm gap, and 30 total interleaved slices. To allow for scanner equilibration and for IPAT reference, 3 TRs at the beginning of the scan were discarded. The total sequence time for the fMRI was 11 minutes and 26 seconds, with 340 volumes acquired. We additionally acquired a matched-bandwidth structural scan with parameters TR=5 seconds, TE=34 ms, Flip-Angle=90°, Matrix=128×128, FOV=192mm, in-plane voxel size 1.5×1.5mm, slice thickness 3mm, and a total sequence time of 1.5 minutes. MPRAGE scans were not acquired for three subjects so their matched-

bandwidth images were instead used for registration. Foam padding was placed around the heads of participants to help dampen motion, stimuli was presented via LCD goggles, and responses were collected by button box.

Image Preprocessing

All preprocessing and analyses were performed within SPM8 (www.fil.ion.ucl.ac.uk/spm/). Subjects' functional volumes were slice-time corrected (Descamps et al., 2007), then motion realigned, coregistered to the MPRAGE structural scan, normalized to a T1-weighted standard brain in MNI space, resliced 2 mm isotropically, and smoothed with a 6 mm FWHM Gaussian kernel. All subjects had maximum translational head movements of less than 2.2 mm, with means and standard deviations across subjects for three translation parameters (x, y, z): 0.179(0.21), 0.147(0.15), 0.307(0.38) and three rotation parameters (pitch, roll, yaw; radians): 0.007(0.01), 0.004(0.004), and 0.003(0.004).

Within-subject general linear model (GLM) analysis

First-level GLMs of the preprocessed functional images for each subject included convolving the task design blocks with a canonical hemodynamic response function, high-pass filtering at 128 seconds, and adding regressors of the rating periods and six additional regressors for each subject's motion realignment parameters as covariates of no interest. We additionally specified an explicit whole-brain mask derived from an optimal thresholding of the subject masks (Ridgway et al., 2009) to ensure coverage of the ventrolateral prefrontal cortex.

We performed three different analyses using two regression designs of the reappraisal contrast (*decrease negative* > *look negative*): a standard, *"full"* analysis where the entire 7 second duration of negative stimuli presentation was modeled as a single regressor (Figure 1A; "model 1"), and two other analyses with the full epoch divided into two "*early"* and "*late"* halves

of 3.5 seconds each (Figures 1B and 1C). We modeled these halves as a separate regressors within the same design ("model 2"). In these latter analyses, contrast vectors were specified with the *early* regressor assigned a "1" and *late* assigned "0", or the *early* regressor assigned a "0" and *late* assigned "1". In this way we covaried out overlapping variance associated with *late* while looking at early, and conversely covaried out overlapping variance associated with *early* while looking at *late*. Interpretations of resulting statistical maps should take this into account (Figures 1D and 1E). All contrasts used the entire 7-sec period of *look negative* as baseline in which subjects were asked to simply look at negative photographs and respond the way they would naturally. We also assessed evidence that cognitive reappraisal had a predicted and often-replicated dampening effect on the amygdala, our primary emotion-generating region of interest. This was tested with the reverse contrasts of the three just described: *look negative* > *decrease negative*, *look negative* > *decrease negative (early)* and *look negative* > *decrease negative (late)*.

We note that although the adjacent *early* and *late* blocks are temporally non-overlapping, they did partially overlap after each was independently convolved with a canonical hemodynamic response function. The correlation of these two regressors was 0.48, and shared 23% of their variance (Figure 1E), which presents a potential multicollinearity issue (Monti, 2011). To test if this multicollinearity would be detrimental to the analysis, we measured the variance inflation factor for these two regressors in the context of the design matrix using SPSS 21.0, which quantifies the severity of multicollinearity in an OLS regression analysis. We found these to be well under conservative recommendations of 5 (Mumford, 2013; Rogerson, 2001) at values of 2.4 and 1.4 for the *early* and *late* regressors, respectively.

Psychophysiological interaction analyses

To assess changes in functional connectivity during reappraisal we performed two

psychophysiological interaction (PPI) analyses of the *early* and *late* stages. The PPI method identifies voxel-level interactions between a psychological process and activity within a specific brain region, revealing task-induced changes in coupling between that region and the rest of the brain (Friston et al., 1997). We chose the same left ventrolateral prefrontal cortex (vlPFC) seed region and its time series for both PPI analyses because it (a) was robustly active in the *full* GLM analysis and would allow assessment of its contributions during the *early* and *late* temporal subsets and (b) has been strongly implicated by other research in emotion regulation processes in general as well as reappraisal in particular; see (Cohen et al., 2011) for review. With PPI, context-specific changes in functional connectivity are generally interpreted as contributory when the regression coefficient is positive, or antagonistic when the coefficients are negative (i.e., activity in seed region X "suppresses" region Y). It should be emphasized that these are interpretations, however, and a PPI cannot determine excitation vs. inhibition or the direction of connectivity.

Three regressors were used to construct the PPI model: 1) a physiological regressor representing the seed activity (time series) within an 8mm radius sphere around the group GLM peak in the full *decrease negative* vs. *look negative* contrast (left vlPFC (BA 47); [-48 16 -4]), adjusted for effects of interest; 2) a psychological regressor for the task condition (*early* or *late* reappraisal) used to determine task-induced changes in functional connectivity between the vlPFC and other regions across the brain; and 3) the PPI variable formed by deconvolving the BOLD time series to represent the interaction at the neuronal level, computing the element by element product of the first two variables and reconvolving this time series to create a regressor for the PPI analysis (Gitelman et al., 2003). To determine which areas reflect this psychophysiological interaction, a second general linear model was formed with these three regressors. Assigning contrast vector values of +1 or -1 for the PPI regressor and 0 for the other two produced statistical images showing voxels that possessed a significant, task-induced

increase (positive coupling) or decrease (negative coupling) with activity in the left vlPFC during the *early* or *late* phases of reappraisal.

Second level (between-subject) group analyses

For both group GLM and PPI analyses, individual contrast maps were grouped in a second-level random effects analysis for population-level inference using one-sample t tests. Whole brain, voxel-level results were thresholded at $p<0.001$, $k=35$, FDR corrected at $p<0.05$. Peak coordinates and cluster-level significance are additionally reported in Table 1. Axial slices were visualized using xjView (http://www.alivelearn.net/xjview8/).

Results

Behavioral data

Subjects demonstrated a significant reduction in self-reported negative affect for the reappraisal trials following negative photographs compared to look trials following negative photographs (means(SD) = 2.15(0.5), 2.57(0.6), respectively; $p=0.0002$). Self-reported negative affect following look neutral trials was 1.04(0.06) and was significantly lower compared to the other two conditions (Figure 3A).

GLM analyses

As mentioned above, we performed three separate analyses on the same data set: (1) a *full* analysis with the entire 7-sec reappraisal trial modeled, (2) an *early* analysis with only the first half modeled (0-3.5 sec), and (3) a *late* analysis corresponding to the second half (3.5-7 sec) of the reappraisal period to better elucidate the temporal dynamics during cognitive reappraisal. Figures 2A-D illustrate select whole-brain axial slices corresponding to each of the three analyses, with cluster and peak-level coordinate results provided in Table 1A-C.

The results from the standard analysis (*full* model; decrease negative > look negative) are consistent with a large meta-analysis of cognitive reappraisal of emotion tasks (Buhle et al., 2013). As expected, we found that cognitive reappraisal recruited key brain regions involved in cognitive control, including bilateral ventrolateral prefrontal cortex (vlPFC; BA 47), dorsolateral prefrontal cortex (dlPFC; BA 9), and superior and anterior frontal gyri (BA 10). Activation results were somewhat left-lateralized (e.g. see vlPFC and inferior parietal lobule (IPL) in right column of Figures 2B and 2D). To assess the effects of reappraisal, we reversed the reappraisal contrast to determine whether the amygdalae were substantially more responsive during the 'look' negative condition versus the decrease negative condition during the full epsiode of reappraisal. This contrast (*look negative > decrease negative (full))* did not yield significant activations in either left or right amygdala at our whole-brain threshold (Figure 3B).

We then divided the reappraisal epoch into two phases, with each phase represented by a unique regressor and both regressors retained in the same design (Figure 1, model 2). In the *early* phase we found significant activations in regions that were not present during either the *late* phase or the *full* period of reappraisal – namely the right amygdala and bilateral inferior temporal (fusiform) gyri (left column in Figure 2A).

In the *late* phase we found significant activations that are present but much *weaker* in the *full* analysis – namely bilateral superior frontal gyri (BA 10; middle column of Figure 2C) and right dlPFC (middle column of Figure 2D). Additionally, we found significant activations in the second half of the reappraisal period that were not at all present during either the *early* phase or the *full* period. For example, the middle column in Figures 2C and 2D show regions emerging *late* such as the right anterior cingulate cortex (ACC), caudate and inferior parietal lobule. Lastly, the *look negative > decrease negative (late)* contrast showed significant bilateral amygdala activations (Figure 3B) not detectable within the *look negative > decrease negative (full)* analysis.

Psychophysiological Interaction analyses

Within both the *early* and *late* reappraisal periods we assessed changing functional connectivity with the left vlPFC. Within the early reappraisal period we observed significant task-induced positive connectivity between the vlPFC and primary and extrastriate visual regions (Figure 4A). We also observed significant negative connectivity between the vlPFC and ACC and dorsal midline structures. Within the *late* reappraisal period we observed continued positive coupling between left vlPFC and primary visual regions but reduced positive connectivity with extrastriate visual regions (Figure 4B). Additionally, we observed a much stronger and broader negative coupling with the ventromedial PFC (vmPFC) as well as greater negative coupling with the dorsal midline regions.

Discussion

The cognitive reappraisal of emotion is a commonly studied form of explicit emotion regulation with particularly complex internal dynamics. While most analyses of reappraisal do not focus on its temporal evolution, notable exceptions have modeled linearly increasing or decreasing brain activity across the reappraisal epoch (Kalisch, 2009; Paret et al., 2011). In addition to examining the entire reappraisal period, we employed a unique and complementary approach to "uncover" brain activity during the *early* and *late* phases of reappraisal. We expected that reappraisal-related brain activity would globally shift from left posterior to right anterior brain regions throughout the course of the reappraisal period and we further assessed changing connectivity patterns across the two temporal phases.

Consistent with a large number of published studies using similar paradigms (Buhle et al., 2013; Diekhof et al., 2011; Ochsner et al., 2012), we found that the full period of reappraisal (*decrease negative (full) > look negative)* was associated with robust prefrontal and parietal activation clusters, regions known to subserve explicit emotion regulation in general and

cognitive reappraisal in particular. Behaviorally, we assessed negative affect by subjects reporting a change following the reappraisal trials versus the look trials and found a significant reduction in negative affect following reappraisal. Assessing the effects of reappraisal in the neuroimaging context, however, proved more difficult, as we additionally looked at the reverse contrast (*look negative* > *decrease negative (full)*) for evidence that the amygdala was more active during looking at negative photographs versus the reappraising them and found no such evidence at our corrected threshold.

In comparison to the standard analysis examining the *full* period of reappraisal, the *early* and *late* contrasts offer additional insights into the dynamics of the reappraisal process. By focusing the statistical contrasts toward *early* and *late* periods we observed significant activity in regions that the *full* model 'dilutes'. In some regions activations are still present but weaker when modeled in *full* rather than only during the *late* stage (i.e. smaller cluster peak statistic and cluster size). Examples include the left superior frontal gyrus (Figure 2C) and right dorsolateral prefrontal cortex (Figure 2D). This observation has multiple implications. Outside *a priori* regions of interest, for example, neuroimaging researchers often focus their interpretations on large regional effects. If an area is only weakly respresented in standard analyses its significance within the reapparaisal process may be overlooked. Even if the region is reported in a table, however, its statistical representation would bias some quantitative meta-analysis approaches that partly weigh regional contributions to the composite analysis by reported effect size (Anticevic et al., 2012). As already shown (Kalisch, 2009), quantitiative meta-analyses of cognitive reappraisal are currently meta-analyses of standard (*full*) models that implicitly make assumptions about a static reappraisal process. The *early/late* division therefore offers a way to bring attention to and perhaps even prioritize the contribution of certain brain regions in the reappraisal process.

Our approach provides another insight into the reappraisal process: activation that is not

seen in the *full* analysis can also be “uncovered” by the *early* or *late* analyses. Examples of this include activation in the right amygdala and bilateral fusiform gyri during the *early* period (Figure 2A), or in the body of the caudate, anterior cingulate (Figure 2C) or right inferior parietal lobule (Figure 2D) during the *late* period. In particular, the *early* stage reappraisal map suggests greater processing of visual aspects of the negative stimuli in extrastriate and inferior temporal regions as well as an initially strong emotional response in the amygdala. These activations recede during the *late* stage of reappraisal. This is interesting in light of the historical distinction between antecedent and response-focused emotion regulation strategies (Goldin et al., 2008; Gross, 1998). Antecedent-focused strategies, like reappraisal, were thought to anticipatorily target the appraised meaning of a stimulus. Conversely, response-focused regulatory strategies, such as expressive suppression, were thought to target an already experienced emotional and/or physiological response. Here, anticipatory targeting is a reasonable assumption given that our instructions to ‘look’ or ‘decrease’ were provided before the onset of the stimulus. However, our results suggest instead such a distinction is misleading as it appears reappraisal is actually acting upon an already initiated emotional response, demonstrated by amygdala activity in the *decrease negative (early)* > *look negative* contrast.

This notion of “uncovering” the signficance of a region’s involvement is further relevant to whether reappraisal had neuroanatomical effects for our subjects that correspond to their self-reports. Only when we specifically probed the latter half of the reappraisal epoch with the reverse contrast *look negative* > *decrease negative (late)* were we able to observe that amygdala activity was much stronger during looking than reappraising during this period (Figure 3). This is relevant because reporting of amygdala modulation in reappraisal studies is inconsistent, with upwards of a quarter of studies not reporting it at all (see Table 1 of (Ochsner et al., 2012)). It would be interesting to see if the researchers of those studies reanalyzed their data in an *early / late* manner if amygdala modulation would then become apparent.

Demonstrating dynamic profiles of regional responses across two broad phases of reappraisal still leaves many questions regarding the mechanisms behind these observations. For example, there are different possible interpretations as to why activity in some regions recede from the early to the later stage: attention could be drawn from them to higher-level cognitive demands, the early regions may habituate, they may possess unique physiological properties (i.e. the amygdala as a “novelty detector”), the shared variance removed during the regression may represent the continued activity of those earlier regions, or latter regions may be dampening the early-responsive ones. Further research is necessary to sort and revise these possibilities.

We did, however, offer additional insight into the mechanisms behind our two phase results by performing an analysis of how task-based functional coupling with a seed region changes across the reappraisal period. We observed that areas that process visual stimuli possess a positive connectivity with the vlPFC earlier in the reappraisal process which appears to diminish in the later phase. We also observed other areas, such as the vmPFC, are negatively coupled with the vlPFC and that this coupling strengthens across the reappraisal process (Figures 4A, 4B).

Limitations and future directions

Our study probed the temporal evolution of cognitive reappraisal via a novel partitioning of the reappraisal epoch. We addressed the potential confound of multicollinearity between the early and late GLM regressors and do not consider it to negatively impact the accuracy of the final results. However, one must be cognizant of the different variances explained across all three statistical maps and to interpret them appropriately (Figure 1E). For example, covarying out shared variance likely produces false negatives, and the *early* and *late* statistical maps should not be thought to ‘add up to’ the *full* map.

A potential limitation to our *early* / *late* analysis is that we contrasted the half of *decrease negative* with the entire *look negative*. We wished to retain as much data for statistical comparison as possible, but by doing so we also implicitly assumed a less dynamic experience looking at the IAPS stimuli than reappraising them. Given the large difference in cognitive demand between the two conditions, we feel that this is not an unreasonable assumption. However, it could be empirically addressed in future studies by contrasting *early decrease* with *early look* and *late decrease* with *late look*.

As previously noted, there is recent interest among emotion regulation researchers in specifying in finer detail the dynamics of reappraisal. Some psychologists have modeled the differential efficacy of deploying regulatory processes within different periods of "emotion generating cycles" (Sheppes and Gross, 2011; Urry, 2009), however these models do not describe the underlying neural dynamics of these cycles. Artificially partitioning the reappraisal epoch as we have adds to our description of these underlying reappraisal dynamics, and yet, also greatly simplifies them. Indeed, all modeling efforts are simplifications of the phenomenon one is modeling (Box and Draper, 1987) and the standard GLM approach to fMRI analysis, whether by box car design or a linearly increasing or decreasing one, is no exception. For example, one might consider that reappraisal entails a non-linear sequence of perceiving and reacticing to an aversive stimulus, regulating, assessing its effects, perhaps altering one's tactic, regulating again, and converging on a functional strategy held in working memory continuously deployed until the end of the trial. Because of these prospects, our *early* / *late* analysis is agnostic to the details of "emotion generating cycles" and simply concentrates on BOLD-signal variance within the beginning and the ending stages of the process. Further examinations of within-stage as well as transitional neural dynamics may benefit from other approaches such as designing a much longer reappraisal epoch amenable to finer analytical divisions, modeling the

directed influences between regions (i.e. dynamic causal modeling) or alternative imaging modalities with finer temporal resolution (i.e. electroencephalography).

Our connectivity findings demonstrated that task-based modulations in functional coupling with the ventrolateral PFC change across the early and late periods as well. However, one interesting aspect of these findings is that some regions in the *early* and *late* GLM maps did not appear at all in the PPI analyses (i.e. note the lack of BA 10 connectivity in figure 3B, bottom left, despite its clear involvement in the activation maps (Figure 2C). This suggests the involvement of multiple networks during reappraisal, some of which were not accessed via the vlPFC "window" of our analysis. Therefore a single-seed PPI analysis only reveals a subset of multiple ongoing and interacting networks required for reappraisal. This is plausible given the multiple psychological sub-processes which psychologists think are involved, such as those outlined in the previous paragraph. Future neuroimaging studies of reappraisal would benefit from more comprehensive connectivity approaches such as those measuring task-based changes in coupling between dozens or more nodes across the brain (Fornito et al., 2012).

A detailed understanding of the neurobiological mechanisms underlying reappraisal would benefit multiple domains of basic and translational research. The cognitive reappraisal of emotion is a uniquely human ability which enables us to return to baseline when internal or external events divert us from emotional homeostasis. Strength in emotion regulation is, for example, key to successful mindfulness-based and cognitive behavioral therapies (Leahy et al., 2011). Furthermore, multiple kinds of psychiatric or developmental disorders, from those involving anxiety and mood (Phillips et al., 2008a) to externalizing disorders (Halligan et al., 2013), have demonstrated weaknesses in the ability to regulate emotion. With future studies an increasingly fine-grained description of what mechanistically occurs during cognitive reappraisal should help clinically-oriented researchers temporally locate where this process breaks down in these populations.

Figures

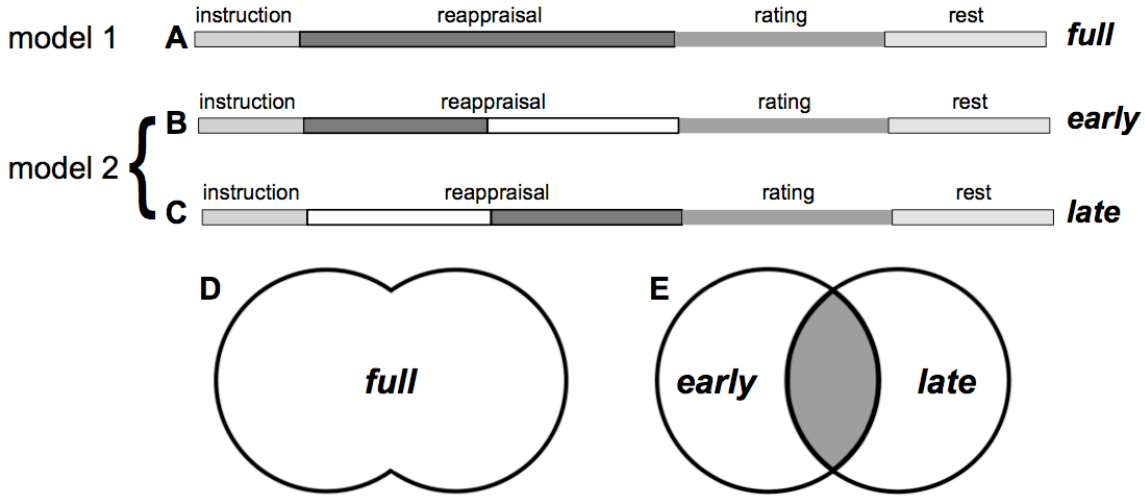

Figure 1. A-C: *full, early* and *late decrease negative* variants of the *decrease negative* > *look negative* contrast. Darkest gray represents the periods of modeled reappraisal. D. Schematic of the variance contained within the *full* (standard) GLM design for reappraisal. E. Schematic of shared variance (23%) between the HRF-convolved *early* and *late* reappraisal regressors. Gray portion is covaried out in both maps.

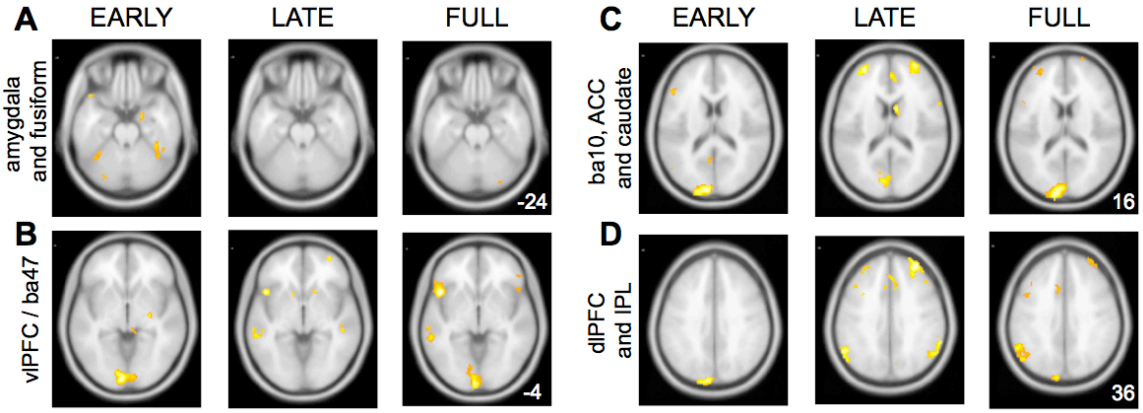

Figure 2. (A-D) Four select axial slices from ventral to dorsal across all three analyses: *early*, *late* and *full*. N=47 subjects; all maps FDR corrected at p<0.001, k=35; left is left; numbers represent Z coordinates in MNI space. vlPFC = ventrolateral prefrontal cortex; ba = Brodmann's area; ACC = anterior cingulate cortex; dlPFC = dorsolateral prefrontal cortex; IPL = inferior parietal lobule.

A) FULL

		Brodmann area	cluster p (FDR-cor)	cluster size	cluster p (unc)	peak Z	peak p (unc)	MNI x, y, z
L	Inferior Frontal Gyrus	BA 47	0.000	604	0.000	6.04	0.000	-48 16 -4
L	Cuneus	BA 18	0.000	1911	0.000	5.83	0.000	-8 -94 20
L	Superior Frontal Gyrus	BA 6	0.000	2018	0.000	5.32	0.000	-4 2 64
L	Angular Gyrus	BA 39	0.000	689	0.000	4.77	0.000	-52 -70 38
L	Medial Frontal Gyrus	BA 8	0.001	153	0.000	4.76	0.000	-4 26 46
L	Middle Temporal Gyrus	BA 22	0.003	119	0.000	4.33	0.000	-58 -38 -4
L	Superior Temporal Gyrus	BA 38	0.061	52	0.010	4.08	0.000	-34 22 -30
L	Middle Frontal Gyrus	BA 10	0.015	79	0.002	3.95	0.000	-36 58 20
L	Precuneus*	BA 7	0.137	35	0.029	3.42	0.000	-6 -70 42
R	Inferior Frontal Gyrus	BA 47	0.000	199	0.000	4.7	0.000	52 32 -10
R	Middle Frontal Gyrus	BA 10	0.000	193	0.000	3.95	0.000	30 52 22
R	Fusiform Gyrus	BA 19	0.085	45	0.015	3.74	0.000	30 -84 -22
R	Supramarginal Gyrus	BA 40	0.088	43	0.017	3.59	0.000	56 -52 28

B) EARLY

		Brodmann area	cluster p (FDR-cor)	cluster size	cluster p (unc)	peak Z	peak p (unc)	MNI x, y, z
L	Cuneus	BA 19	0.000	2530	0.000	5.96	0.000	-4 -94 22
L	Medial Frontal Gyrus	BA 6	0.002	127	0.000	4.74	0.000	-2 0 66
L	Middle Frontal Gyrus	BA 6	0.029	70	0.003	4.36	0.000	-40 2 62
L	Inferior Frontal Gyrus	BA 44	0.005	110	0.000	4.16	0.000	-58 20 10
L	Inferior Frontal Gyrus	BA 47	0.076	50	0.008	4.14	0.000	-44 24 -18
L	Middle Temporal Gyrus	BA 39	0.010	92	0.001	4.08	0.000	-36 -66 26
L	Posterior Cingulate	BA 30	0.001	155	0.000	3.87	0.000	-6 -52 12
R	Fusiform Gyrus	BA 37	0.000	396	0.000	5.47	0.000	34 -58 -16
R	Lentiform Nucleus*	Globus Pallidus	0.125	41	0.015	4.61	0.000	28 -16 -2
R	Thalamus	Pulvinar	0.150	36	0.022	4.54	0.000	8 -30 0
R		Amygdala	0.131	39	0.018	4.21	0.000	20 -6 -22
R	Lingual Gyrus	BA 18	0.000	245	0.000	4.17	0.000	22 -80 -16
R	Inferior Frontal Gyrus	BA 47	0.029	68	0.003	3.98	0.000	30 34 -12

C) LATE

		Brodmann area	cluster p (FDR-cor)	cluster size	cluster p (unc)	peak Z	peak p (unc)	MNI x, y, z
L	Inferior Parietal Lobule	BA 40	0.000	823	0.000	5.22	0.000	-50 -66 50
L	Superior Frontal Gyrus	BA 10	0.000	265	0.000	4.94	0.000	-30 52 18
L	Middle Frontal Gyrus	BA 8	0.000	289	0.000	4.88	0.000	-44 24 48
L	Middle Frontal Gyrus	BA 6	0.000	242	0.000	4.82	0.000	-28 14 62
L	Anterior Cingulate	BA 32	0.000	711	0.000	4.69	0.000	-4 34 26
L	Insula*	BA 13	0.002	115	0.000	4.61	0.000	-46 16 -4
L	Cuneus	BA 17	0.000	441	0.000	4.53	0.000	-8 -82 10
L	Caudate	Caudate Body	0.045	50	0.010	4.46	0.000	-14 18 4
L	Insula	BA 13	0.028	60	0.006	4.34	0.000	-36 12 6
L	Lentiform Nucleus*	Putamen	0.091	37	0.024	4.33	0.000	-26 -6 6
L	Middle Frontal Gyrus	BA 11	0.002	118	0.000	4.25	0.000	-38 50 -10
L	Medial Frontal Gyrus	BA 6	0.000	160	0.000	3.86	0.000	-4 -4 62
L	Middle Temporal Gyrus	BA 22	0.002	115	0.000	3.83	0.000	-58 -38 -4
L	Superior Frontal Gyrus	BA 9	0.014	75	0.003	3.56	0.000	-28 48 30
R	Superior Frontal Gyrus	BA 6	0.000	307	0.000	5.27	0.000	18 4 70
R	Inferior Frontal Gyrus	BA 44	0.000	297	0.000	5.24	0.000	56 16 8
R	Superior Frontal Gyrus	BA 9	0.000	1230	0.000	5.23	0.000	34 48 34
R	Inferior Parietal Lobule	BA 40	0.000	763	0.000	4.76	0.000	58 -56 42
R	Caudate	Caudate Body	0.022	65	0.004	4.38	0.000	8 6 16
R	Superior Frontal Gyrus	BA 8	0.016	72	0.003	4.34	0.000	44 18 54
R	Middle Temporal Gyrus	BA 21	0.010	83	0.002	4.16	0.000	62 -24 -12
R	Insula*	BA 13	0.045	51	0.010	4.05	0.000	36 18 4
R	Caudate*	Caudate Head	0.052	47	0.012	3.93	0.000	14 18 0
R	Superior Frontal Gyrus	BA 6	0.064	43	0.016	3.75	0.000	2 10 66

Table 1. A-C, *full, early* and *late* GLM analysis results, respectively. P<0.001, k=35. All reported clusters contain more than one local maxima except where indicated *.

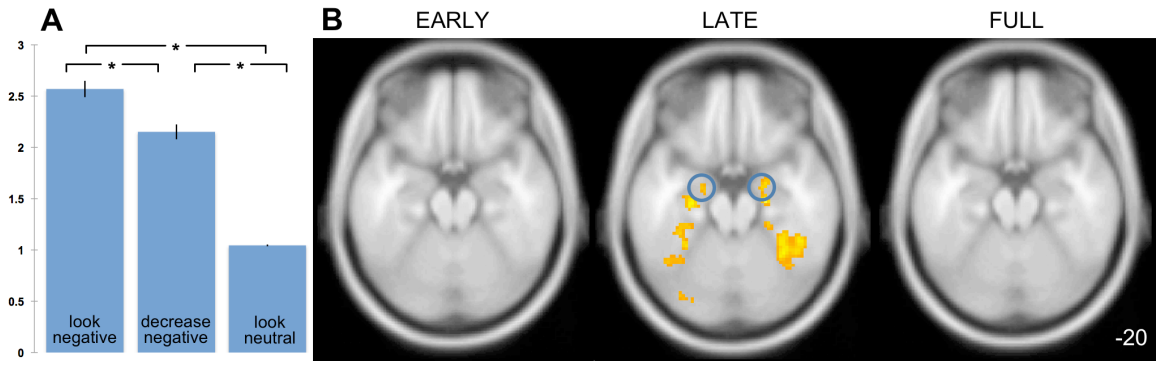

Figure 3. **A**. Self-reported negative affect following the three conditions. Error bars = s.e.m. **B**. Significantly less amgydalae activity (circled) during the late reappraisal period observed in the *look negative* > *decrease negative (late)* contrast. Maps FDR corrected at p<0.001, k=35.

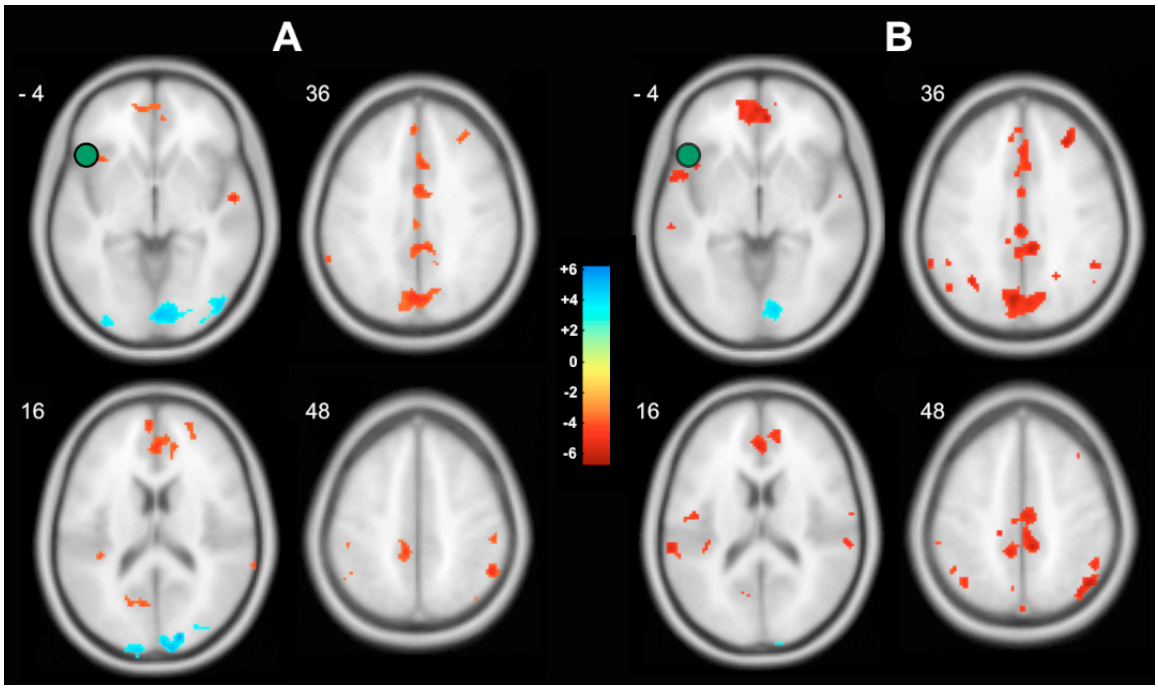

Figure 4. Preliminary psychophysiology (PPI) results. **A**. PPI of early reappraisal period. Left vlPFC seed region (green circle) derived from the *full* analysis in the *decrease negative* > *look negative* (full) contrast (recall Figure 2B; same time series for each subject was used in both the *early* and *late* analyses). **B**. PPI of late reappraisal period. Blue = positive functional connectivity with vlPFC (t test values), red = negative functional connectivity. Non-colorbar numbers indicate the z level in MNI space. p<0.001, k=35.

CHAPTER 3: Early and late stage activation differences during reappraisal in bipolar disorder

Salvatore Torrisi[a], Kateri McRae[b],

Nathalie Vizueta[a], Susan Y. Bookheimer[c], Lori L. Altshuler[a]

Semel Institute for Neuroscience & Human Behavior, Dept. of Psychiatry, UCLA[a];
Dept. of Psychology, University of Denver[b]; Center for Cognitive Neuroscience, UCLA[c]

Introduction

Neuroscientific research in healthy subjects is generally designed to delineate the biological mechanisms that serve the range of normal cognition. Understanding which brain regions are involved in particular physiological states or psychological processes and how those regions interact in a network provides the logical starting point for investigating how aspects of that network may be dysfunctional in psychiatric diseases. It can be beneficial, therefore, to first elucidate what occurs in the healthy brain, and then apply that approach to a particular disorder. Here we apply the *early* / *late* temporal approach to the cognitive control of emotion described in the previous chapter to a group of individuals in the euthymic state of bipolar disorder, type I.

As outlined in Chapter 1, bipolar disorder is a serious psychiatric illness with a profile of chronic mood episodes, from serious depressions to manias, and with some periods of respite between them called euthymia. Because of the fluctuating but cyclical nature of the disease, researchers believe that there are some biological properties in the bipolar brain that are constant throughout the life of the patient (that are, in effect, synonymous with them identifying with the diease and them being successfully diagnosed as such), and some biological properties that either cause or are reflective of the different mood states. Researchers often

refer to these as trait- and state-related biomarkers, respectively. Therefore a description of what occurs within the brain in all three mood states (depression, mania and euthymia) is instrumental to understanding which neural substrates, and characteristics of their connectivity, are consistently problematic (a trait), and which substrates track with mood (a state).

The capacity to regulate one's emotion (where emotion is operationally a component a mood) is considered one of the fundamental problems in bipolar disorder (Phillips et al., 2008a). The cognitive reappraisal of emotion is furthermore one of the most well-studied types of explicit emotion regulation (Ochsner et al., 2012). The few studies that have used this paradigm applied to bipolar disorder found hypoactivity in the ventrolateral prefrontal cortex (vlPFC) and hypoconnectivity with the amygdala in the vlPFC (Townsend et al., 2013; Townsend and Altshuler, 2012). In general, however, little is known about where and how this particular process is aberrant in bipolar.

In this chapter we explore the temporality of where reappraisal breaks down in bipolar disorder with the early / late analysis by using fMRI to investigate differences between the healthy and euthymic groups. We recruited euthymic subjects because results found during this period point to trait, as opposed to state, differences. We additionally tested the normal *(full)* period of reappraisal, as well as self-reports of reappraisal efficacy and tactic use, to connect this work with extant and novel research. We hypothesized that we would behaviorally observe: (1) a lesser amount of self-reported change in affect following 'decrease' trials in the bipolar subjects and (2) a difference in tactic use among bipolar subjects (an exploratory analysis). We further hypothesized that we would neurobiologically see in bipolar disorder: (3) hypoactivity in vlPFC during the *full* epoch of reappraisal, relative to healthy subjects, (4) no difference in amygdala activation while looking during the *early* epoch and (5) hypoactivity in cognitive control regions during the *late* epoch.

Materials and Methods

Participants provided written and informed consent in accordance with the Institutional Review Boards at UCLA and the Veterans Affairs Greater Los Angeles Healthcare System. Subjects with bipolar disorder type I (BP; N=42) were recruited through the outpatient UCLA Mood Disorders Clinic, the outpatient Bipolar Disorders Clinic of the VA Greater Los Angeles Health Care System and through local advertising in the community. Healthy control subjects (HC; N=47) were recruited by advertisement in newspapers and campus flyers. All participants were first interviewed using the Structured Clinical Interview (SCID) (First, 2002) for DSM-IV to confirm a bipolar diagnosis or absence of. Participants with bipolar were excluded if they met criteria for any other current Axis I disorder. Demographics and clinical variables of the healthy and bipolar groups are listed in Table 1. There were no significant differences in age ($p=0.51$) or gender (Chi squared $p=0.83$) between groups.

Behavioral analyses were conducted using SPSS 21.0. We fit a 2x2 repeated measures ANOVA with group (healthy or bipolar) as the between-subjects factor and condition prior to reporting (look or decrease). Tactic coding was performed independently by two raters who classified self-reported tactics into nine categories (Mcrae et al., 2012). Between group results with poor rater reliability (Chronbach's α <0.6) are not reported.

All bipolar subjects' MRI and fMRI data were identically preprocessed and analyzed as the healthy subjects' data. Because these procedures were described in the previous chapter they are not detailed here. There were no significant differences in the six head motion parameters during scanning between groups. First-level *full*, *early* and *late* GLM maps were brought to a random effects group level for between-group comparisons using 2-tailed, 2-sample t-tests. Between-group maps were thresholded at $p<0.001$, $k=20$.

Results

Self-reported negative affect following each trial revealed a significant reduction in both groups after reappraisal trials relative to look trials (figure 1; HC p=0.0002, BP p=0.043), however the condition*group interaction showed the bipolar subjects trending towards less decrease in negative affect after reappraisal than the healthy subjects (p=0.088). Reappraisal tactic coding also showed a significantly greater use of "*agency"* by the bipolar subjects with independent samples t-test with unequal variance (HCμ=0.15$\pm$0.06(s.e.m), BPμ=0.31$\pm$0.11; *t*=-1.3; p=0.019; α=0.77). This type of tactic is categorized as such when the subject has specifically mentioned "…a person with skills to change the current situation" when describing which tactic they used most often (Mcrae et al., 2012).

Between-group *full* GLM results demonstrated significant hypoactivity in the bipolar group in left vlPFC (BA47; cluster peak at [-48 28 -14]: *t*=4.04, k=25; figure 2A) and in the right anterior cingulate cortex (BA32; cluster peak at [6 46 16]: *t*=4.44, k=28; figure 2B). As hypothesized, we also found no group differences in either amygdala at the whole brain level during the *look negative (full) vs look neutral* contrast, lending support to our hypothesis that amygdala reactivity tracks with mood state, as we have previously found it to be hyperactive during mania, hypoactive during depression, and not significantly different during euthymia (Altshuler et al., 2008; 2005a; Foland-Ross et al., 2012).

Between-group *early* GLM results demonstrated hypoactivity in a number of posterior brain regions in the occipital, temporal and parietal lobes in the bipolar group during reappraisal (*decrease negative (early) vs look negative*; figure 3). We found no significant hyperactivations in the bipolar group in the *early* period. Between-group *late* GLM results revealed greater activation in left hippocampus and right inferior parietal lobule (IPL) in the bipolar group (bipolar

> healthy; not shown). We found no significant hypoactivations in the bipolar group in the *late* period.

Discussion

We tested behavioral and neuroactivation differences during reappraisal between healthy subjects and an age- and gender-matched group of euthymic subjects with bipolar disorder, type I. The bipolar subjects reported slightly less success at downregulating their emotional responses to negative photographs by reappraisal than the healthy group, and also reported more frequent use of the *agency* reappraisal tactic. Our hypothesis of hypoactivation in vlPFC in the bipolar subjects was supported, as we found a significant cluster in the left vlPFC that was more strongly active during the *full* reappraisal epoch in healthy subjects. This result corroborates other results from our laboratory using a similar version of this task but with entirely different groups of healthy and euthymic bipolar type I subjects and using entirely different fMRI analysis software as well (Townsend et al., 2013). This lends strong support to hypoactivity in the vlPFC being consistently problematic in bipolar disorder and is a potential trait-related biomarker for the disease. Our hypothesis of no difference in amygdala reactivity to the negative photographs was also supported at the whole brain level.

The *early* / *late* analyses, however, yielded unexpected results for which we had no *a priori* hypotheses. Therefore, detailed interpretations of them would be in error of speculation and reverse inference. Nonetheless, bipolar subjects appear to have generally less activity in posterior brain regions during the *early* period of reappraisal and more activity in left hippocampus and right IPL during the *late* period, relative to healthy subjects.

Limitations and future directions

One limitation of this study is that most of our bipolar subjects were taking psychotropic medications, while our healthy group was not. This is common among studies of BP type I, but unfortunately we did not have enough subjects to look at sub-groups based on medication type. It has, however, been shown via two non-overlapping meta-analyses that the effects of psychotropic drugs on the fMRI signal in bipolar disorder yields no appreciable effect (Hafeman et al., 2012; Phillips et al., 2008b). Further research that directly tests this is warranted.

A number of sub-analyses still need to be performed to solidify the reliability of the *early / late* results. For example, a region of interest (ROI) analysis with an *a priori* vlPFC mask will need to be conducted to determine if the healthy > bipolar, *decrease negative (full)* > *look negative* contrast survives cluster correction (Figure 2A), as well as confirmation that there was no difference in amygdala reactivity between groups using an ROI approach on the healthy > bipolar *look negative (full)* > *look neutral* contrast maps. Finally, future directions may also include a psychophysiological interaction analysis as performed in the previous chapter.

Subject Demographics	**Control Subjs** (N=47)	**BP I Subjs** (N=42)
Age (μ ± SD)	38.9± 12 yrs.	40.5± 12 yrs.
Gender (M,F)	27,20	26,16
Duration of current euthymia (μ ± SD) °	-----	118 ± 295 wks
YMRS*	0.5 ± 0.95	1.8 ± 2.0
HAMD-21*	0.96 ± 1.2	4.0 ± 2.4
unmedicated lithium antipsychotic antidepressants anticonvulsant benzodiazapine	-----	24% 0% 64% 45% 43% 2%

YMRS=Young Mania Rating Scale; HAMD=Hamilton Depression Rating Scale
° = two outliers >1,000 wks included. * = two-sample T-Test p<0.05

Table 1. Demographic and clinical variables.

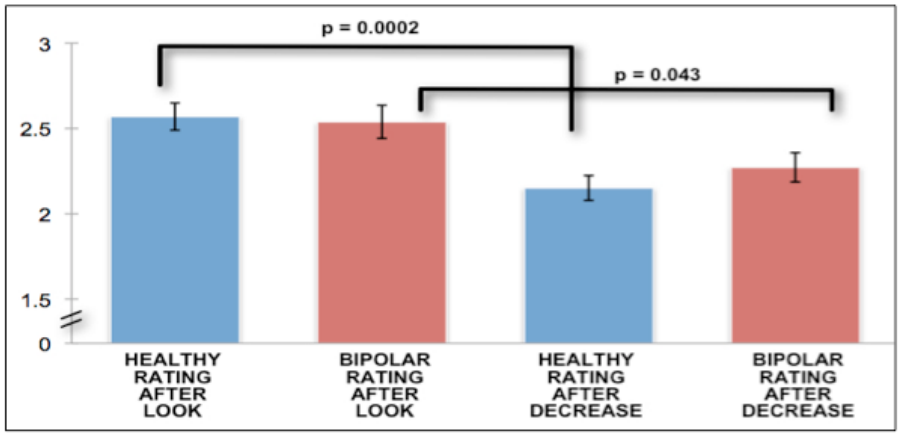

Self-reported negative affect. Scale 1-4. error bars: SEM. interaction: p=0.088

Figure 1. Averaged self-reported negative affect following look and decrease trials.

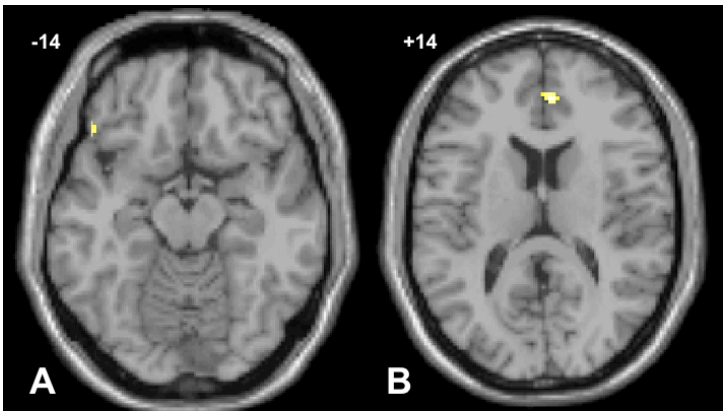

Figure 2. Between group reappraisal, healthy > bipolar. A: Hypoactivity in vlPFC in bipolar subjects. B: Hypoactivity in ACC in bipolar subjects. Both axial slices from *decrease negative (full)* > *look negative* contrast, visualized on a canonical T1-weighted brain. Left=Left.

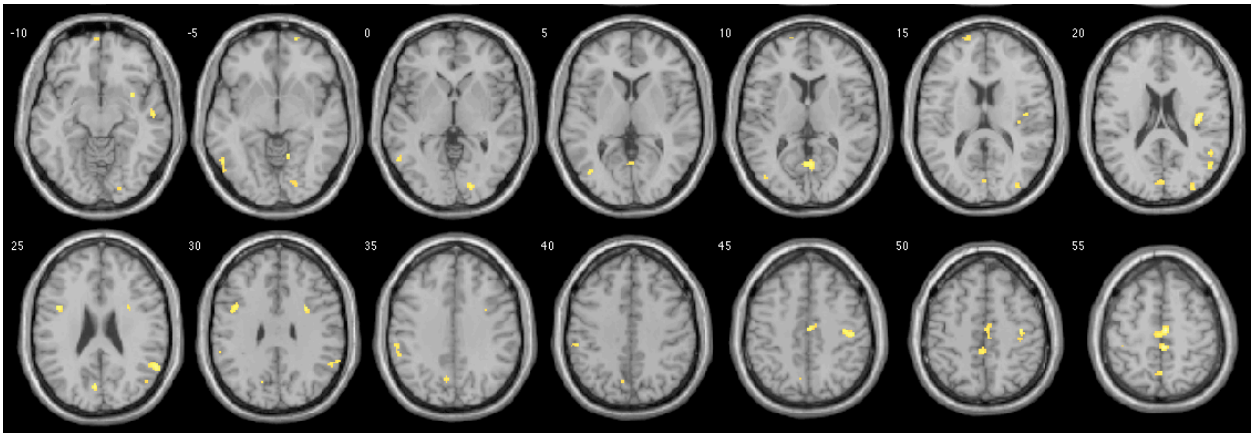

Figure 3. Healthy > bipolar, *decrease negative (early)* > *look negative* contrast. Left=Left, visualized on a canonical T1-weighted brain.

CHAPTER 4: Advancing understanding of affect labeling with dynamic causal modeling

Salvatore J. Torrisi[a], Matthew D. Lieberman[b], Susan Y. Bookheimer[c], Lori L. Altshuler[a]

Semel Institute for Neuroscience & Human Behavior, Dept. of Psychiatry, UCLA[a]; Department of Psychology, UCLA[b]; Center for Cognitive Neuroscience, UCLA[c]

Introduction

In this chapter we shift our orientation toward an effective connectivity technique, to investigate causal relations among brain regions, and to a form of implicit emotion regulation, to see if latent disfunction in a disease can be tapped via a task where the individual is not effortfully trying to regulate. Before including bipolar subjects in our analysis, however, this chapter focuses on the mechanics of affect labeling in the healthy brain.

The unique human ability to consciously control one's emotional experience also counts among the more difficult to execute. Nonetheless the psychology and neuroscience of explicit emotion regulation have been fruitfully studied for over two decades, yielding much understanding of the neural mechanisms of emotions and behavioral control (Gross, 2007). Neurobiologically, we are now aware of major prefrontal and emotional regions involved (Ochsner et al., 2012; Ochsner and Gross, 2005) and are beginning to understand the important connections between emotion regulation and health (DeSteno et al., n.d.). However, research has more recently suggested that there is a disconnect between self-reported use of explicit emotion regulation strategies and their spontaneous use in daily life (Gruber et al., 2012; Volokhov and Demaree, 2010). One reason for this may be due to the substantial cognitive resources and time required to enact such strategies (Mauss et al., 2006). As a result, research

on emotion regulation at a non-conscious level has emerged as an equally interesting and alternative avenue of investigation into how we commonly control our emotional experiences (Berkman and Lieberman, 2009; Koole and Rothermund, 2011).

By explicit emotion regulation we refer to strategies such as reappraisal of an emotional stimuli or suppression of an emotional response, while in contrast non-conscious emotion regulation (also called implicit or incidental emotion regulation) refers to those cognitive processes that result in the lessening of emotional reactivity and where this effect was not consciously intended by the person engaging in it (Lieberman et al., 2011). Although incidental emotion regulation at a non-conscious level cannot easily be self-reported, functional magnetic resonance imaging (fMRI) offers a window into the process. This technology can reveal the presence of incidental emotion regulation via lessened emotional reactivity and the extent to which prefrontal regions are recruited that overlap those used to explicitly control emotion (Burklund et al., 2012; Payer et al., 2012).

There are a variety of psychological paradigms currently being used to probe non-conscious forms of emotion regulation using fMRI (Berkman et al., 2009; Egner et al., 2008; Meyer et al., 2011). One frequently studied cognitive process is affect labeling (Hariri et al., 2000; Lieberman et al., 2007) which is gaining increasing evidence as a form of incidental emotion regulation (Kircanski, Lieberman, & Craske, 2012; Lieberman et al., 2011). This paradigm lies at the confluence of emotion, control, and language systems. Labeling emotional faces results in decreased amygdala response and the increased recruitment of prefrontal control and language regions, particularly the ventrolateral prefrontal cortex (vlPFC) in the right hemisphere and Broca's area (BA 44/45) in the left. To this end, a task-induced negative coupling between the activity in the amygdala and vlPFC has been shown using regression-based techniques (Foland-Ross et al., 2008; Hariri et al., 2000) and has been interpreted as a dampening of amygdala reactivity by the vlPFC. However, causal inferences using such

methods remain circumspect. To advance beyond the simple identification of activation patterns or the changes in coupling between only two regions one must use more sophisticated analyses (Friston, 2011).

In this study, we examined the nature of the vlPFC-amygdala coupling (specifically, the directed influences between these regions) during affect labeling, and additionally assessed the understudied contribution of Broca's area to amygdala activity. To do so we used Dynamic Causal Modeling (DCM), a validated and reliable Bayesian statistical framework for effective connectivity analysis which encourages the comparison of multiple user-defined models of causal interactions between a set of brain regions (Friston et al., 2003; Rowe et al., 2010; Schuyler et al., 2010). Ours is, to the best of our knowledge, the first application of this method to this common paradigm.

Materials and Methods

Subjects

Fifty-two healthy subjects were recruited as part of a larger study of emotion regulation in bipolar disorder by advertisement in local newspapers and campus flyers. They provided informed consent in accordance with the Institutional Review Boards at the University of California, Los Angeles (UCLA). All participants completed the Structured Clinical Interview for DSM-IV Structured Clinical Interview for DSM-IV Axis I Disorders (SCIDI/P; (First, 2002)). Exclusion criteria included any concurrent or past psychiatric diagnosis (including history of substance abuse), neurological illness, left-handedness, metal implants, a history of skull fracture or head trauma with loss of consciousness of more than 5 minutes, or taking any medications with psychotropic effects.

Experimental design

The affect labeling paradigm consisted of three experimental conditions: 'match facial affect,' 'label facial affect,' and 'match forms' (Figure 1) (Hariri et al., 2000). They were presented as nine experimental 30-second blocks: four displayed emotional faces and were interleaved with five control blocks displaying geometric forms. Of the four displaying faces, two required the subject to match a facial expression with one of two other facial expressions (*match faces* condition). Faces were shown with neutral or negative affect such as fear, surprise or anger. The other two blocks required subjects to choose one of two presented words (e.g., 'ANGRY', 'AFRAID') that best matched an emotional face (*label faces*). For each affect condition, 12 different faces were used, taken from a standard set of photographic stimuli (Ekman and Friesen, 1976). Each emotion was randomized across blocks and the order of task presentation was counterbalanced among subjects. Subjects responded with one of two buttons with their right hand and were told to answer "…as quickly as possible without making too many mistakes". Response times were collected and accuracy was calculated for each condition.

Image acquisition

All subjects were scanned on a 3T Siemens Trio scanner. A high resolution structural T1 MPRAGE was acquired with parameters of TR=1.9 seconds, TE=2.26 ms, Flip-Angle = 9°, Matrix = 256×256, FOV=250mm, voxel size 1mm isotropic, and total sequence time 6 minutes and 50 seconds. The fMRI scan was acquired using a T2*-weighted EPI gradient-echo pulse sequence with IPAT, with TR=2.5 seconds, TE = 25 ms, Flip-Angle = 78°, Matrix=64×64, FOV=192mm, in-plane voxel size 3×3 mm, slice thickness 3mm, 0.75mm gap, and 30 total interleaved slices. To allow for scanner equilibration, 2 TRs at the beginning of the scan were discarded. The total sequence time was 5 minutes and 45 seconds, with 135 volumes acquired. For co-registration we additionally acquired a matched-bandwidth structural scan with

parameters TR=5 seconds, TE=34 ms, Flip-Angle=90°, Matrix=128×128, FOV=192mm, in-plane voxel size 1.5×1.5mm, slice thickness 3mm, and a total sequence time of 1.5 minutes. We were not able to acquire MPRAGE scans for four subjects, so their lower resolution matched-bandwidth images were used instead for registration. Foam padding was placed around the heads of participants to suppress motion, responses were recorded by button box, and stimuli was presented by LCD goggles.

Image Preprocessing

All preprocessing and analyses were performed within SPM8/DCM10 (www.fil.ion.ucl.ac.uk/spm/). Subjects' functional volumes were slice-timing corrected (Descamps et al., 2007; Kiebel et al., 2007), then motion realigned, coregistered to the MPRAGE, normalized to a T1-weighted standard brain in MNI space, resliced 3mm isotropically, and smoothed with a 6mm FWHM gaussian kernel. All subjects had maximum translational head movement of less than 2.5mm, with means and standard deviations across subjects for three translation (x, y, z; in mm) parameters: 0.16(0.2), 0.10(0.11), 0.29(0.31) and three rotation (pitch, roll, yaw; in radians) parameters: 0.005(0.005), 0.003(0.004), 0.003(0.005).

First level (within-subject) analysis

First-level general linear modeling (GLM) of the preprocessed functional images included convolving task design blocks with a canonical hemodynamic response function, high-pass filtering at 128 seconds to remove low frequency drifts, adding six motion realignment parameters as covariates of no interest and specifying an F-statistical contrast for subsequent VOI extraction (i.e. when adjusting for effects of interest). The first level statistical maps were run twice; the second time with an explicit whole-brain mask derived from an optimal thresholding of the initial masks to ensure coverage of vlPFC (Ridgway et al., 2009).

Second level group GLM analysis

The standard mass univariate summary statistics approach was used to bring single-subject contrast images into a group random effects analysis. The contrast *label emotion vs match forms* was of interest to elucidate the incidental emotion regulation network while the contrast *label emotion vs match emotion* more specifically revealed those regions involved in labeling (thresholds: $p<0.0005$, cluster size 10 voxels; $p<0.05$ AlphaSim-corrected (http://www.restfmri.net/)). Furthermore, the contrast *match emotion vs match forms* robustly activates the amygdala and was used to guide functionally defined node extraction (see below).

Region of interest analyses

To demonstrate and confirm with our data the expected labeling-induced increase of right vlPFC activity with the decrease of right amygdala activity we performed region of interest (ROI) analyses on both these regions with independently defined anatomical masks. We brought a histologically-defined probabilistic right amygdala (Amunts et al., 2005) and a Tailarach Daemon right vlPFC (BA 47) mask into the MarsBaR toolbox (Brett et al., n.d.) across the 45 subjects that survived a time series extraction procedure (see below). For the amygdala the contrast *match emotion vs label emotion* was used to verify that its activity is significantly greater during matching emotional faces than during labeling emotional faces, while the reverse contrast was used to verify greater activity of vlPFC.

Dynamic Causal Modeling and model space construction

To perform a dynamic causal modeling analysis of a network one first selects nodes for which one has a priori knowledge and hypotheses, but bases the selection on GLM maps of significant task-induced activation. We chose four regions that were shown to be activated in the group *match emotion vs match forms* or *label emotion vs match forms* contrasts which we

hypothesized either launched the cognitive process (through visual input) or potentially caused the dampening of amygdala activity previously noted (Foland-Ross et al., 2008; Lieberman et al., 2007; 2005). These regions were the right inferior occipital gyrus (IOG), the right amygdala (both coordinates chosen at the individual subject level with the *match emotion vs match forms* contrast), the right ventral lateral prefrontal cortex (vlPFC; BA 47) and Broca's area (aka left posterior inferior IFG; pars triangularis; BA 44/45) (Figure 2 top row; both coordinates chosen at the individual subject level with the *label emotion vs match forms* contrast). Two of these regions, Broca's area and vlPFC, also appeared in the targeted *label emotion vs match emotion* contrast (Figure 2 bottom row), supporting their specific involvement in affect labeling over and above matching or perceiving affect. However, coordinates for the latter two nodes were not chosen at the individual subject level within this latter contrast because of a decrease in sensitivity. After choosing these four regions based on their response profiles to affect labeling, DCM then allowed us to advance our research question from *what* occurred regionally during labeling to *how* it occurred mechanistically.

Dynamic causal modeling is a Bayesian framework to infer effective connectivity between brain regions in a neural system of interest (Friston et al., 2003). The investigator specifies a given model (i.e. hypothesis) by assigning an endogenous architecture to the regions, the location(s) of a stimulus input that drives the system, and specifies which connections' couplings are modulated by a particular task condition. The evaluation of a model results in posterior parameter estimates on the model's uni- or bidirectional edges, as well as a 'score' of the model as a whole. The negative free energy approximation to the model evidence is the score used to compare multiple models (which constitute a model space) in a Bayesian Model Selection (BMS) scheme. The negative free energy value represents a balance between a model's goodness of fit to the data and the model's complexity which additionally takes into account interdependencies or covariances among parameters (Penny, 2012). Given a particular

network, a model space is generally a subset of all theoretically testable models built by the investigator to probe specific questions in a computationally pragmatic manner. The inferences one makes with DCM are therefore relative to the model space one tests. Multiple models can further be grouped into families (Penny et al., 2010), which contain a common element of interest and can be compared in this manner if one asks specific questions about that common element. Finally, one can test not only model architectures as a whole but specific connection strengths and their 'sign' (positive or negative) with Bayesian Model Averaging (BMA) (Penny et al., 2010) within a model family.

In service of these analytical options, we systematically constructed a factorial model space that embodied our neuroscientific assumptions and the hypotheses we wished to test. The basic model was constructed to investigate both forward and backward information propagation centered on the right amygdala. The presence of some connections among regions was held constant throughout all models while others were systematically permuted, resulting in eight basic patterns of endogenous connectivity (figure 3). Based on recent research on 'multiple routes' in the processing of written words, emotion and emotional faces (Dima et al., 2011; Pessoa and Adolphs, 2010; Richardson et al., 2011), we chose to keep the information propagation from IOG to right vlPFC constant across all models, along with the more obvious assumption of affective stimuli also entering the amygdala via IOG. The inclusion of IOG as the visual processing node, rather than, e.g. the fusiform face area, also follows previous theory and empirical research on the effective connectivity of face processing (Cohen Kadosh et al., 2011; Dima et al., 2011; Fairhall and Ishai, 2007; Haxby et al., 2000). By conflating the matching and labeling emotional faces conditions into a single regressor we specified the driving input to our models, which as such contained mostly face stimuli. However, one third of what a participant saw during these conditions were affective words, and so each model was also crossed with two driving input hypotheses (families): entering only at the right IOG or at both the right IOG

and the left Broca's Area. For the latter family it was assumed that language information entered previously via left hemisphere regions upstream from Broca's not explicitly included in our models. Naturally the same assumption applies to our choice of IOG, a higher-order visual processing region, however the degree of synaptic distance from sensory input is different between these regions. Finally, to investigate the specific changes in coupling that labeling affect engenders, our primary interest in this study, we created four families of amygdala afferent modulation. These were where labeling modulated either the Broca's to amygdala connection, the right vlPFC to amygdala connection, the Broca's to Amygdala *via* right vlPFC pathway (i.e. these two connections simultaneously) or all three of these directed edges simultaneously. This resulted in an 8(endogenous) × 2(driving) × 4(modulatory) = 64 element model space, where each model was separately estimated for all 45 subjects.

Time series extraction

The peak coordinates of these four volumes of interest (VOIs) as observed in the second level group maps were the right IOG [42 -82 -16], right amygdala [24 -4 -13], right vlPFC [42 23 -7], and left Broca's Area [-57 20 23], located within the *label emotion vs match forms* contrast (figure 2A). Left Broca's area and right vlPFC were also shown in the language specific contrast *label emotion vs match emotion* (figure 2B). Within each subject we then manually chose peak coordinates around these group peaks within anatomical constraints and within a threshold of $p<0.05$ uncorrected overlaid on the subjects' own normalized structural images (Leff et al., 2008). Because the quality and extent of a given region's atlas representations are quite variable (Bohland et al., 2009), we chose those anatomical reference tools we reasoned would optimize our selection for a particular region in our tested network. Threshold-crossing subject-specific activations were thusly considered within the IOG if they conformed to the Harvard-Oxford probabilistic atlas, within the amygdala or Broca's Area (BA 44/45) if they conformed to the Jülich histological/probabilistic atlas (Eickhoff et al., 2005) and within the vlPFC (BA 47) if

they conformed to the Tailarach Daemon (www.talairach.org) after non-linear coordinate conversion from MNI to Talairach space (www.bioimagesuite.org). All subject-specific coordinates were also within 15mm Euclidean distance of the group peak (supplemental figure 1). If any region for a given subject did not pass any of these constraints they were eliminated from the study. Seven subjects were lost in this manner, which produced our final subject pool of 45 subjects. All DCM and ROI results are based on this group (Table 1 for demographics). Finally, the principal eigenvariate time series was extracted from each peak, adjusted for effects of interest, within a 5mm radius sphere.

Model Comparisons and Bayesian Model Averaging

Our first DCM model comparison step was to exploit the factorial nature of our space and compare two large model families that differed only in the anatomical locations of the driving inputs. We chose to run a random-effects (rfx) bayesian model selection because we could not assume that the optimal model was uniformly used by each individual in our group (Stephan et al., 2010). We looked at a given family or model's exceedance probability, which is the probability of a particular model being more likely than any other model in the space. Exceedance probabilities across all models sum to 1, providing a relative measure of fit specific to one's model space. We then performed rfx BMS on the winning half of the model space and included the BMA procedure. BMA averaged the connectivity parameters within each subject's 32 models, weighted by their posterior probabilities, which yielded estimates for their strength and directions in the form of posterior distributions (means and standard deviations) at both the subject and group levels. Because we tested 11 parameters of interest (8 endogenous plus 3 modulatory) we applied Bonferroni correction (α= 0.05/11= 0.0046) to two-tailed, one-sample tests.

Correlations with behavioral measures

To explore the potential connection between the strengths of subject-specific effectivity connectivity parameters with behavioral measures, we ran correlations with reaction time and percent accuracy with the parameter estimates from BMA. We applied Bonferroni correction for multiple comparisons to these tests as well.

Results

Behavioral data

All participants performed at a high level of accuracy for both the match emotion and label emotion conditions (Table 1).

GLM analysis

As predicted, second level group GLM maps for the contrast of interest *label emotion vs match forms* replicated previous work by demonstrating a number of known regions activated by the affect labeling paradigm: most prominently bilateral occipital and fusiform regions, amygdalae, vlPFC, dlPFC (BA 6), a medial region of the superior frontal gyrus (BA 8), Broca's area and posterior superior temporal sulcus (Wernicke's Area; BA 22) in the left hemisphere (Figure 2a and supplemental table 1A). The more targeted contrast *label emotion vs match emotion* revealed that a subset of these regions responded specifically to the linguistic stimuli (Figure 2b and supplemental table 1B). After elimination of 7 subjects due to node finding for DCM all GLM second level analyses were re-run and the results were marginally less robust but consistent with those of the primary analysis (supplemental figures 2A, 2B).

For the region of interest analyses the *match emotion vs label emotion* contrast was used to confirm that activity within the amygdala during matching emotion was significantly greater than during labeling emotion (t=2.0, p=0.026 corrected). The reverse contrast *label*

emotion vs match emotion was used to confirm that activity within the vlPFC during affect labeling was significantly greater than during affect matching (t=2.37, p=0.011 corrected).

DCM analysis

Comparing families of models

We first split our model space to determine the better of two general hypotheses regarding the driving input to affect labeling (Penny et al., 2010), i.e. whether the driving input was best modeled as entering the right IOG alone or in conjunction with the left Broca's area. Random-effects bayesian model selection showed that the family with driving input entering only at the right IOG strongly won over the family where the driving input entered additionally at the left Broca's area (respective posterior means: 0.9493, 0.0507; exceedance probabilities: 100%, 0%).

Comparing individual models (BMS) and Bayesian Model Averaging (BMA)

The family-level result allowed us to focus on the winning family of 32 models in a comparison using rfx Bayesian Model Selection. This would help answer further questions: (1) are any of the three permuted connections especially important to the basic model structure? (2) If so, which connections are? (3) Does affect labeling produce significant changes in regional coupling over endogenous coupling? (4) If so, which connections are significantly modulated?

We found model 1 to outperform the other models with an exceedance probability of 22% (Figure 4). This model had a basic endogenous architecture without any of the three permuted connections (Figure 3, template 'a') and with modulation under affect labeling targeting the Broca's area to amygdala connection. Model 17 was the second-best model with an exceedance probability of 17%. In this model the same endogenous architecture as model 1 is present, although labeling modulates the Broca's area to amygdala *via* vlPFC pathway.

However, neither of these modulatory hypotheses emerged as very clear winners at the BMS level, i.e. if we calculate the ratio of model posterior means between these two models (their Bayes Factor) we return 0.0804/0.0685=1.1737, which constitutes weak evidence in favor of model 1 (Penny et al., 2004). However, what emerged from this 32-model comparison was that the third and fourth strongest winning models also possessed that basic endogenous architecture that lacked amygdala afferents and the vlPFC to Broca's projection (Figure 4, asterisks). In other words, while the top four models were dissimilar in the location of modulation under labeling, they all shared an identical endogenous architecture (Figure 3, template 'a'), seemingly providing strong support about the best-fit endogenous architecture of the labeling task. To quantify this observation we next 'post hoc' grouped our model space into eight families of those endogenous architectures. Of these, the family with the first model's architecture strongly won the Bayesian model comparison with a family posterior mean of 0.479 and exceedance probablity of 88% (supplemental figure 3). As a parallel, exploratory analysis we also performed BMA (see below) on this smaller group of models and the main results below did not change (supplemental Table 2).

For greater insight into our main apriori interest of labeling-induced modulation of regional coupling we looked at the results of our Bayesian model averaging (BMA) of the 32 models that won the family-level driving input test. This provided subject and group-level posterior distributions for the endogenous and modulatory parameters. For a given parameter, i.e. a directed edge between two regions, we performed two-tailed, one-sample T-tests for significance on their mean values. Four endogenous connections survived Bonferroni correction: the IOG projections to amygdala and vlPFC as well as the bidirectional connections between vlPFC and Broca's area (Table 2; Figure 5). With the exception of the Broca's area to vlPFC connection, all of these values were positive, meaning that an increased rate of a source region's neural population-level activity results in an increase in the neural population-level

activity of its target. Finally, the modulatory effect of affect labeling showed the right vlPFC to right amygdala influence to be very significantly negative, meaning we can infer that an increased rate of vlPFC activity under the labeling condition causes a decrease in the rate of amygdala activity ($p<0.0001$). The modulatory effect of labeling showed Broca's area to also significantly decrease the rate of amygdala activity, albeit not as strongly as the vlPFC. Finally, the Broca's to vlPFC modulatory connection was found to be significantly negative, but did not survive correction. In sum, affect labeling appears to induce a dampening effect across the corticolimbic network where one of these connections becomes *more negative* under modulation than its endogenous coupling (Broca's to vlPFC) and the other two couplings (vlPFC to amygdala and Broca's to amygdala) become significantly negative where there was previously no significant endogenous coupling present.

DCM parameter correlations with behavior and external variables

There were no significant correlations between BMA parameter estimates and reaction time or percent accuracy.

Discussion

To our knowledge, the current study is the first application of an effective connectivity technique to investigate causal neural interactions during a task of affect labeling, a paradigm acquiring increasing evidence as a form of incidental emotion regulation. By including a strongly language-involved brain region in our network modeling we have advanced a mechanistic understanding of what occurs while 'putting feelings into words' and, namely, how the often-replicated observation of decreased amygdala activity may arise. Our findings reinforce common interpretations of previous regression and correlation-based analyses of vlPFC-amygdala negative connectivity, however they both solidify and extend them, as dynamic causal

modeling permits stronger claims about causal interactions and allows the testing of multiple connections simultaneously.

As predicted, we found the right vlPFC *to* right amygdala connection to be strongly modulated, negatively, by labeling facial affect. This means that during this task the vlPFC exhibits a dampening effect on the activity of the amygdala that is not endogenously present but rather manifests during the labeling of affect. The DCM model results additionally support a causal role for Broca's area during labeling affect, in that its involvement directly and negatively modulates the amygdala as well, and may additionally indirectly modulate the amygdala *via* the vlPFC. We also found strong evidence at the model level of the data supporting a most minimal endogenous architecture. Taken together, our results demonstrate that the most significant regulatory effect on amygdala originates from the right vlPFC, yet also present are weaker but nonetheless substantial labeling-induced contributions from Broca's area to both the amygdala and to the vlFPC. Finally, we found that the endogenous connection from IOG to vlPFC that we modeled was strongly supported by our data, corroborating recent work on parallel routes for the visual processing of facial affect (Dima et al., 2011; Pessoa and Adolphs, 2010).

This study has several limitations. It is only practical to test a small number of nodes with Dynamic Causal Modeling, and although this is common practice, we may have missed crucial players in the network that forms the basis of affect labeling. The dampened amygdala activation observed could additionally be caused or mediated by the left middle temporal gyrus (Wernicke's Area; BA 22) or the medial superior frontal gyrus (BA 8) which were both shown as active in the *label emotion vs match emotion* GLM contrast (supplemental Table 1). Future DCM studies of affect labeling should systematically add these regions as other nodes to tested models, as well as the contralateral homologues of the regions investigated here. Additionally, other areas implicated by previous research may be important to this regulatory network. For example, in animal models ventromedial PFC activity has been demonstrated to dampen

amygdala activity (Quirk et al., 2003) or mediate its dampening in humans (Lieberman et al., 2007). Other incidental emotion regulation paradigms have additionally shown increases in rostral anterior cingulate cortex (Berkman and Lieberman, 2009; Cohen et al., 2011), however, our task did not significantly recruit either the vmPFC or rACC, where significant recruitment is required for node inclusion in DCM analyses (Stephan et al., 2010).

As for brain regions whose effective connectivity we did investigate, the vlPFC and Broca's area were revealed in the targeted contrast *label emotion vs match emotion* and yet they are both regions that have been studied in cognitive contexts other than affect labeling. For example, and as previously mentioned, the right vlPFC has more broadly been considered a candidate mechanism for self-control of several types, as it additionally activates during many tasks of response inhibition, risk-taking (gambling) and temporal discounting (delaying gratification) (Cohen et al., 2011). Additionally, the right vlPFC has been implicated in attentional switching (reflexive reorienting) (reviewed in Levy and Wagner, 2011), although the relation of this function to our affect labeling paradigm is unclear. The vlPFC has also been implicated in language studies, and in particular the processing of semantic information, however the evidence more strongly suggests hemispheric lateralization to the left (Dapretto and Bookheimer, 1999; Noesselt et al., 2003; C. J. Price, 2012). To this end we did observe bilateral vlPFC activation in the *label emotion vs match emotion* contrast (supplemental Table 1) and so we may speculate that the left vlPFC could be processing semantic (affect-related) aspects of affect labeling while the right vlPFC acts as a regulating mechanism. Our paradigm, however, precludes more targeted contrasts or factorial interactions to better tease apart these relations. Likewise, Broca's area is a heterogeneous region (BAs 44/45) that has been studied in multiple contexts, most prominently as serving multiple sub-functions of affect-neutral language processing (extensively reviewed in (C. J. Price, 2012). Therefore, given their known functional heterogeneity, our study offers greater understanding of how to interpret the changing roles of

these regions given a “neural context” of affect labeling (Henson, 2005; McIntosh, 2004).

In sum, the present study investigated causal mechanisms ostensibly responsible for the effect of greater vlPFC and dampened amygdala during tasks of affect labeling, and in doing so helps situate affect labeling within a broader context of emotion regulation (Gyurak et al., 2011). While there are overlaps between the mechanisms and effects of explicit and incidental forms of emotion regulation, the latter offers advantages to evoking this cognitive process less directly. For instance, explicit emotion regulation paradigms, such as reappraisal, additionally test an individual’s *capacity* to regulate their emotions following a set of directed instructions. As such, the subject’s capability of quickly and creatively producing a scenario that achieves the desired goal is tested along with their regulatory abilities. In contrast, regulation of emotion that occurs incidental to intentionally instructed goals may reflect an individual’s *tendency* to regulate more automatically in domains outside the laboratory (Berkman and Lieberman, 2009). Following this logic, if incidental emotion regulation lends insight into an individual’s tendency to regulate, be it genetic or learned, it may also be used to probe ‘latent’ disfunction caused by, or reflective of, disease states such as post traumatic stress disorder, anxiety, or mood disorders. In the case of affect labeling, for example, research has already been conducted with spider phobic subjects and suggests a pronounced effect in mitigating fear responses by labeling affect versus cognitive reappraisal (Kircanski et al., 2012; Tabibnia et al., 2008). Future behavioral and neuroimaging work leveraging an individual’s tendency to spontaneously regulate emotion with incidental emotion regulation strategies and the ability for this to additionally inform disorders characterized by deficits in emotion regulation will be highly valued.

Figures and Tables

Figure 1. Affect Labeling paradigm. (A) Match emotion condition (B) label emotion (C) match geometric forms. (Hariri et al., 2000)

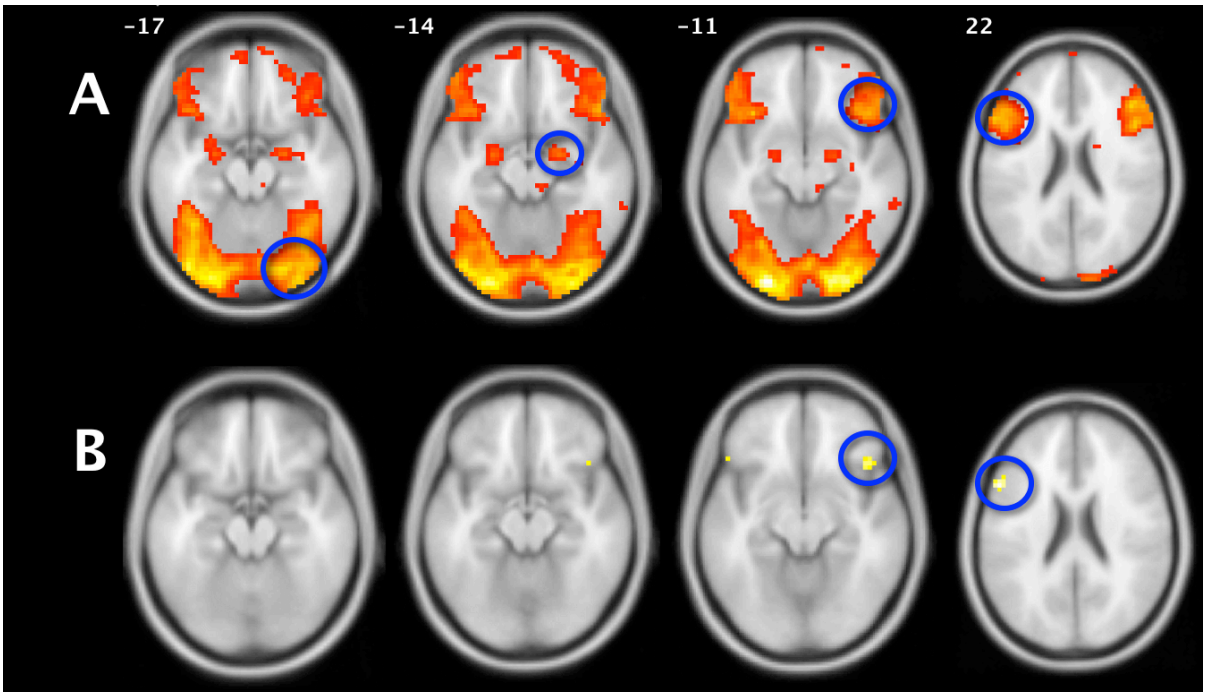

Figure 2. (A) *Label emotion vs Match forms*. The map (N=52) used to determine node peak selection, (four peaks circled) before the loss of seven subjects due to node extraction. (B) *Label emotion vs Match emotion*, the targeted affect labeling contrast. See supplemental Table 1 for cluster-specific information. Axial slices (R=R) at indicated Z coordinates overlaid on standardized brain in MNI space. Both maps $p<0.0005$, $k=10$.

demographics and behavior

N=45	
Age	41.9 (12.1)
Gender	20F 25M
Years education	15.5 (2.2)
Race	
Caucasian	34 (76%)
African American	9 (20%)
Asian	2 (4%)
match emo accuracy	0.94 (0.09)
match emo RT (sec)	2.09 (0.51)
label emo accuracy	0.84 (0.08)
label emo RT (sec)	2.01 (0.47)

Table 1. DCM subject demographics (mean and SD) and behavior during task.

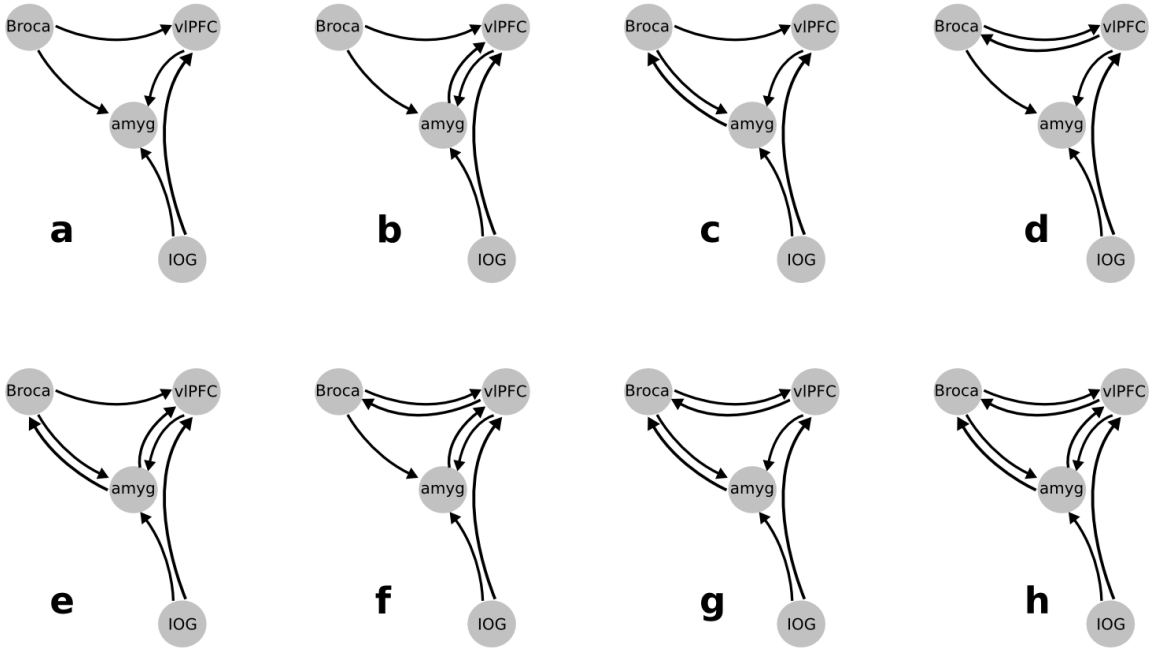

Figure 3. Eight templates of endogenous connectivity in schematic axial slice orientation. These were crossed with 2 different driving input and 4 different modulatory hypotheses, creating a 64-element model space.

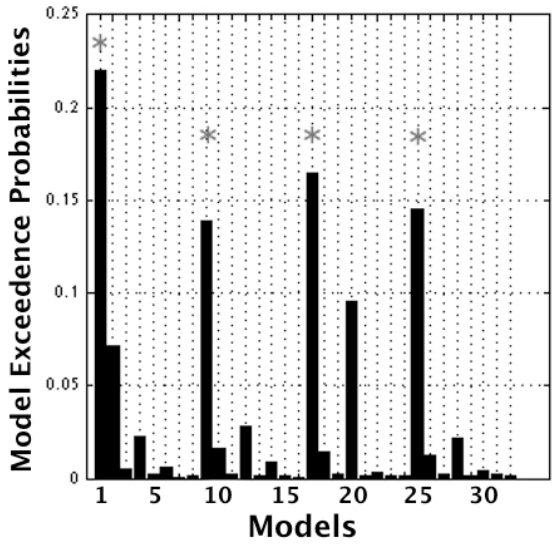

Figure 4. Bayesian Model Selection for 32 models from the winning driving input family (input to lOG). Asterisks above the four models with the highest exceedance probabilities.

BMA results

Endogenous	**Mean**	**SD**	**P Value**	
lOG to Amyg	0.17	0.11	0.0000000110	**
lOG to vlPFC	0.15	0.10	0.0000001550	**
Amyg to vlPFC	0.04	0.10	0.0336	*
Amyg to Broca's	0.03	0.07	0.0124	*
vlPFC to amyg	0.00	0.18	0.9549	
vlPFC to Broca's	0.20	0.09	0.0013	**
Broca's to amyg	-0.03	0.20	0.2228	
Broca's to vlPFC	-0.11	0.20	0.0038	**
Modulatory				
vlPFC to amyg	-0.27	0.12	0.0000000173	**
Broca's to amyg	-0.06	0.11	0.0013	**
Broca's to vlPFC	-0.09	0.10	0.0090	*

Table 2. Parameter-level results (as distributions) from Bayesian Model Averaging across 32 models and 45 subjects. SD = standard deviation. **Bonferroni corrected, *p<0.05 uncorrected.

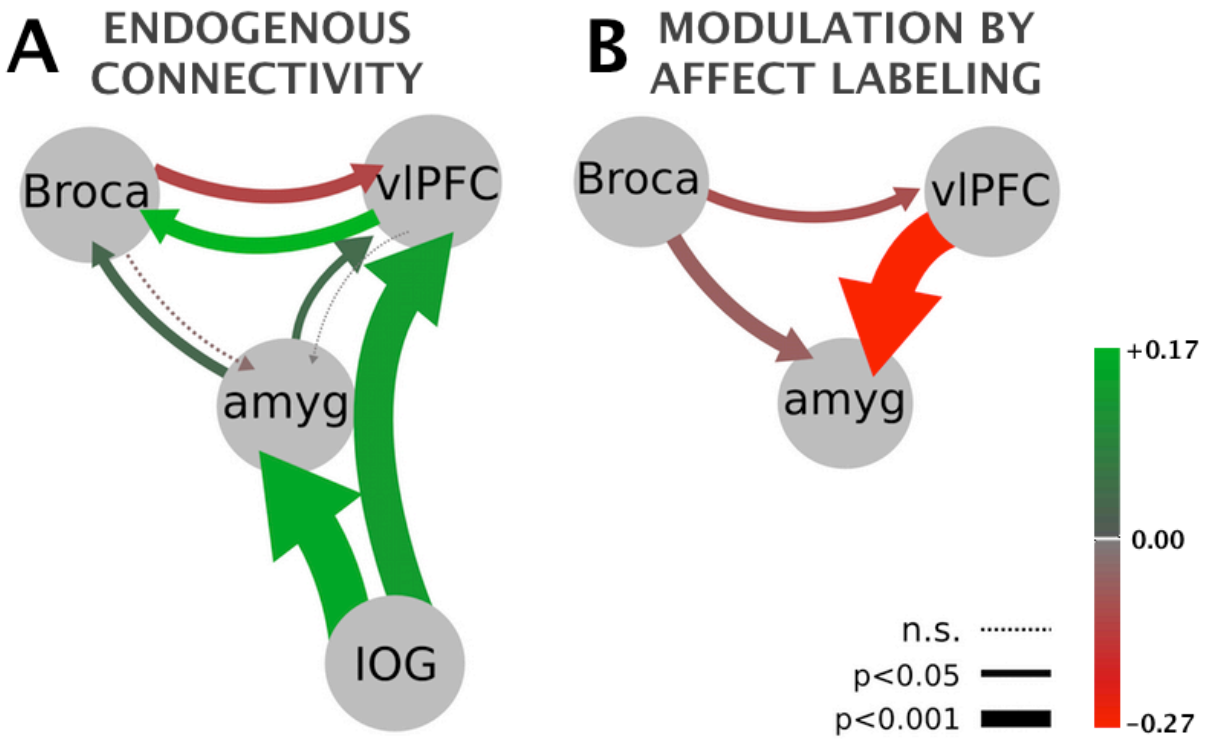

Figure 5. Graphic depiction of Bayesian Model Averaging results (Table 2). Color saturation values map to mean effective connectivity parameters (in hertz) while arrow thickness maps to statistical significance proportional to *log(1/p-value).* (A) Endogeneous connectivity. (B) Modulation of connectivity by affect labeling representing the three tested connections. Due to the basic bilinear DCM equation the modulation values add to the endogenous values. Driving input (not shown graphically) enters the IOG in both states.

Supplemental Material:

52 subjects:

(A) label emotion vs match forms

p<0.0001, k=10

		BA	cluster P (FWE)	cluster size	peak Z	MNI x,y,z {mm}
L	Inferior Occipital Gyrus	18	0	3997	Inf	-24 -97 -7
R	Inferior Occipital Gyrus	18			Inf	27 -97 2
R	Lingual Gyrus	18			Inf	21 -91 -7
L	Insula	13	0	1770	Inf	-33 23 -1
L	IFG: pars opercularis	44/45			7.73	-54 17 32
L	Middle Frontal Gyrus	6			7.71	-45 2 47
L	Superior Frontal Gyrus	8	0	885	7.8	0 17 56
L	Superior Frontal Gyrus	8			7.1	-6 29 47
L	Superior Frontal Gyrus	8			6.99	-3 38 47
R	MFG: pars triangularis	46	0	1571	7.56	45 29 23
R	MFG: pars opercularis	44/45			7.56	51 20 32
R	Ventral Lateral IFG	47			7.52	42 20 -7
R	Thalamus		0	73	6.91	24 -31 2
R	Thalamus				4.59	6 -28 -1
R	Cerebellum: Culmen				4.39	9 -28 -13
L	Thalamus		0.003	22	6.17	-18 -34 -1
R	Amygdala		0	44	5.67	21 -7 -13
R	Amygdala				4.9	27 -4 -19
L	Middle Temporal Gyrus	22	0	162	5.66	-54 -31 -4
L	Middle Temporal Gyrus	22			5.39	-60 -43 -1
L	Middle Temporal Gyrus	39			5.28	-48 -49 5

L	Amygdala		0	38	5.47	-24 -7 -13
L	Amygdala				4.53	-27 2 -16
R	Middle Temporal Gyrus	22	0	99	5.33	57 -40 -1
R	Middle Temporal Gyrus	22			4.9	48 -46 8
R	Middle Temporal Gyrus	37			3.89	63 -43 -13
L	Superior Parietal Lobule	7	0	55	4.8	-33 -64 47
L	Middle Occipital Gyrus	7			4.39	-30 -67 38
R	Thalamus		0.052	10	4.5	6 -13 5
R	Angular Gyrus	7	0.052	10	4.15	33 -64 47

(B) label emotion vs match emotion

p<0.0005, k=10

		BA	cluster p (FWE)	cluster size	peak Z	MNI x,y,z {mm}
L	IFG: pars triangularis	44/45	0.001	49	4.77	-54 17 26
L	IFG: pars triangularis	45			4.35	-51 26 17
L	Middle Temporal Gyrus	22	0.05	21	4.69	-66 -31 5
L	Middle Temporal Gyrus	22			4.14	-69 -40 2
L	Cingulate Gyrus	32	0.001	46	4.61	-3 26 38
L	Superior Frontal Gyrus	8			4.19	-6 29 47
R	Ventral Lateral IFG	47	0.085	18	4.59	42 20 -7
L	Middle Frontal Gyrus	6	0.03	24	4.59	-45 11 50
L	IFG: pars triangularis	44/45	0	60	4.57	-54 20 -1
L	Ventral Lateral IFG	47			4.5	-42 35 -4
L	Ventral Lateral IFG	47			3.58	-48 44 -4
L	Superior Frontal Gyrus	6	0.003	38	4.44	-3 8 65
L	Superior Frontal Gyrus	6			4.12	-12 14 65
L	Superior Frontal Gyrus	8	0.001	44	4.41	-6 41 44

L	Middle Temporal Gyrus	21	0.011	30	4.4	-51	-31	-4
L	Middle Temporal Gyrus	39			3.89	-48	-49	5
R	Inferior Parietal Lobule	40	0.05	21	4.37	54	-58	44
L	Superior Frontal Gyrus	6	0.011	30	4.25	-21	26	59
L	Superior Frontal Gyrus	6			3.8	-12	32	59
R	Superior Frontal Gyrus	6	0.013	29	4.15	6	29	62
R	Superior Frontal Gyrus	8			3.72	15	32	56
R	Superior Frontal Gyrus	9	0.085	18	3.97	3	44	35
L	Superior Frontal Gyrus	9	0.149	15	3.9	-6	56	35

Supplementary table 1. Voxel-level results from general linear model analysis, corresponding to Figure 2 of main text. (A) Label emotion vs match forms contrast. (B) Label emotion vs match emotion contrast. BA = Brodmann's area.

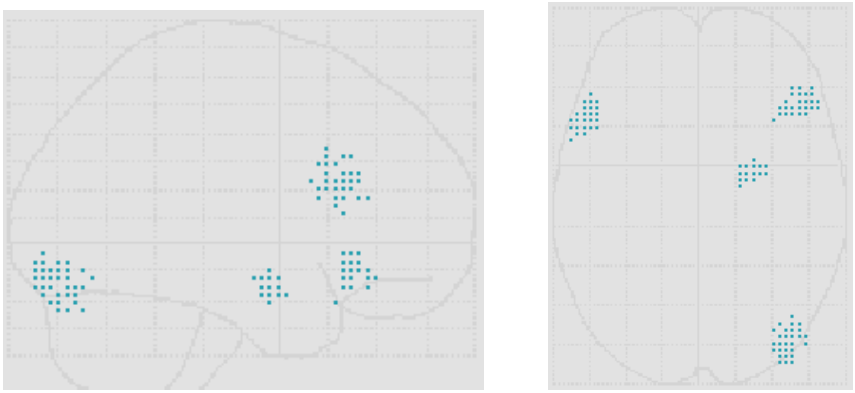

Supplementary figure 1. Sagittal (left) and axial (right) glass brain projections of the locations of all coordinate peaks specific to each individual in the DCM analysis (N=45). Peaks chosen after reslicing during normalization. *Mip_maker.m* visualization tool courtesy of Darren Gitelman. Means and (SDs) for each region are IOG = [X: 39.7 (4.2), Y: -82 (5.4), Z: -15 (5.2)]; AMYG = [X: 22 (3.1), Y: -3.7 (2.8), Z: -16 (2.8)]; vlPFC = [X: 45.2 (4.7), Y: 27 (3.8), Z: -9.3 (3.9)]; Broca's area = [X: -54 (3.6), Y: 21.3 (4.8), Z: 23.2 (5.3)].

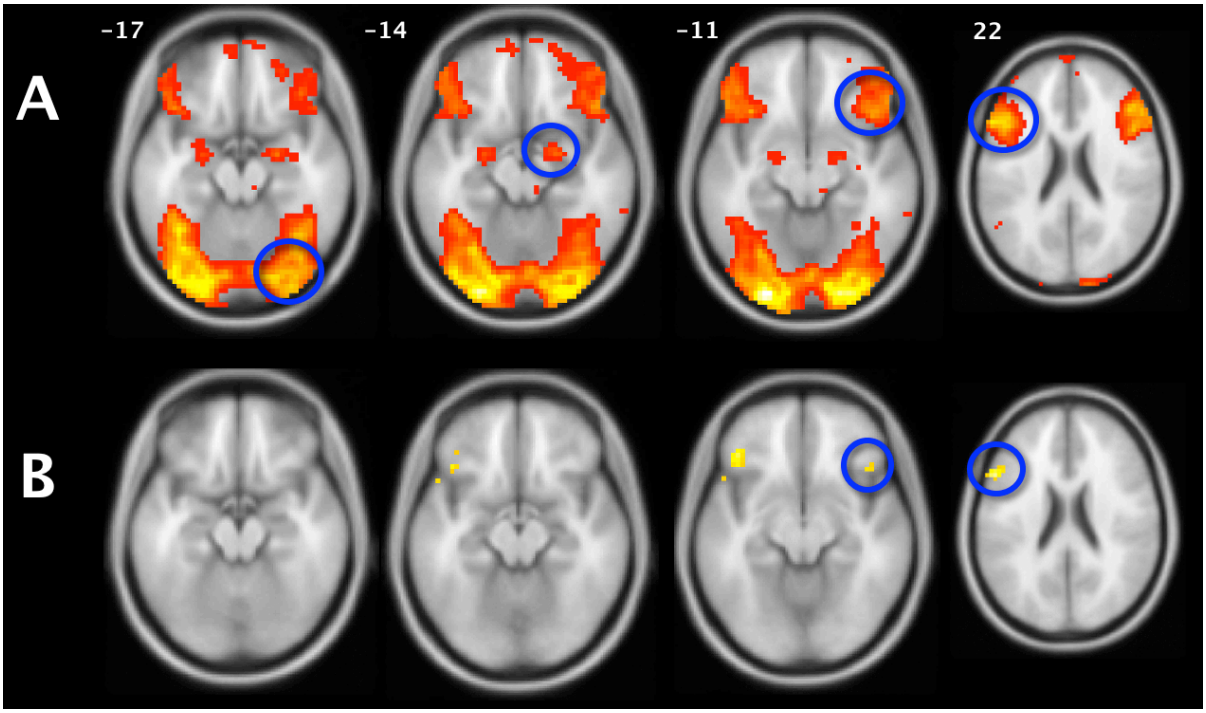

Supplementary figure 2. N=45 subjects, after removal of seven, i.e. the subject pool that the DCM and ROI analyses were performed with. (A) GLM contrast *Label emotion vs Match forms*. (B) GLM contrast *Label emotion vs Match emotion*. Both maps p<0.001, k=5.

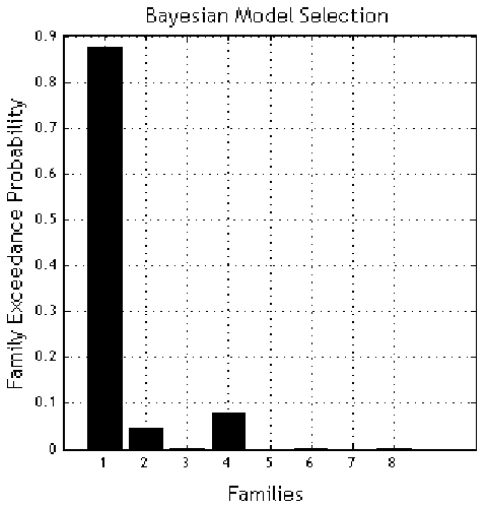

Supplementary figure 3. Post-hoc, family-level Bayesian Model Selection of 32 models (the driving input winning half of the original model space) grouped by endogenous architecture. Each family contained 4 different models of modulation. BMS demonstrates that model family 1 wins, with the most minimal endogenous architecture (see main text Figure 3a), with an exceedance probability of 88%

BMA of winning endogenous connectivity family:

endogenous	**mean**	**sd**	**p value**	
lOG to Amyg	0.1933	0.11	0.000000004	**
lOG to vlPFC	0.1137	0.10	0.0000000005	**
vlPFC to amyg	-0.0992	0.18	0.0277	*
Broca's to amyg	0.0043	0.21	0.0775	
Broca's to vlPFC	0.0073	0.21	0.0033	**
modulatory				
vlPFC to amyg	-0.2588	0.11	0.000000008	**
Broca's to amyg	0.0017	0.12	0.1672	
Broca's to vlPFC	0.0002	0.10	0.7795	

Supplementary table 2. Parameter-level results (as distributions) from Bayesian Model Averaging of the 4 models within the winning endogenous connectivity family following a post-hoc BMS procedure (figure 3). sd = standard deviation. **Bonferroni corrected, *p<0.05 uncorrected.

CHAPTER 5:

Effective connectivity alterations in bipolar disorder during affect labeling

Salvatore Torrisi[a], Nathalie Vizueta[a], Susan Y. Bookheimer[c], Lori L. Altshuler[a]

Semel Institute for Neuroscience & Human Behavior, Dept. of Psychiatry, UCLA[a]; Department of Psychology, UCLA[b]; Center for Cognitive Neuroscience, UCLA[c]

Introduction

The ability to characterize a brain network not only by its functional connections but additionally by the directed influences among those connections gives us a finer degree of "resolution" through which to see pathophysiology in a psychiatric disease. Because bipolar disorder is considered in part a disorder of emotion regulation (Phillips et al., 2008a; Townsend and Altshuler, 2012), probing this particular network may yield insights into which connections are aberrant. If we know these connections, then we know where to look for changes under different conditions such as mood state (which may assist the diagnostic process) or talk or pharmacological therapies (to track the success of and even guide treatments).

Labeling with words one's own affect or the affect within a stimulus has been shown for some time to cause largely the same self-reported and neural effects that forms of explicit emotion regulation produce. For example, subjects report feeling less negatively after labeling a stimulus and consequently have *less* amygdala activity but *more* activity in prefrontal control (and language) related regions. Therefore it is useful to probe potential network dysfunction in bipolar disorder with this seemingly innocuous task of implicit emotion regulation.

Our work in this chapter directly builds on the previous one. In this chapter we investigate differences in brain activity and connectivity between healthy subjects and subjects

with bipolar disorder while they label emotional facial expressions. We hypothesized that we would observe weaker vlPFC *to* amygdala negative connectivity in bipolar subjects relative to healthy subjects during a task of affect labeling. We began by using the standard fMRI analysis method to find activation differences and then went one step farther with the dynamic causal modeling (DCM) method to probe model and parameter-level differences in the bipolar brain. We constructed a large dynamic causal model space because they are advantageous when the true underlying functional network is not precisely understood. DCM procedures such as bayesian model averaging exploit the benefits of large model spaces through weighted averages over parameter results. This increases one's confidence in the final averages. Finally, we address some of the issues and difficulties that arise from the application of this novel method to this fMRI paradigm.

Materials and Methods

Participants provided written and informed consent in accordance with the Institutional Review Boards at UCLA and the Veterans Affairs Greater Los Angeles Healthcare System. Subjects with bipolar disorder type I (BP; N=48) were recruited through the outpatient UCLA Mood Disorders Clinic, the outpatient Bipolar Disorders Clinic of the VA Greater Los Angeles Health Care System and through local advertising in the community. Healthy control subjects (HC; N=53) were recruited by advertisement in newspapers and campus flyers. All participants were first interviewed using the Structured Clinical Interview (SCID) (First, 2002) for DSM-IV to confirm a bipolar diagnosis or absence of. Participants with bipolar were excluded if they met criteria for any other current Axis I disorder. Other exclusion criteria are listed in the previous chapter. Demographic and clinical variables of the healthy and bipolar groups are given in Table 1. There were no significant differences in age or gender between groups.

All bipolar subjects' fMRI data were identically preprocessed and analyzed as the healthy subjects' data. The GLM procedure up through the first levels, time series extractions

and model space construction for the DCM procedure were all described in detail in the previous chapter and so are not repeated here. First-level GLM maps were brought to a random effects group level for between-group comparisons using 2-tailed, 2-sample t-tests. Between-group second level maps were thresholded at $p<0.001$, $k=20$. For the dynamic causal modeling analysis it should be noted that manual coordinate-finding for each node was performed blind to diagnosis for the work in both chapters. There were no significant differences in the six head motion parameters during scanning between groups, either before or after subject removal. In addition, there were no significant differences in MNI coordinate locations of the four nodes between groups (individual peaks were also chosen in relation to 2nd level peaks in pooled group maps). See Appendix 2 for a two group DCM protocol. Finally, two-tailed, two-sample t-tests were performed between groups for each of the 11 tested model parameters (e.g. a particular directed connection such as Broca's area to vlPFC) as estimated by Bayesian Model Averaging (BMA).

Results

Second level between-group GLM analyses revealed significant hypoactivation in the right vlPFC in the bipolar subjects (Figure 1). This cluster was in a slightly more anterior and lateral position than the right vlPFC cluster that was chosen with both groups' *label emotion vs match forms* contrast images pooled. Both peaks, however, were within the general region "ventrolateral prefrontal cortex" as labeled by standard atlases. The bipolar subjects also demonstrated hyperactivation in the ventromedial PFC, as indicated in Table 2.

The dynamic causal modeling analysis was performed in three stages. First, the family level 'driving input' division (half of the original 64-element model space) yielded the same winner in the bipolar subjects as the healthy controls (right IOG only; exceedence probability=100%, not shown). In stage two, bayesian model selection (BMS) was performed among those winning 32 bipolar models. These results, along side the healthy subject BMS

results, are shown in Figure 2. The same four model pattern was shown with the bipolar subjects (i.e. the endogenous architecture winner, see chapter 4, figures 3a and supplemental figure 3), although one model additionally stood out (#28) as being more highly preferred by the bipolar than the healthy subjects (Figures 2 and 3, red arrow; see also Figure 4). We performed post-hoc exploratory correlations between the posterior probabilites of this model across the bipolar subjects and some of their clinical variables (HAMD, YMRS, years ill, weeks euthymic, etc) and found no significant correlations. The third stage, using BMA, also yielded no significant differences between groups for any of the 11 model parameters.

Discussion

The current study was the first dynamic causal modeling analysis of bipolar subjects using a large model space. We tested for differences between groups of euthymic bipolar and healthy subjects in their network functional architecture and connectivity of a four-node subnetwork of affect labeling, a form of implicit emotion regulation. At the activation level we observed hypoactivation in the bipolar subjects in their right vlPFC during labeling, relative to the control subjects. At the DCM model level we observed a difference in model preference, one which contains as its endogenous architecture a structure that is more connected than the main winning architecture. In other words, with this model there is back propogation in its endogenous architecture from vlPFC to Broca's area, something we saw very little preference for in the healthy subjects' BMS results. This might be considered a kind of functional "hyperconnectivity" in the bipolar subjects, something our group found with a group of much the same subjects while simply resting (see chapter 6). However, DCM and resting state results should not be expected to mirror each other (Rehme et al., 2013). Some researchers have stated that different winning models between patient and control groups is an interesting finding in itself (Seghier et al., 2010). Unfortunately, however, probing this model for correlations to

subject-level clinical variables yielded no significant results and so the value of this model-level finding as an index or marker of bipolar pathophysiology is currently unclear.

Limitations and Future Directions

There are a number of limitations and considerations with this study. Some of these involve issues of general interpretability and comprehension of the DCM method and will be discussed in greater detail in chapter 7, while others are more specific to the current study. The major issue is as follows: between-group GLM results revealed a weakened right vlPFC in the bipolar subjects during affect labeling, and yet there appears to be no weakening of the connections to or from this node in the DCM parameter-level analysis. How is this seemingly paradoxical situation possible? In the following sections we speculate on a few potential explanations.

Our first is that the DCM vlPFC node chosen (based on pooled data) and the between-group vlPFC GLM results are actually in different functional sub-regions. The vlPFC is a neuroanatomical area whose functional and structural heterogeneity has been acknowledged and studied (Carmichael and J. L. Price, 1995; Chiavaras et al., 2001), but for which we human neuroimagers currently have few standardized tools with which to work. It could be that we would have detected parameter level differences if we had picked the DCM nodes based on the between-group GLM map. This may have produced an error of “double dipping”, of course, and would have also made the manual node-choosing unblind. Using anatomical masks, for example, may have alleviated the issue of a biased or different location, but then, for example, would have skirted DCM authors’ recommendation that coordinates be specifically chosen based on activation to one’s task (Stephan et al., 2010). These kinds of best-practice procedural details still need to be worked out in the DCM community.

Another explanation for the paradox could be that the statistics used for the between-group BMA comparison were suboptimal, and that a non-parametric Wilcoxon rank-sum test would be preferable (Eickoff, 5/17/13; personal communication). We plan to follow up on this. We also acknowledge that the between-group effects we hypothesized to find may be rather subtle and therefore could be undetectable by DCM, which has built-in conservative and generally un-adjustable "shrinkage priors" that require strong effects in the data to overwhelm them (Friston et al., 2003).

An explanation for the null results of clinical variable correlations with the model (BMS) level results is that the posterior probability measurements for each model for each subject are highly abstract values that are difficult to correlate with the more concrete measures of clinical variables (but which are also susceptible to different kinds of noise). Careful consideration of which clinical variables would be most appropriate to connect to the strength of the evaluation of a model as a whole would be highly valued. We may eventually find that model-level posterior results are simply too far removed from the underlying biology that finding linear correlations between them is impossible. The posterior results are, after all, a variational free energy approximation to the model evidence (Penny, 2012), which is an estimation of how probable the observed data is given a model ($p(y|m)$). Strength of probability in this context might mean more, therefore, if the underlying model is already known in advance (e.g. as with our current neuroscientific knowledge of most sensory processes). In contrast, the DCM approach we took, using a large model-space designed to capture the most probable configurations of a network, is still more exploratory than perhaps it should ideally be to correlate model-level results with clinical variables. Nonetheless there remain potential exploratory analyses to be perforrmed here, including using these subject-specific matrices of posterior model probabilities as inputs to a cluster analysis blind to diagnosis.

Finally, we may have found no results at the BMA parameter level between groups simply because the subjects were in the euthymic state. While a number of researchers have observed differences in the euthymic bipolar brain, that does not imply that all aspects of their brains are abnormal at all times, or that even if the abnormality existed in a known area or connection would we observe its functionality affected in a directly corresponding manner. As previously mentioned, our laboratory has collected and published on data using this labeling task on all three mood states in bipolar, type I. Therefore our “null” BMA results may be better couched within a larger, future study that tests the effective connectivity in this network across depression and mania as well.

Figures and Tables

Final Subject Pool (6 BP and 8 HC removed)	**Bipolar I** (N=42)	**Control** (N=45)
Age (μ ± sd)	42.5 ± 12	41.9 ± 12
Gender (M , F)	25 , 17	25 , 20
Duration euthymic	33 ± 42 wks	-----
YMRS	1.7 ± 2	-----
HAMD-21	3.6 ± 2.5	-----
No medications Antipsychotics Antidepressants Anticonvulsants (valproic acid,lamotrigine)	10 (24%) 5 (12%) 26 (62%) 19 (45%)	-----

Table 1. Demographics for Dynamic causal modeling. YMRS = Young Mania Rating Scale; HAMD = Hamilton Depression Rating Scale.

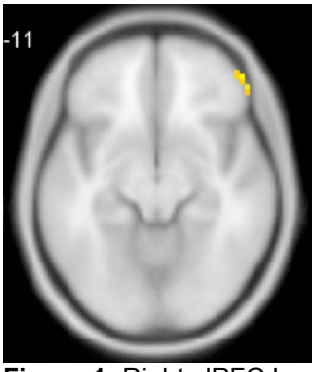

Figure 1. Right vlPFC hypoactivity in bipolar subjects: GLM contrast of healthy > bipolar for *label emotion vs match forms*. Axial slice at -11 z MNI level, visualized on MNI averaged brain. N= 53HC and 48BP subjects, before node finding. p<0.001, k=20.

Label vs Forms	**Region**	**Cluster size**	**Z stat**	**Voxel unc**	**Cluster p**	**MNI coords**
HC > BP	R vlPFC	21	3.62	0.000	0.048	51 47 -10
	R BA 8	27	3.88	0.000	0.028	9 32 53
BP > HC	vmPFC	31	3.26	0.001	0.02	12 35 -13
	L BA 9	21	3.88	0.000	0.048	-30 50 35

Table 2. Between group GLM contrasts. N= 53HC and 48BP subjects, before node finding.

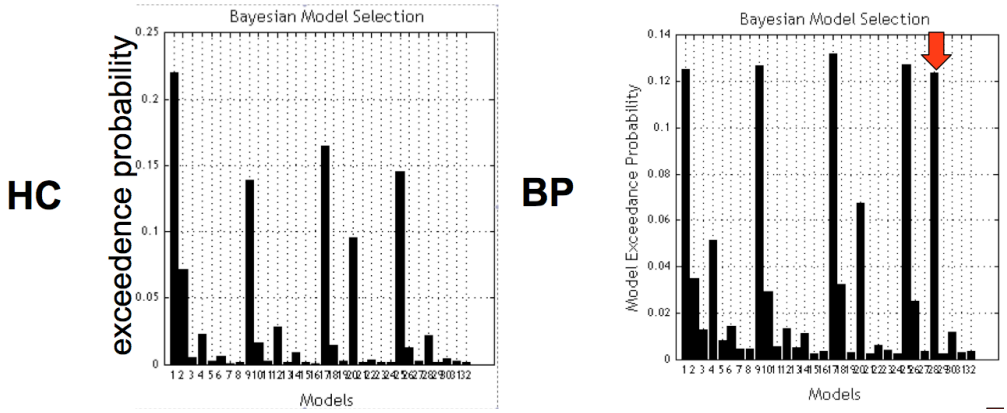

Figure 2. Two group DCM bayesian model selection results. N= 45HC and 42BP subjects, after node finding. On right: red arrow points to model #28 with substantially greater probability among the bipolar than the healthy subjects.

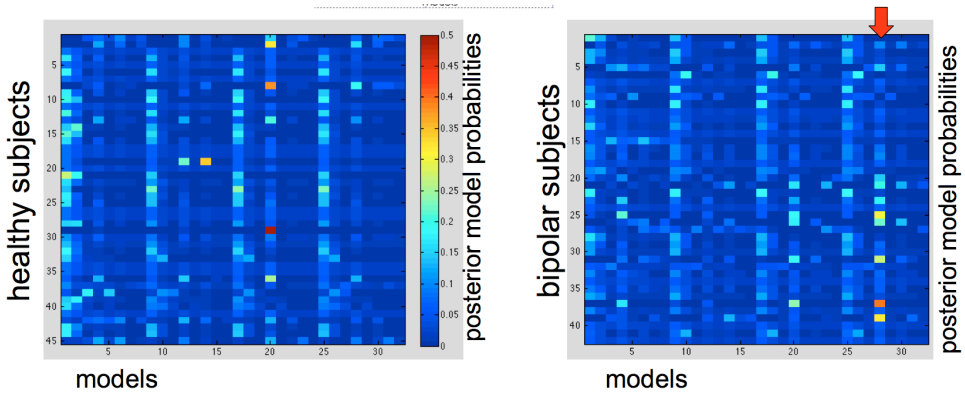

Figure 3. Two group subject-specific posterior model probabilities (the data summarized in Figure 2). On right, red arrow points again to model 28.

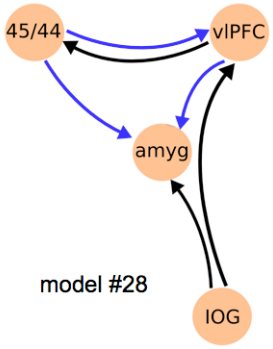

Figure 4. Graphic of the model that stands out as particularly different between healthy and bipolar subjects.

CHAPTER 6: Differences in Resting Corticolimbic Functional Connectivity in Bipolar I Euthymia

Salvatore Torrisi[a], Teena D. Moody[d], Nathalie Vizueta[a], Moriah E. Thomason[b], Martin M. Monti[c], Jennifer D. Townsend[a], Susan Y. Bookheimer[d], Lori L. Altshuler[a]

Semel Institute for Neuroscience & Human Behavior, Dept. of Psychiatry, UCLA[a];
Dept of Pediatrics, Wayne State University School of Medicine[b];
Department of Psychology, UCLA[c]; Center for Cognitive Neuroscience, UCLA[d]

Introduction

After the previous literature reviews of the emotion regulation network, its dysfunction in sample populations with bipolar disorder, and our own results showing differences in activation and connectivity between healthy indviduals and those with bipolar disorder in this network, we have gained confidence for knowing, *a priori*, which regions to particularly focus on. This chapter therefore takes a region-of-interest approach to investigating these areas in the resting brain. Resting state analyses generally focus on a lower end of the frequency spectrum than task-based analyses do, giving them a separate but equally valuable place in the neuroimaging field. Their ease of acquisition is additionally a benefit to those researchers interested in studying psychiatric populations, such as bipolar disorder.

Bipolar disorder (BP) is a serious psychiatric illness thought to involve deficits in the neural substrates for emotion regulation because of its characteristic profile of lifetime depressed and manic mood episodes (Green et al., 2007; Phillips et al., 2008a). Neuroimaging research in healthy subjects has revealed a number of brain areas involved in emotional regulation, including subcortical (e.g., amygdala) and ventrolateral prefrontal cortical (vlPFC) regions (Lieberman et al., 2007; Ochsner et al., 2004). Research in both humans and primates has additionally demonstrated strong anatomical projections between these areas, forming the

substrate for which functional coupling (connectivity) is possible (Ghashghaei and Barbas, 2002; J. L. Price and Drevets, 2009). The amygdala, for example, is functionally responsive to emotional stimuli, while the vlPFC is instrumental in the regulation of that response. In healthy subjects, during down-regulation of emotion, the functional connectivity between these areas has been observed to increase (Banks et al., 2007; Hariri et al., 2000).

The above referenced fMRI studies of emotion regulation involve observation of brain activity while subjects perform a task. Recent studies that have evaluated subjects while not performing any cognitive tasks –-e.g. resting state studies-- have also revealed intrinsic activation patterns in the brain. Resting state fMRI provides complementary information to task-based fMRI in that both provide a platform for examining functional brain networks. Spatially distributed large-scale brain networks can be reliably derived and interrogated by either kind of fMRI experiment (Biswal et al., 1995; Smith et al., 2009; Van Dijk et al., 2010) and one could argue that both contribute different dimensions to a full characterization of brain activity. A variety of methods have been used to analyze such data (Fox and Raichle, 2007) and have been applied to diverse clinical populations in the effort to delineate disease-related dysfunctions in connectivity (Fox and Greicius, 2010).

While there are a handful of studies that have investigated functional connectivity in bipolar disorder, few are resting state studies (Table 1). Of these, there is some overlap with the regions used as seeds such as the medial prefrontal cortex (Anand et al., 2009; Chai et al., 2011b) or amygdala (Cerullo et al., 2012; Chepenik et al., 2010) but the findings show differences in connectivity in lateralization (left or right hemisphere), sign (positive or negative coupling) and between group differences (HS > BP or BP > HS). Three of these studies investigated bipolar mania and/or depression (Anand et al., 2009; Cerullo et al., 2012; Chai et al., 2011b), however one combined several mood states into its bipolar sample (Chepenik et al., 2010) while another combined bipolar subtype (type I and II) (Anand et al., 2009). This latter

issue is particularly problematic as there is evidence to suggest that patterns of activation and connectivity change with different mood state and subtype of BP (Cerullo et al., 2012; Townsend et al., 2010; Vizueta et al., 2012b). For a clearer picture of the underlying pathophysiology of bipolar disorder further research is necessary which investigates common regions in both hemispheres in single mood states and in single bipolar subtypes.

The goal of the present resting state study was to elucidate differences in intrinsic functional connectivity that might contribute to mood lability in bipolar disorder type I. We therefore took a focused approach to assessing connectivity in two bilateral brain regions strongly implicated in emotion regulation (four regions in total: right and left amygdalae and right and left vlPFC) in a group of euthymic bipolar type I subjects. We hypothesized that subjects with bipolar disorder would demonstrate aberrant functional connectivity relative to healthy subjects between amygdalae and lateral ventrolateral PFC - regions that subserve emotion regulation. Furthermore, observed alterations of brain connectivity during the euthymic state may be considered a potential biomarker of trait aspects of the disease.

Methods and Materials

Participants

Participants provided written informed consent in accordance with the Institutional Review Boards at UCLA and the Veterans Affairs Greater Los Angeles Healthcare System. Subjects with bipolar disorder, type I, were recruited through the outpatient UCLA Mood Disorders Clinic, the outpatient Bipolar Disorders Clinic of the VA Greater Los Angeles Health Care System, and through local advertising in the community. Healthy subjects were recruited by advertisements in local newspapers and campus flyers. All participants were first interviewed using the Structured Clinical Interview (SCID) (First, 2002) for DSM-IV to confirm a bipolar diagnosis or absence thereof. Participants with bipolar were excluded if they met criteria for any

other current Axis I disorder. Healthy subjects were excluded if they had a current or past psychiatric diagnosis (including history of substance abuse) or were taking any medications for medical reasons. Additional exclusion criteria for all participants included left-handedness, neurological illness, metal implants, and a history of skull fracture or head trauma with loss of consciousness of more than 5 minutes.

In total, 21 bipolar and 26 healthy subjects (HS) were scanned. Mood symptoms were evaluated in all participants on the day of the scan, using the Young Mania Rating Scale (YMRS; (Young et al., 1978)) and the 21-item Hamilton Depression Rating Scale (HDRS; (Hamilton, 1960)) to assess for any symptoms of mania or depression. Participants were considered appropriate for this study if they had a YMRS score of < 7 (BP: 1.9±1.9; HS: 0.74±1.19, p=0.03), a 21-item HDRS score of < 7 (BP: 3.55±2.5; HS: 0.79±0.9, p<0.001) and had been euthymic by self-report and by SCID for at least 1 month prior to scanning.

Following the removal of seven subjects due to excessive head motion, 20 bipolar (10f, age 42.1±11.4 yrs) and 20 (10f, 39.8±12.6 yrs) age (p=0.55) and gender matched (p=1.0) healthy subjects were included in the final analysis. Based on their age at first episode, they had been ill an average of 22.7±11 years and currently euthymic an average of 34.5 ± 38.9 weeks. Length of formal education was 14.1±1.9 years for bipolar subjects and 15.6±2.1 for healthy subjects. Employment rate was 10% for bipolar subjects and 95% for healthy subjects. Three (15%) of these bipolar subjects were unmedicated and had been off medications for ≥ 2 months. The remaining 17 subjects were on a range of medications including, antipsychotics (15%), antidepressants (75%), and anticonvulsants (valproic acid: 25%, lamotrigine: 20%).

Image Acquisition

Subjects were scanned on a 3T Siemens Trio scanner. They were asked to rest with eyes closed during the scan but to not fall asleep. A structural T1 MPRAGE was acquired with

parameters of TR=1.9 seconds, TE=2.26 ms, Flip-Angle = 9°, Matrix = 256x256, FOV=250mm, voxel size 1mm isotropic, and total sequence time 6 minutes and 50 seconds. The resting state fMRI scan was acquired using a T2*-weighted EPI gradient-echo pulse sequence with IPAT, with TR=2 seconds, TE = 25 ms, Flip-Angle = 78°, Matrix=64x64, FOV=192mm, in-plane voxel size 3x3 mm, slice thickness 3mm, 0.75mm gap, and 30 total interleaved slices. To allow for scanner equilibration, 2 TRs at the beginning of the scan were discarded. The total sequence time was 7 minutes and 2 seconds, with 208 volumes acquired.

fMRI Analysis

Following slice-timing correction of functional volumes, we performed motion realignment, gray matter/white matter/cerebral spinal fluid structural segmentation, normalization of both structural and functional scans to MNI space, 3mm isotropic voxel re-slicing, and 6mm FWHM Gaussian smoothing. To perform the statistical analysis we used the CONN-fMRI functional connectivity toolbox, version 12.p (www.nitrc.org/projects/conn(Whitfield-Gabrieli and Nieto-Castanon, 2012)), built on SPM8 (www.fil.ion.ucl.ac.uk/spm/).

Head movement can be a serious confound with resting state studies because it can introduce spurious correlations across the brain (Power et al., 2011; Van Dijk et al., 2010). We took several precautions to ensure that it would not be a factor in our results. First, at a gross level subjects were excluded if they had translational movement greater than 1 voxel (3mm). Second, we tested whether the maximum head motion values (three translation and three rotation) were different between groups and we found no differences (all p-values > 0.05). Third, for each subject we calculated two different combinations of the six motion parameters that indicated total displacement (TD) along the scan or framewise displacement (FD; i.e. scan-to-scan). Both metrics took into account each subject's individual head sizes to accurately assess the effects of rotation (Wilke, 2012). We tested whether there were differences between groups

for these metrics as well. TD did not differ between groups (BP: μ=0.69±0.3, HS: μ=0.89±0.5, p=0.14) but FD did (BP: μ=0.14±0.07, HS: μ=0.1±0.04, p=0.01). Therefore subject-specific FD mean values were added as a separate covariate of non-interest during subsequent analysis and was found to exert no significant influence on the final reported results.

To account for movement and other noise confounds during the preprocessing of the functional images, and to avoid known issues with regressing out the global signal (Murphy et al., 2009), the CONN-fMRI toolbox uses the anatomical component correction (aCompCor) method of flexibly removing physiological noise and movement confounds on a voxel-by-voxel basis (Behzadi et al., 2007; Chai et al., 2011a). The aCompCor approach enhances the sensitivity and specificity of positive correlations and can reveal non-artifactual anticorrelations. We used this method to regress out 5 principal components from the noise regions of interest (ROI) obtained from the anatomical segmentation as well as the six realignment parameters and their first temporal derivatives for each subject. The functional scans were further band-pass filtered between 0.01 and 0.1 hertz (100 to 10 second cycles) to investigate low frequency correlations, which are most consistently produced within this range (Van Dijk et al., 2010).

The CONN-fMRI toolbox implements a default set of (eighty-eight) Tailarach Daemon masks that may be augmented by additional regions of interest. Thus, although the present study was mainly concerned with a focused set of connectivity pairings, the averaged time series from each of 88 cortical and 2 subcortical anatomical ROIs across the brain were extracted and bivariate Pearson correlations were calculated from each of these time courses at the voxel-level. The two additional subcortical ROIs added to the default Tailarach Daemon masks were the 75% probabilistic Harvard-Oxford's left and right amygdalae (Harvard Center for Morphometric Analysis).

We performed an analysis among regions of interest (ROI-to-ROI) by calculating statistics for all possible connections for a selected subset of ROIs (right and left amygdalae, right and left BA 47). This effectively performs a small volume correction on (Fischer-transformed) correlation values by setting the FDR correction to assure that only 5% or less of significant effects could be false positives. Results from this ROI-to-ROI analysis were then checked at the whole brain level to confirm that they were not driven by a very small number of voxels (the ROI-to-ROI analysis works on the averaged time series of all voxels within the ROI). For this whole-brain (seed-to-voxel) analysis the amygdala was chosen as the seed region from the bi-directional right amygdala-vlPFC finding from the ROI-to-ROI analysis (see results below) to allow comparison with other studies that used the amygdala as a seed in connectivity analyses during rest (Chai et al., 2011b; Chepenik et al., 2010) and in studies of emotion regulation (Foland-Ross et al., 2008; Hariri et al., 2000; Townsend et al., 2013). The toolbox creates T-statistic volumes, which were brought into SPM8 for whole-brain investigations of within and between-group maps. A voxel statistical height threshold of $p<0.001$, $k=10$ with a cluster height of $p<0.05$ was used to identify significant correspondences between right amygdala whole-brain connectivity in the within and between-group contrasts. These results were then tabulated (Table 3), with anatomical and Brodmann labels automatically determined by the Tailarach Client (www.talairach.org/client.html) after nonlinear coordinate conversion (www.bioimagesuite.org). These labels were then checked and revised against a probabilistic Anatomy toolbox (Eickhoff et al., 2005) and an atlas in MNI space (Oishi et al., 2011).

For confidence that findings in the tested model were not simply a reflection of global differences between the bipolar and healthy subject groups, we ran additional analyses between brain areas in which we did not expect to observe connectivity differences between groups. Specifically, we tested correlations of a number of primary sensory areas with the rest of the brain and compared groups.

Post-hoc associations between correlation values of right amygdala-vlPFC functional connectivity and patient course of illness variables (illness duration, number of depressive and manic episodes) and clinical variables (HAMD and YMRS scores) were assessed through correlations and 2-tailed T-Tests with right amygdala to right vlPFC beta values. These beta values were extracted from each bipolar subjects' individual ROI correlation matrices. Prior to conducting these correlational analyses, an outlier correction was applied in which outlying connectivity parameter estimate values were winsorized to a value of 2.5 standard deviations from the group mean as in recent fMRI work (Vizueta et al., 2012a). These correlations were performed in PASW version 18.0 (SPSS Inc; Chicago, USA).

To explore regions outside our *a priori* model that may have driven our within-group bipolar functional connectivity results, a 'connectivity conjunction map' of two different statistical maps was performed – the map of whole brain correlations with the right amygdala and the map of whole brain correlations with right vlPFC -- using the toolbox xjView (www.alivelearn.net/xjview8/). Strong correlations common to both connectivity maps outside our regions of interest were identified by conjunction (i.e. a logical AND), with each map individually set at $p<0.0001$, $k=10$. A third brain region was identified in this manner and was included in a group-level mediation analysis, along with the amygdala and vlPFC nodes, to determine whether that region was responsible for a full or partial mediating effect on the main results. The mean times series from the third region was extracted from each of the bipolar subjects- preprocessed and filtered as the other ROIs- and was included as the mediator in a mixed effects group level mediation analysis. Regressions for the mediation analysis were performed in four steps (Baron and Kenny, 1986) using the all-in-one model described by Beckmann and colleagues which retains the variance of each subject throughout (C. F. Beckmann et al., 2003).

Results

Figure 1a shows the main region of interest ROI-to-ROI model investigated, with the six labeled functional correlations between the four a priori nodes (left and right amygdalae and left and right vlPFC). Figure 1b shows the between group ROI-to-ROI positive connectivity result in graphical form. Only the connection "IV" (right amygdala with right vlPFC) survived FDR multiple comparison correction ($T(38)=3.07$, FDR $p=0.024$). Adding head movement measurements TD and FD as covariates of non-interest left this result virtually unchanged (TD: $T(37)=2.93$, FDR $p=0.035$; FD: $T(37)= 2.74$, FDR $p=0.028$). Table 2 lists the within and between group results for this ROI-to-ROI analysis. The strength of within group connectivity between all nodes survived FDR correction in both groups with the exception of weaker V (R amygdala with L vlPFC) and VI (L amygdala with R vlPFC) connections in healthy subjects ($p<0.05$, FDR corrected). There were no whole brain connectivity differences between bipolar and healthy subjects in primary somatosensory (BA 1), auditory (BA 41, 42), or visual (BA 17) regions.

As stated, whole brain connectivity from the right amygdala seed was also assessed to confirm that the ROI-to-ROI results were not driven by a very small number of voxels, as is possible when averaged time series are extracted from an anatomical mask. Figures 2a and 2b (top and middle rows) show within group axial slices, while figure 2c shows the between group contrast (circled cluster size =11 voxels, cluster $p<0.05$; peak at MNI: [51 41 -8], $p<0.0001$, $Z=3.52$). Consistent with the ROI-to-ROI result our between group results (BP>healthy subjects) confirmed significant hyperconnectivity between the right amygdala and right vlPFC, but also revealed significant regional hyperactivity between a number of other regions such as the right and left medial frontal gyri (BAs 10 & 11, respectively), the right superior temporal gyrus (BA 41) and the precentral gyrus (BA 6). Table 3 lists these within and between group right-amygdala-to-whole-brain connectivity results.

We found no significant correlations between right amygdala with right vlPFC connectivity and any of the five illness or clinical variables collected (illness duration, number of depressions, number of manias, HAMD and YMRS scores). We also checked for medication effects on connectivity parameter estimates to make sure our few unmedicated bipolar subjects were not actually outliers driving our results.

Finally, we conducted a post-hoc test for possible 'third' regions outside our model that may have driven, through mutual coupling, our right amygdala with right vlPFC result in the bipolar subjects. A significant cluster in the anterior cingulate cortex (ACC; BA 32, center of gravity [1.9 44 0.63]) was found to be strongly and positively functionally connected to both the right amygdala and the right vlPFC using the 'connectivity conjunction map' procedure (Figure 3a). We constructed our mediation model with the ACC mediating the influence of vlPFC to amygdala, which is what we hypothesized based on previous regression-based connectivity analyses of these regions (Foland-Ross et al., 2008; Hariri et al., 2000). A diagram and group-level betas for the analysis are shown in Figure 3b. We found the ACC to partially mediate the influence of vlPFC on the amygdala and this mediation effect was significant with the Sobel test (Z=7.88).

Discussion

Bipolar disorder is associated with a trait dysregulation of the corticolimbic network (Green et al., 2007; Phillips et al., 2008a), which may in turn result in fluctuations of mood states over time. Here we investigated the corticolimbic network using a focused, seed-based correlation analysis of resting state data in one mood state of one subtype of BP. Our results demonstrate an altered intrinsic connectivity in euthymic bipolar type I compared to healthy subjects between brain regions vital for emotion regulation. Specifically, we observed hyperconnectivity of the right hemisphere vlPFC (BA 47) and right amygdala in BP and its

partial mediation by the anterior cingulate cortex. Here 'hyperconnectivity' refers to greater positive correlations in low-frequency fMRI signal in one group than a reference group (Whitfield-Gabrieli et al., 2009), which in this case are healthy subjects. Our within-group maps clearly support this difference in magnitude; subjects with bipolar disorder have greater positive connectivity between these two regions in comparison to healthy subjects (figures 2b and 2a). Additionally, we found this resting hyperconnectivity elsewhere in the BP brain between amygdala and, for example, the ACC and the middle frontal gyrus (BAs 10 and 11) (see also Table 3).

One interpretation of our hyperconnectivity result is that functional coupling between vlPFC and may be especially sensitized in bipolar disorder and that this may contribute to or reflect the characteristic mood lability of the disease. Whether this sensitization stems from differences in right hemisphere white matter structural connections is unclear and warrants further research (Honey et al., 2010). The lateralization of differences of brain coupling in BP also warrants further exploration and replication in general, however what we report here is consistent with prior neuroimaging research documenting right lateralization for emotion-processing effects (Noesselt et al., 2005).

The present findings are also consistent with four other studies in bipolar subjects that have shown increases in seed-based connectivity between or involving at least one of these regions. For example, hyperconnectivity, as measured by mutual information, has been observed in bipolar disorder between ventromedial PFC and right amygdala while labeling sad facial expressions (Versace et al., 2010). During a psychophysiological interaction, hyperconnectivity was observed in BP subjects between right vlPFC and insula (Pompei et al., 2011), and during rest hyperconnectivity was observed during mania between medial and ventrolateral PFC (Chai et al., 2011b) as well as between left and right ventral PFC in a variety of mood states (Chepenik et al., 2010) (c.f. Table 1.)

We also found that an area of the anterior cingulate cortex (ACC; BA 32) was significantly coupled with both right amygdala and right vlPFC. The ACC is known to have anatomical and functionally reciprocal connections with the amygdala within humans (M. Beckmann et al., 2009; Bracht et al., 2009; Stein et al., 2007), has been strongly implicated in mood disorders (J. L. Price and Drevets, 2009), and has been found by one group to mediate the coupling between right vlPFC and amygdala during incidental emotion regulation (Lieberman et al., 2007). The functional connectivity between the ACC and the amygdala has been found by another group to be decreased in bipolar disorder relative to healthy subjects during the processing of fearful and happy faces (Wang et al., 2009). Therefore one interpretation of our results is that the ACC is dysfunctionally mediating the relationship of the vlPFC and amygdala which creates the hyperconnectivity we observed in our BP subjects. There exist multiple white matter pathways connecting these three regions and so we may speculate that healthy subjects during rest posess less distributed patterns of information flow across these potential pathways and that, conversely, bipolar subjects have an ACC-mediated disinhibition of one or more of these paths not normally as engaged by healthy subjects. Which precise pathways are involved, and whether it is a disinhibition or simply greater excitation, however, is not identifiable from the present analysis. It is interesting that Chai, et al (Chai et al., 2011b) also found hyperconnectivity during rest between the vlPFC and this area in manic bipolar subjects, however not between this area and the amygdala, as we did. This suggests this connection could be dependent on mood state, and other research which shows the coupling between ACC and amygdala tracking with anxiety (Kim et al., 2011) supports this. Further investigation is necessary to elucidate the resting effective connections of the ACC.

There are several limitations to the current study. First, the volumes of the anatomical ROIs we used for this seed-based functional connectivity analysis, especially the vlPFC, were based on an atlas and as such will contain certain errors. If, for example, the time-series

extracted from an atlas-derived brain region averages over both gray and non-gray matter signals the resulting series will not properly represent that region's activation, which can result in unreliable measures. However, the aCompCor algorithm, which incorporates a high-resolution, subject-specific anatomic segmentation into its noise reduction procedure, takes such variability into account and attempts to compensate by higher weighting of gray matter voxels, thereby minimizing the effect of this issue (Nieto Castañón, personal communication; (Chai et al., 2011a)). Nonetheless, there is likely some degree of functional heterogeneity within both the vlPFC and amygdala atlas ROIs used, which would add variability to the extracted time series. The effect of this, however, could likely dilute our results. Thus, our observed significant effects would likely only become more significant if this limitation were corrected.

A second limitation, characteristic of any bivariate correlation, is that significant couplings between two brain regions could be the result of their being driven by a third. We explored this possibility and found that the ACC is a region potentially driving the apparent coupling between right hemisphere amygdala and vlPFC (see results above and figure 3a). We investigated this further and found partial mediation of the ACC with the vlPFC to amygdala connection. Despite our standard "arrowed" diagram (figure 3b) the causality in such a mediation should be interpreted cautiously, as it represents 'soft' causal links that stem from the DV/IV regression relation. The mediation analysis does, however, provide a more mechanistic description of the hyperconnectivity between amygdala and vlPFC. Future studies which systematically expand our four-node model and assess effective connectivity between regions are needed to further elucidate the causal relationship of functional pathology of bipolar disorder (Palaniyappan and Cousins, 2010). Such work is ongoing in our laboratory.

Certain characteristics of our sampled subjects are also limitations. First, many of our bipolar subjects were medicated. There were too few subjects in each medication group to investigate the effects of specific medications, but this is something future work should address.

We did, however, examine the correlation beta values of the three unmedicated subjects in our bipolar pool to make sure their connectivity estimates were not driving the results and found them to be well within 1 standard deviation of the group mean. Despite the potential, but inconclusive, impact of medications on BOLD signal in subjects with bipolar disorder (Phillips et al., 2008b), we argue that including medicated subjects ensures that our subject population is representative of the bipolar population at large, thereby increasing the generalizability of our results. Second, there was a significant difference in employment between the two groups: the vast majority of BP subjects were unemployed while the majority of HS were employed. This is not something commonly controlled for in BP studies, although future studies would benefit from taking a closer look at this issue. We note that unemployment is often correlated to BP severity (Goodwin and Jamison, 2007), but the relationship of the variable to resting state functional coupling has, to our knowledge, not been studied.

Finally, and not so much a limitation to our particular study as a reminder to exert interpretive caution with resting state studies, the current state of MRI-based imaging does not yet have a clear explanation of the relationship between task-based and resting state functional brain activity. The extent to which findings from experimental manipulations of cognitive states should and can map to resting states studies is still being actively investigated (Smith et al., 2009; Van Dijk et al., 2010). Many resting state studies have focused on a small set of reliably produced large-scale networks across the brain and yet for two decades the majority of cognitive neuroscientists have studied the activity and connectivity in a variety of different networks specific to cognitive processes and which have not been reliably uncovered within resting state analyses. One likely explanation for this discrepancy is that analyses of resting state data are conducted on a much lower and usually non-overlapping end of the fMRI signal frequency spectrum than standard task-based studies (Fox et al., 2006; Van Dijk et al., 2010). Knowledge coming from advances by those researchers actively investigating these important

relationships will, no doubt, inform the types of studies, like this one, performed by clinical neuroscientists.

In summary, we took a focused approach to exploring resting state brain patterns in subjects with bipolar disorder during the euthymic mood state. Specifically, we investigated intrinsic connectivity between four regions of interest that have been implicated in emotion regulation and have been previously shown to be functionally altered in bipolar disorder. Our results of hyperconnectivity between the right vlPFC and the right amygdala in bipolar subjects are in accordance with the few prior studies of bipolar that have found either hyperactivation or hyperconnectivity in these brain regions. We further observed a mediating effect from the ACC, which was functionally coupled to both amygdala and vlPFC. Together these findings suggest a maladaptive misallocation of neural resources in bipolar disorder. Intrinsic hyperconnectivity in the bipolar group between regions, in the “normal” euthymic state and while at rest, could be evidence of a trait marker of disease pathophysiology.

Figures and Tables

	AUTHOR	TASK/REST	BP MOOD	METHOD	SEED/ROI	BP > HS	HS > BP
FUNCTIONAL CONNECTIVITY STUDIES							
	Foland, et al. 2008 (29)	labeling emotional faces	manic	PPI	left AMYG	negative FC; ACC (BA32 & 24) & BA10	negative FC; LH amygdala —bilateral vlPFC
	Pompei, et al. 2011 (40)	color-word stroop	euthymic	PPI	right vlPFC	positive FC; RH vlPFC — insula	negative FC; RH vlPFC — LH vACC
	Townsend, et al. 2012 (30)	explicit emotion regulation	euthymic	PPI	left AMYG		negative FC; L AMYG—L vlPFC
	Versace, et al. 2010 (39)	labeling sad and happy faces	depressed & euthymic	seed-based FC	omPFC (BA11) & AMYG	sad; RH AMYG—vmOFC	happy; LH AMYG—vmOFC
	Anand, et al. 2009 (14)	rest	manic & depressed	seed-based FC	pgACC		LH & RH pgACC — dmTHAL, AMYG, & striatum
	Chai, et al. 2011 (15)	rest	manic	seed-based FC	mPFC, AMYG, dlPFC, insula, vlPFC	mPFC — LH insula mPFC— RH BA47	
	Chepenik, et al. 2010 (16)	rest	rapid cyclers, euthymic, depressed, & mixed	seed-based FC	vlPFC, AMYG	LH vPFC— RH vPFC	negative FC; LH AMYG—vPFC
	Cerullo, et al. 2012 (17)	steady state	manic & depressed (longitudinal)	seed-based FC	left & right AMYG	N/A	N/A

Table 1. A selection of fMRI connectivity studies of bipolar disorder. BA, Brodmann's Area; AMYG, amygdala; FC, functional connectivity; "—", correlation (coupling); PPI, psychophysiological interaction; LH, left hemisphere; RH, right hemisphere; omPFC, orbitomedial prefrontal cortex; vlPFC, ventrolateral PFC; dlPFC, dorsolateral PFC; mPFC, medial PFC; dmTHAL, dorsomedial thalamus; IFG, inferior frontal gyrus; HS, healthy subjects; BP, bipolar disorder; N/A, these direct contrasts were not performed.

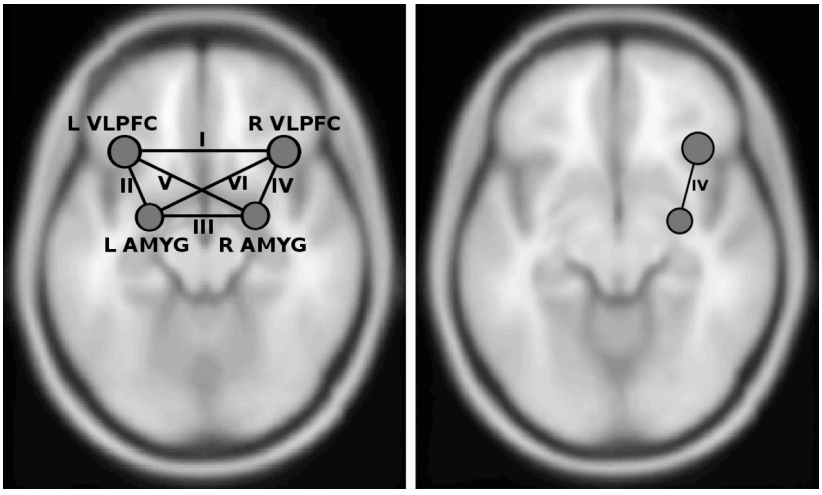

Figure 1a (left)**.** The four node (six correlation) connectivity model that was tested. Node locations at center of mass of anatomical ROIs. **Figure 1b** (right). Result of greater positive connectivity between right amygdala and right vlPFC in bipolar subjects relative to healthy subjects.

	Healthy Subjects						BP euthymic						BP>HS
connection	I	II	III	IV	V	VI	I	II	III	IV	V	VI	IV
betas*	0.52	0.11	0.31	0.07	0.04	0.04	0.51	0.12	0.26	0.2	0.14	0.1	0.12
T-scores	10.74	3.19	6.76	2.71	1.67	1.08	11.81	4.28	5.71	6.89	3.89	3.66	3.07
Z-scores	7.24	2.98	5.44	2.58	1.63	1.07	7.61	3.84	4.82	5.52	3.55	3.37	2.88
FDR p-values	0.0000	0.0096	0.0000	0.0207	0.1335	0.2947	0.0000	0.0006	0.0000	0.0000	0.0012	0.0017	0.0237
*Fisher-transformed correlation coefficients													

Table 2. Within and between group ROI-to-ROI analysis results with connections labeled as in Figure 1a.

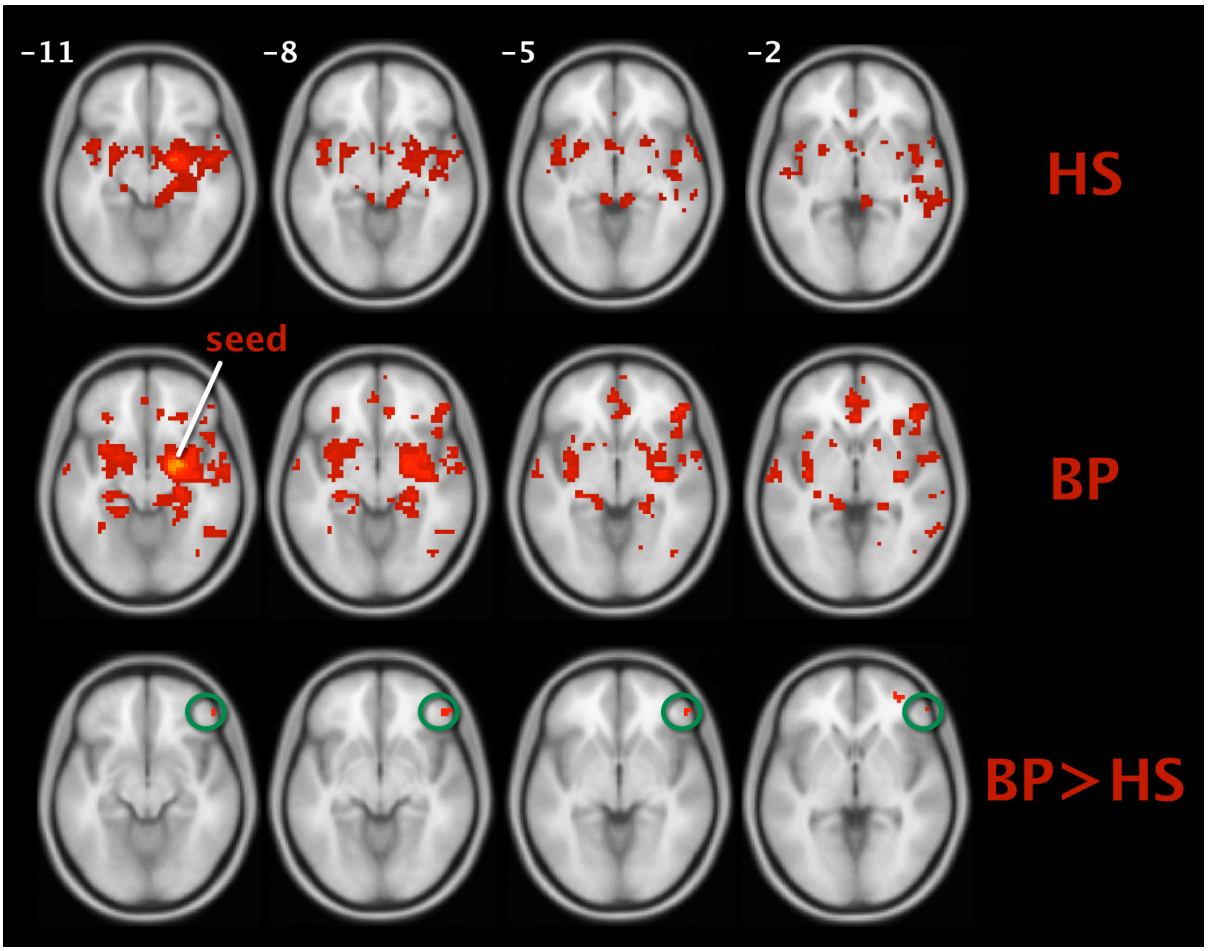

Figure 2. Positive connectivity with right amygdala. Top and middle rows (2a and 2b): within group maps for healthy subjects (HS) and bipolar subjects (BP). Bottom row (2c): between group contrast. Right vlPFC cluster circled. Voxels visualized on an average T1-weighted brain in MNI space, p<0.001, k=10.

Healthy subjects right amydala connectivity

	Brodmann Area	cluster size	cluster p	peak Z	MNI x, y, z
POSITIVE					
R Amygdala		2391	0.000	Inf	21 -4 -17
R Temporal Pole	BA 38			0.000	45 23 -26
L Superior Temporal Gyrus				0.000	-54 -16 7
L Medial Temporal Pole				0.000	-33 8 -32
L Insula				0.000	-42 8 -8
R Parahippocampal Gyrus	BA 36			0.000	39 -19 -32
L Hippocampus				0.000	-27 -22 -17
L Superior Temporal Gyrus	BA 13			0.000	-45 5 -14
L Superior Temporal Gyrus				0.000	-39 2 -20
R Postcentral Gyrus	BA 3			0.000	63 -1 22
R Superior Temporal Gyrus	BA 22			0.000	48 -19 1
L Middle Temporal Gyrus	BA 22	12	0.027	4.56	-66 -55 10
L Middle Temporal Gyrus	BA 39	10	0.041	3.51	-60 -64 10
Anterior Cingulate Gyrus		10	0.041	3.57	0 35 1
R Insula	BA 13	53	0.000	4.51	36 -13 19
R Thalamus		16	0.013	3.66	3 -10 7
NEGATIVE					
L Middle Frontal Gyrus	BA 10	70	0.000	4.72	-24 47 25
L Inferior Parietal Lobule	BA 40	33	0.001	4.6	-48 -52 40
L Precuneus	BA 7	14	0.019	4.07	-9 -64 49
L Superior Parietal Lobule	BA 7	29	0.002	3.85	-39 -49 61
L Middle Orbital Gyrus		16	0.013	3.5	-42 56 -11
R Precuneus	BA 7	18	0.009	4.28	6 -70 58
R Middle Frontal Gyrus		18	0.009	3.84	33 50 13

Bipolar Euthymic right amydala connectivity

	Brodmann	cluster	cluster p	peak Z	MNI

	Area	size			x, y, z
POSITIVE					
R Amygdala		2020	0.000	Inf	27 -4 -20
R Inferior Temporal Gyrus				5.2	51 -55 -17
R Hippocampus				5.18	33 -13 -35
R Parahippocampal Gyrus				5.14	24 -25 -14
R Inferior Frontal Gyrus	BA 45			5.04	54 32 10
R Ventrolateral PFC	BA 45			4.93	45 35 -2
R Fusiform Gyrus	BA 36			4.8	24 -40 -17
R Middle Temporal Gyrus				4.77	60 -7 -14
R Inferior Frontal Gyrus	BA 47			4.66	48 38 -5
R Temporal Pole	BA 38			4.3	42 20 -38
R Thalamus (somatosensory)				4.18	21 -19 4
R Superior Temporal Gyrus	BA 41	67	0.000	4.58	66 -22 4
R Posterior Insula	BA 13	58	0.000	4.33	42 -28 22
R Angular Gyrus	BA 39	32	0.001	4.2	54 -67 34
R Posterior Cingulate	BA 30	32	0.001	4.12	15 -58 7
R Insula	BA 13	17	0.011	4.08	39 5 10
R Superior Temporal Gyrus		95	0.000	4.03	54 -46 19
R Middle Frontal Gyrus	BA 11	42	0.000	4.01	18 29 -14
R Precuneus	BA 19	13	0.022	3.99	36 -85 37
R Precentral Gyrus	BA 6	15	0.015	3.99	51 2 37
R Precentral Gyrus	BA 6	14	0.018	3.84	54 -7 31
R Middle Occipital Gyrus		16	0.013	3.81	36 -73 25
R Middle Frontal Gyrus		12	0.027	3.66	45 20 28
R Inferior Temporal Gyrus		10	0.041	3.65	45 -70 -5
L Fusiform Gyrus	BA 37	40	0.000	4.22	-42 -49 -26
L Middle Occipital Gyrus	BA 19	29	0.002	4.2	-42 -85 25
L Rolandic Operculum		13	0.022	4.03	-51 -4 7
L Inferior Frontal Gyrus		36	0.001	3.82	-30 35 -8
L Posterior Cingulate		11	0.033	3.64	-18 -64 13
L Medial Frontal Gyrus	BA 10	10	0.041	3.59	-6 62 16
Cingulate Gyrus	BA 24	50	0.000	5.29	0 2 34

BP > HS right amydala connectivity

	Brodmann Area	cluster size	cluster p	peak Z	MNI x, y, z
POSITIVE					
L Middle Frontal Gyrus	BA 10	16	0.021	3.5	-30 62 13
R Middle Frontal Gyrus	BA 9	14	0.029	4.3	45 20 40
R Inferior Temporal Gyrus	BA 20	11	0.049	3.58	33 -4 -47
R Ventral Lateral PFC	BA 47	11	0.049	3.52	51 41 -8

p<0.001 (k=10)

Table 3. Within and between group voxel-level functional connectivity from right amygdala in healthy and bipolar subjects. There were no significant negative connectivity results with bipolar subjects. Rows in gray represent subclusters within a large cluster. Within and between group maps thresholded at p<0.001, k=10.

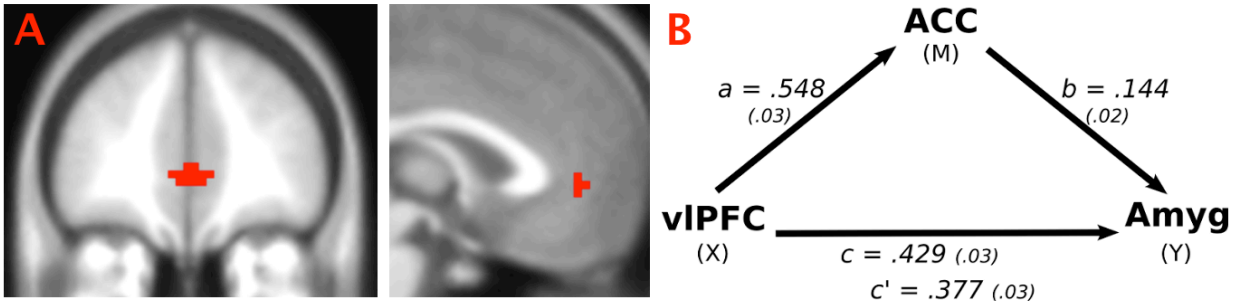

Figure 3a. Connectivity conjunction map shows a cluster in the anterior cingulate cortex (BA 32) that is strongly positively functionally connected to both the right amygdala and right vlPFC regions in bipolar subjects. **Figure 3b.** Group-level analysis of ACC mediating vlPFC to amygdala. Path coefficients labeled with traditional mediation nomenclature and standard errors in parentheses. All paths were significant (p<0.0001), indicating partial mediation of vlPFC to amygdala by ACC.

CHAPTER 7: SUMMARY AND DISCUSSION

The work for this dissertation involved the use of multiple advanced fMRI analysis techniques to elucidate functional and effective connectivity in the emotion regulation circuit in healthy subjects and in subjects with bipolar disorder. In particular, this work focused on the connections between two brain regions, the amygdala and the ventrolateral prefrontal cortex, both of which have been strongly implicated in the pathophysiology of bipolar disorder. This work has contributed novel findings to the understanding of normal emotion regulation, including an investigation into the little-explored temporality of cognitive reappraisal (chapter 2), and a novel application of an effective connectivity technique to the form of implicit emotion regulation known as affect labeling (chapter 4). After applying our novel approaches to these forms of emotion regulation in healthy subjects, we then applied those approaches to groups of euthymic bipolar type 1 patients (chapters 3 and 5). Finally, we tested differences in the resting brain between these bipolar subjects and healthy subjects in an analysis that identified the anterior cingulate as mediating intrinsic hyperconnectivity between the right amygdala and ventrolateral PFC in bipolar (chapter 6).

While each study has been valuable in itself, there are some common findings that run throughout. The main one of these is that the vlPFC is shown to be consistently hypoactive in bipolar disorder. Our group has already observed this with BP I subjects in mania (Altshuler et al., 2005b), depression (Altshuler et al., 2008) and euthymia (Foland-Ross et al., 2012; Townsend et al., 2013). However, as suggested by the findings in chapters 3 and 5, the laterality of this finding may be a function of which hemisphere a task preferentially recruits, i.e. right-lateralized vlPFC activation (or dysfunction) during affect labeling and left-lateralized vlPFC activation (or dysfunction) during the cognitive reappraisal of emotion. This offers some clue as to why laterality of dysfunction remains unclear across neuroimaging studies of bipolar disorder

(Chen et al., 2011), but nonetheless speaks of the (perhaps bilateral) vlPFC hypoactivation as a general trait marker for bipolar.

How many of the other major findings relate to each other, however, is difficult to understand at this point in time. It may be some years before we, as a neuroimaging field, are capable of comprehending how the varying results from different techniques precisely connect and inform each other. It will be important to know whether any two techniques reveal to us entirely different phenomena, different 'angles' on the same phenomena, or perhaps phenomena at one scale hierarchically contained within or containing another (Smith, 2012). A concrete example is the still unclear relationship between higher cognitive-based GLM analyses and seed- and ICA-based analyses of the resting state, despite the breadth of research using both approaches. While some of the same intrinsic networks repeatedly appear in data-driven analyses of rest (Smith et al., 2009), conscious, cognitive tasks seem to probe a broader configuration of networks that largely but not entirely fall within the jurisdiction of the intrinsic networks and which often recruit sub- or super-sets of resting state intrinsic networks. The fact that these two kinds of analyses are performed at largely non-overlapping ends of the fMRI frequency spectrum has prompted some researchers to test the idea that the phenomena represented by each superimpose (Barnes et al., 2009; Fox et al., 2006). This may explain why we found both hypoactivation and hyperconnectivity of the vlPFC in our bipolar subjects. Relevant to understanding 'inter-method' relationships, one study has shown that a resting state analysis of a neuroscientifically understood motor network could not be replicated when that same network (and exact time series) was subjected to a dynamic causal modeling analysis. The authors suggest the divergent findings were not due to a difference in method, but rather to the different mental states engaged during task-based and resting paradigms (Rehme et al., 2013).

Other issues preventing clear interpretability of the totality of findings presented in this dissertation are more intra- than inter- method concerns. Some of these were alluded to in the discussion section of chapter 5. Indeed, despite a very helpful paper of recommendations for practical implementations of DCM (Stephan et al., 2010), there remain a number of detailed questions about the technique, worth noting here: (1) At the individual subject level, is it imperative, highly recommended, or simply preferred that a particular statistical contrast show the node one is interested in for selection (Stephan et al., 2010)? Some regions, for example, respond to more than one condition at the group level, and yet during node selection at the individual level the given region is sometimes only visible during one of these contrasts. (2) To what extent does a *weak* time series (i.e. extracted from a small cluster with a small statistical effect or from a particularly noisy region) influence the model's overall evidence and parameter values? (3) To what extent could a *weak* node in a psychiatric population be considered a "missing node" in the neurological sense (Seghier et al., 2010). For example, investigators researching brain-damaged aphasics found patient-specific differences after not directly testing brain damaged areas but instead intact areas *upstream* from the damaged ones (Brodersen et al., 2011; Schofield et al., 2012). Would such an approach be recommended for psychiatric diseases like bipolar disorder where we already have strong clues as which areas are problematic? (4) Is a more diverse and larger model space better for Bayesian model averaging, seeing that the averaging is already performed in a weighted manner? While more computationally expensive, this would allow for more exploratory model spaces than are currently tested (but see (Friston et al., 2011)). (5) How does one perform a between-group study with a large model space that 'narrows in on' a best model (i.e. with successive family divisions) but *also* maximizes the potential for individuals of either population to express preferred model(s)? This is one potential issue with the analysis performed in chapter 5. Finally, (6) How can we make quantitative inferences at the model level between groups? This is

another problem encountered in chapter 5. Karl Friston, the main inventor of the DCM technique wrote recently in the SPM listserve (posted May 29, 2013; https://www.jiscmail.ac.uk/cgi-bin/webadmin?A0=spm):

> To make inferences about different architectures or models it is, in principle, possible to add a hierarchical level to the random effects Bayesian model selection, to test the hypothesis that models were selected at random from two different distributions for two groups. We have not actually implemented this ...

These are, of course, largely empirical questions, and one hopes that in the following few years such matters will be settled by both DCM authors and expert users.

As for resting state data, an unambiguous interpretation of what low frequency BOLD signal fluctuations neurobiologically represents is also not currently possible. However, this issue is not being ignored and many researchers are actively investigating the mysteries of the resting state (see (Raichle, 2011) for review). Some of the most sophisticated attempts to understand the resting brain, however, do so using computer modeling and dynamic systems theory to build complex but biologically-plausible simulations (Deco et al., 2011; Ritter et al., 2013).

This raises an interesting issue for researchers of psychiatric diseases. Although neuroimaging is a very interdisciplinary enterprise with many kinds of information informing different strata of skills and knowledge required to execute a study, one must not become complacent towards uncomfortable or unfamiliar domains of knowledge. Because the human brain is as complex as it is, it should come as no surprise that mathematics and engineering offer very useful empirical tools and even metaphors to help us understand it. It is also well known that these tools are making neuroimaging increasingly computationally sophisticated. However, many neuroimagers fall victim to using them without deeply understanding how they work or how their results arise from the underlying machinery. Interpretations of results should be dependent on one's understanding of how the results were gotten at. Of course this situation

is expected given the typical educational background of today's neuroimager interested in higher cognitive functions. Similarly, tool makers do not usually have a sophisticated understanding of a particular disease, which is also understandable given their backgrounds. One important and common bridge between this gap is through collaboration, with some individuals from both 'sides' working on the same data set and contributing coauthorship. Another solution, however, which may yield more appropriate and nuanced applications of techniques to particular disease properties, would be to try to close this gap by each side spending more time and effort informing and understanding the other side. First, bioengineers, statisticians, programers and other tool-makers can make more concerted efforts to explain what they are doing to clinical imagers. This will likely entail more creative thinking and use of metaphors and visualizations than they are perhaps used to. Second, clinically-minded imagers must continue to supplement their knowledge of math and engineering principles throughout their careers through continuing education. This will likely entail (re-) taking courses in programming and especially mathematics and perhaps even swallowing a little pride to do so.

This dissertation reflects the desire of the principle author of these chapters to create a middle ground between these two extremes. Through the novel application of sophisticated fMRI analysis techniques to the psychology of emotion regulation, and applied to bipolar disorder, I hope that some of this distance between method and relevance has been shortened. I hope that I have advanced our understanding of the neural networks involved in normal emotion regulation, and contributed to understanding why there are some perhaps methodologically-based discrepanicies within the field. I additionally believe my efforts over the past five years have incrementally advanced our understanding of neural network abnormailites in persons with bipolar disorder. I sincerely hope that the imaging approaches I have utilized to make some of the discoveries reported on above will contribute to future of translational neuroimaging research.

Appendix 1

Seven Major Matlab Scripts to Accomplish the Above

```
================================== mediate.m ================================

% Regression-based MFX mediation analysis of fMRI time series
% at the group level, retaining subject variances throughout.
% bpSubjs.mat was extracted and compiled with another script.
% note: variable naming is kinda lame
% Salvatore Torrisi and Martin Monti. August, 2012

load bpSubjs.mat; clear subj* acc vlPFC;

why = threeRegions(:,1); % column 1 = amygdalae concatenated
em = threeRegions(:,2);  % column 2 = ACCs concatenated
ex = threeRegions(:,3);  % column 3 = vlPFCs concatenated

numSubjs = 20;
tsl = 208;               % time series length

subjColumns = zeros(size(why),numSubjs-1); % minus 1 for no colinearity
for i=1:numSubjs-1          % make columns of 1s to distinguish time series
    subjColumns((1+tsl*(i-1)) : (tsl*i), i) = 1;
end

% STEP 1: is the predictor (ex) related to the mediator (em)?
X = [ex subjColumns];
stats=regstats(em, X,'linear',{'beta','covb','rsquare','tstat'});
a=stats.beta(2); a(2)=stats.tstat.t(2); a(3)=stats.tstat.pval(2);
sea = stats.tstat.se(2); % standard error of a

% STEP 2: Is the predictor related to the outcome (why)?
stats=regstats(why, X,'linear',{'beta','covb','rsquare','tstat'});
c=stats.beta(2); c(2)=stats.tstat.t(2); c(3)=stats.tstat.pval(2);

% STEP 3: is the mediator related to the outcome?
X = [em subjColumns];
stats=regstats(why, X,'linear',{'beta','covb','rsquare','tstat'});
b=stats.beta(2); b(2)=stats.tstat.t(2); b(3)=stats.tstat.pval(2);
seb = stats.tstat.se(2); % standard error of b

% STEP 4: full or partial mediation? (full mediation if cPrime p>0.05)
X = [ex em subjColumns];
stats=regstats(why, X,'linear',{'beta','covb','rsquare','tstat'});
cPrime=stats.beta(2); cPrime(2)=stats.tstat.t(2);
cPrime(3)=stats.tstat.pval(2);
bPrime=stats.beta(3); bPrime(2)=stats.tstat.t(3);
bPrime(3)=stats.tstat.pval(3);

% Sobel test of significance:
me = a(1)*b(1); % mediated effect
seme = sqrt(((a(1)^2)*(seb^2))+((b(1)^2)*(sea^2))); % standard error of me
Z = me/seme;

a
```

```
b
bPrime
c
cPrime
Z
```

========== pull_SPM_design_timings.m ==========

```
% Pull SPM design timings out of multiple subjects' SPM.mat for FSL.
% This script must be at the same level as the subjects' folders and is
% useful for event-related designs such as go-nogo w/ different designs for
% each subject (e.g. only “correct” trials). Salvatore Torrisi 04.13.12

% Names of folders to iterate through
Folders={'1001'; '1013'; '1014'; '1015'};

numSess = 1;

for i = 1:length(Folders)
    cd (sprintf('%s', Folders{i}))
    cd 'design2'

    load SPM.mat;
    numConditions = length(SPM.Sess.U);

    for j = 1:numSess
        for k = 1:numConditions
            ons = SPM.Sess(j).U(k).ons;
            durs = SPM.Sess(j).U(k).dur;
            height = ones(length(ons),1);
            forFSL = [ons durs height];
            filename = [num2str(Folders{i}), '_', 'session', num2str(j), '_',
SPM.Sess(j).U(k).name, '.txt'];
            stringName =
strcat(filename(1),filename(2),filename(3),filename(4),
filename(5),filename(6),filename(7));
            fid = fopen(stringName{1}, 'w');
            fprintf(fid, '%f %f %f\n', forFSL');
            fclose(fid);
        end
    end

    cd ../..
end
```

========== SummarizeMotion.m ==========

```
% TO HELP Q.C. MOTION (REALIGNMENT) PARAMETERS BETWEEN GROUPS
% This assumes nothing special like regressing out or removing spiky vols has
% occurred. Before running script, change the names of the rp_*.txt files to
% be 'rp_aafaces.txt' in each subject's folder. "-c" added to ends of
% controls' files so i could throw them all in the same folder and then
% retrieve them easily. Salvatore Torrisi 9.8.11

Files = { '1002'; '1004'; '1006'; '1007'; ...
    '1001-c'; '1013-c'; '1014-c'; '1016-c' };

NumBP = 34;
```

```
Sums = [];
pVals = [];

for i = 1:size(Files,1)
    cd (sprintf('%s', Files{i}));
    cd 'raw'

    load 'rp_aafaces.txt'
        xTransMean = mean(abs(rp_aafaces(:,1)));
        Sums(i,1)=xTransMean;
        yTransMean = mean(abs(rp_aafaces(:,2)));
        Sums(i,2)=yTransMean;
        zTransMean = mean(abs(rp_aafaces(:,3)));
        Sums(i,3)=zTransMean;
        pitchRotMean = mean(abs(rp_aafaces(:,4)));
        Sums(i,4)=pitchRotMean;
        rollRotMean = mean(abs(rp_aafaces(:,5)));
        Sums(i,5)=rollRotMean;
        yawRotMean = mean(abs(rp_aafaces(:,6)));
        Sums(i,6)=yawRotMean;
    cd ../..
end

for i = 1:6
    [h,p] =
ttest2(Sums(1:NumBP,i),Sums((NumBP+1):size(Files,1),i),[],[],'equal');
    pVals(1,i) = p;
end

fprintf('\n2-sample t-test btwn groups of 6 realignment parameters:\n');
fprintf('%10s%10s%10s%11s%10s%9s\n','x','y','z','pitch','roll','yaw');
pVals
```

========== mtxPerm.m ==========

```
% This script takes user input to generate DCM model permutations.
% First select the connections in the 'A' adjacency matrix that
% you wish to remain static throughout all models.
% Then select the connections you wish to permutate across models.
% It assumes familiarity with the ordering of VOI selection.
% And it prints in a form that's pasteable into dcm_spm8_batch_fn.m
%
% One can also use it to generate permutations of the 'B' matrix.
% To do so you must conceptualize what you're doing in terms of modularity,
% remove the first "%" in line 88, and then change "DCM.a =" of outputed text
% to, e.g.: DCM.b = zeros(4,4,4); DCM.b(:,:,4)=

% Salvatore Torrisi, UCLA MDRP, 5.28.12, 4.27.13
% This script also makes use of permpos.m by Jos van der Geest (10584):
% http://www.mathworks.com/matlabcentral/fileexchange/11216

clear all; close all;
Finter = figure;
bcolor = get(Finter,'color');
dx     = 40;
r      = 4;     %number of regions (VOIs)
a      = zeros(r,r);
```

```
for i = 1:r
    for j = 1:r
        h3(i,j) = uicontrol(Finter,...
            'Position',[180+dx*j 350-dx*i 020 020],...
            'BackgroundColor',bcolor,...
            'Style','checkbox');
        if i == j
            set(h3(i,j),'Value',1,...
                'enable','off');
        end
    end
end

%now user selects 'static' elements of the 'A' adjacency matrix
uicontrol(Finter, 'String','"A" static', 'Callback','uiresume(gcbf)');
uiwait(Finter);

for i = 1:r
        for j = 1:r
        a(i,j) = get(h3(i,j),'Value');
        end
end

for i = 1:r
    for j = 1:r
        h3(i,j) = uicontrol(Finter,...
            'Position',[180+dx*j 350-dx*i 020 020],...
            'BackgroundColor',bcolor,...
            'Style','checkbox');
        if a(i,j) == 1
            set(h3(i,j), 'enable','off');
        end
    end
end

%now user selects permutable elements of 'A'
uicontrol(Finter, 'String','"A" permute', 'Callback','uiresume(gcbf)');
uiwait(Finter);

for i = 1:r
        for j = 1:r
        permutate(i,j) = get(h3(i,j),'Value');
        end
end

num2perm = sum(permutate(:));
modelPerms = [ ];

%build all permutations of the connections to permute
for i = 1:num2perm+1
    temp  = permpos(i-1, num2perm);  %avoid perms.m redundancies
    modelPerms = [modelPerms; temp]; %concatenate
end

permCells = find(permutate);         %cell indices
models = size(modelPerms,1);
tempPermutate = permutate;
```

```
%prints into Command Window to copy/paste into dcm_spm8_batch_fn.m:
for i = 1:models
      x = modelPerms(i,:);
  for j = 1:length(permCells)
      tempPermutate(permCells(j))= x(j);
  end
      model = a + tempPermutate %- eye(r); %put them together (and remove
self-connections if permuting a B mtx)

      fprintf('%1s%', 'DCM.a = [')
   for k = 1:size(model,1)-1
      fprintf('%1s%1s', num2str(model(k,:)),'; ');
   end
      fprintf('%1s%1s\n', num2str(model(size(model,1),:)), '];');
      tempPermutate = permutate;
end
```

============================== dcm_AhmadFaces.m ============================

```
% This is the DCM script to execute, which calls the function in the block of
% code below (dcm_spm8_batch_fn.m)
% Copyright 2011, UCLA MDRP, Salvatore Torrisi & Ed Lau

DATADIR = ['/Users/storrisi/Desktop/Altshuler/BP1_DCM/controls'];
global SUBJVOITSTATS;

SUBJ = {'1001'; '1013'; '1014'; '1015' };
CB = [1, 2, 1, 1];
load(fullfile(DATADIR, 'VOIs.mat'));
VOI=VOIs;
fid = fopen('TsForAllNodes.txt', 'a');

for i=1:length(SUBJ)
    dcm_spm8_batch_fn(DATADIR, SUBJ{i}, VOI(30+i,:), CB(i)) % change
    subjAndTs = [SUBJ{i} '    ' num2str(SUBJVOITSTATS)];
    fprintf(fid, '%s\n', subjAndTs);
    cd ../..
end
fclose(fid);
```

============================ dcm_spm8_batch_fn.m ==========================

```
% This function analyses Ahmad Hariri's face labeling task (but can be
% adapted). It performs a Dynamic Causal Modeling analysis, currently called
% DCM10 in SPM8. It assumes an entire (1st and 2nd) level GLM analysis has
% already been done with these extant directories: subj*/design/DCM and
% subj*/raw, where the subj*/design has the 1st level files, subj*/design/DCM
% is empty, and subj*/raw has the preprocessed files. btw, if you do >1 model
% selection 'stages' you might want, e.g., at the same level as /DCM a
% /DCM_DI folder (for driving input). Then of course change code accordingly.
%
% It also assumes that subject-specific volume of interest (VOI) coordinates
% (and the contrasts they come from) have been entered into the file called
% VOIs.mat (most likely with fillVOIs.m), and that this file along with
% dcm_AhmadFaces.m and this function (dcm_spm8_batch_fn.m) are
% all in the same directory that has all subject directories in it too.
%
```

```
% The final model space and estimation lines below need study-specific
% specification
%
% DATADIR is the aforementioned directory with all that stuff in it.
% SUBJ is a structure of directory names specified in dcm_AhmadFaces.m.
% VOI comes from VOIs.mat and contains three fields: name, contrast, and
% coords. CB is a subject-specific value that represents one of two stimuli
% counterbalancings
%
% Copyright 2010, Wellcome Trust Centre for Neuroimaging, G. Flandin
% Copyright 2011-2013, UCLA MDRP, Salvatore Torrisi & Edward Lau

function dcm_spm8_batch_fn(DATADIR, SUBJ, VOI, CB)

data_path = fullfile(DATADIR, SUBJ,'design','DCM');

% Initialise SPM
%-----------------------------------------------------------------------
spm('Defaults','fMRI');
spm_jobman('initcfg');
global SUBJVOITSTATS;

% CHANGE WORKING DIRECTORY
%-----------------------------------------------------------------------
clear matlabbatch
matlabbatch{1}.cfg_basicio.cfg_cd.dir = cellstr(data_path);
spm_jobman('run',matlabbatch);

% DCM-NECESSARY GLM SPECIFICATION (i.e. with collinear driving-input
regressor)
%-----------------------------------------------------------------------
clear matlabbatch

matlabbatch{1}.spm.stats.fmri_spec.dir = {data_path};
matlabbatch{1}.spm.stats.fmri_spec.timing.units = 'secs';
matlabbatch{1}.spm.stats.fmri_spec.timing.RT = 2.5;
matlabbatch{1}.spm.stats.fmri_spec.timing.fmri_t = 16;
matlabbatch{1}.spm.stats.fmri_spec.timing.fmri_t0 = 1;
f = spm_select('ExtList', fullfile(data_path,'../../raw'),
'^swa.*nii$',[1:135]);
matlabbatch{1}.spm.stats.fmri_spec.sess.scans = cellstr(f);

for i = 1:length(f)
    matlabbatch{1}.spm.stats.fmri_spec.sess.scans{i} =
[fullfile(data_path,'../../raw/')
matlabbatch{1}.spm.stats.fmri_spec.sess.scans{i} ];
end

if CB == 1
    matlabbatch{1}.spm.stats.fmri_spec.sess.cond(1).name = 'Match';
    matlabbatch{1}.spm.stats.fmri_spec.sess.cond(1).onset = [57.5 122.5];
    matlabbatch{1}.spm.stats.fmri_spec.sess.cond(1).duration = 30;
    matlabbatch{1}.spm.stats.fmri_spec.sess.cond(2).name = 'ID';
    matlabbatch{1}.spm.stats.fmri_spec.sess.cond(2).onset = [187.5 252.5];
    matlabbatch{1}.spm.stats.fmri_spec.sess.cond(2).duration = 30;
else
    matlabbatch{1}.spm.stats.fmri_spec.sess.cond(1).name = 'Match';
    matlabbatch{1}.spm.stats.fmri_spec.sess.cond(1).onset = [187.5 252.5];
```

```
    matlabbatch{1}.spm.stats.fmri_spec.sess.cond(1).duration = 30;
    matlabbatch{1}.spm.stats.fmri_spec.sess.cond(2).name = 'ID';
    matlabbatch{1}.spm.stats.fmri_spec.sess.cond(2).onset = [57.5 122.5];
    matlabbatch{1}.spm.stats.fmri_spec.sess.cond(2).duration = 30;
end

matlabbatch{1}.spm.stats.fmri_spec.sess.cond(3).name = 'faces';
matlabbatch{1}.spm.stats.fmri_spec.sess.cond(3).onset = [57.5 122.5 187.5
252.5];
matlabbatch{1}.spm.stats.fmri_spec.sess.cond(3).duration = 30;
matlabbatch{1}.spm.stats.fmri_spec.sess.cond(4).name = 'crap'; % instruction
screens + fixation crosses
matlabbatch{1}.spm.stats.fmri_spec.sess.cond(4).onset = [0 22.5 55 87.5 120
152.5 185 217.5 250 282.5 315];
matlabbatch{1}.spm.stats.fmri_spec.sess.cond(4).duration = [22.5 2.5 2.5 2.5
2.5 2.5 2.5 2.5 2.5 2.5 20];

spm_jobman('run',matlabbatch);

% EXTRACTING TIME SERIES (specify these in a relevant order in VOIs.mat)
%-----------------------------------------------------------------------

for i = 1:length(VOI)
    clear matlabbatch
    matlabbatch{1}.spm.util.voi.spmmat = cellstr(fullfile(data_path, '..',
'SPM.mat'));
    matlabbatch{1}.spm.util.voi.adjust = 1;
    matlabbatch{1}.spm.util.voi.session = 1;
    matlabbatch{1}.spm.util.voi.name = VOI(i).name;
    matlabbatch{1}.spm.util.voi.roi{1}.spm.spmmat = {''};% using 1st SPM.mat
    matlabbatch{1}.spm.util.voi.roi{1}.spm.contrast = VOI(i).contrast;
    matlabbatch{1}.spm.util.voi.roi{1}.spm.conjunction = 1;
    matlabbatch{1}.spm.util.voi.roi{1}.spm.threshdesc = 'none';
    matlabbatch{1}.spm.util.voi.roi{1}.spm.thresh = 0.1;
    matlabbatch{1}.spm.util.voi.roi{1}.spm.extent = 0;
    matlabbatch{1}.spm.util.voi.roi{1}.spm.mask = struct('contrast', {},
'thresh', {}, 'mtype', {});
    matlabbatch{1}.spm.util.voi.roi{2}.sphere.centre = VOI(i).coords;
    matlabbatch{1}.spm.util.voi.roi{2}.sphere.radius = 6;
    matlabbatch{1}.spm.util.voi.roi{2}.sphere.move.fixed = 1;
    matlabbatch{1}.spm.util.voi.expression = 'i1 & i2';
    spm_jobman('run',matlabbatch);

      % get Tstat for peak voxel of each node:
      V=spm_vol(['spmT_000' num2str(VOI(i).contrast) '.img']); tstat =
      spm_get_data(V,V.mat\[VOI(i).coords 1]');
      % and also print to a .txt file (see also the .m file that calls this)
      SUBJVOITSTATS(1,i) = abs(tstat);

    movefile(['VOI_' VOI(i).name '_1.mat'], './DCM_DI');
    movefile(['VOI_' VOI(i).name '.hdr'], './DCM_DI');
    movefile(['VOI_' VOI(i).name '.img'], './DCM_DI');
end

% DYNAMIC CAUSAL MODELLING
%-----------------------------------------------------------------------
clear DCM
```

```
% SPECIFY MODELS
load(fullfile(data_path,'.','SPM.mat'));

for i = 1:length(VOI)
    load(fullfile(data_path, ['VOI_' VOI(i).name '_1.mat']),'xY');
    DCM.xY(i) = xY;
end

DCM.n = length(DCM.xY);      % number of regions
DCM.v = length(DCM.xY(1).u);
DCM.Y.dt  = SPM.xY.RT;
DCM.Y.X0  = DCM.xY(1).X0;

for i = 1:DCM.n
    DCM.Y.y(:,i)  = DCM.xY(i).u;
    DCM.Y.name{i} = DCM.xY(i).name;
end

DCM.Y.Q    = spm_Ce(ones(1,DCM.n)*DCM.v);
DCM.U.dt   =  SPM.Sess.U(1).dt;
DCM.U.name = [SPM.Sess.U.name];
DCM.U.u = [];

for i=1:length(VOI)
    DCM.U.u    = horzcat(DCM.U.u, SPM.Sess.U(i).u(33:end,1));
end

DCM.delays = repmat(SPM.xY.RT,length(VOI),1);
DCM.TE     = 0.025;
DCM.options.nonlinear  = 0;
DCM.options.two_state  = 0;
DCM.options.stochastic = 0;
DCM.options.nograph    = 1;

% Manually enter your models (here, three are listed as an example):
if length(VOI) ~= 4
    error('change number of VOIs to fit the study!');
end

DCM.a = [1 1 1 1; 1 1 1 1; 1 1 1 1; 1 1 1 1];
DCM.b = zeros(4,4,4);  DCM.b(2,1,2) = 1;  DCM.b(2,3,3) = 1;
DCM.c = [0 0 1 0; 0 0 0 0; 0 0 0 0; 0 0 0 0];
save(fullfile(data_path,'DCM_1A.mat'),'DCM');

DCM.a = [1 1 1 1; 1 1 1 1; 1 1 1 1; 1 1 1 1];
DCM.b = zeros(4,4,4);  DCM.b(2,1,3) = 1;  DCM.b(2,3,2) = 1;
DCM.c = [0 0 0 0; 0 0 1 0; 0 0 0 0; 0 0 0 0];
save(fullfile(data_path,'DCM_2A.mat'),'DCM');

DCM.a = [1 1 1 1; 1 1 1 1; 1 1 1 1; 1 1 1 1];
DCM.b = zeros(4,4,4);  DCM.b(2,1,2) = 1;  DCM.b(2,3,3) = 1;
DCM.c = [0 0 1 0; 0 0 1 0; 0 0 0 0; 0 0 0 0];
save(fullfile(data_path,'DCM_3A.mat'),'DCM');

% ESTIMATE MODELS
%-----------------------------------------------------------------------

DCM_1A = spm_dcm_estimate(fullfile(data_path,'DCM_1A.mat'));
```

```
fprintf('Model evidence: %f (DCM_1A) \n', DCM_1A.F);

DCM_2A = spm_dcm_estimate(fullfile(data_path,'DCM_2A.mat'));
fprintf('Model evidence: %f (DCM_2A) \n', DCM_2A.F);

DCM_3A = spm_dcm_estimate(fullfile(data_path,'DCM_3A.mat'));
fprintf('Model evidence: %f (DCM_3A) \n', DCM_3A.F);

end
```

========== **TTEST_withinGroup_bma.m** ==========

```
% TO TEST BMA MODULATORY OR INTRINSIC PARAMETER ESTIMATES WITHIN 1 GROUP
% Salvatore Torrisi 6.26.12, modified 7.16.12, 9.16.12

load BMS.mat;
NumSubjs = 45;
taskCondition = 2;

meanAs = BMS.DCM.rfx.bma.mEps(1).A;  % mean A matrix values
meanBs = BMS.DCM.rfx.bma.mEps(1).B;  % mean B matrix values
A_dims = length(meanAs);   % we assume mtx B has same 1st & 2nd dimensions

ParameterMeansTTest2 = [];

for r=1:A_dims,                      % rows
    for c= 1:A_dims,                 % columns

        for i=1:NumSubjs, x(i) = BMS.DCM.rfx.bma.mEps(i).A(r,c); end;
        % or change part of the above to .B(r,c,taskCondition);

        [h,p] = ttest(x,[],[],'both');  % matrix 2-tailed diff from 0?
        %[h,p] = kstest(x);             % is distribution normal?

        ParameterMeansTTest2(r,c) = p;  % change p to h for y/n significance
    end;
end;

ParameterMeansTTest2

% Now let's mine the results for graphing (see Fig.5 of my NeuroImage paper).
% We assume the use of Inkscape or comparable software with arrow stroke
% width specifiable in pixels and arrow colors specifiable as hue and
% saturation (HSL or HSV). Firstly we turn positive and negative mean BMA
% values into colors (with diminishing strength moving towards gray), and
% secondly we turn p-values into line widths (the greater the significance
% the thicker the arrow). Run this twice, the second time changing line 17
% and commenting out the upper block of code and uncommenting the lower.

meanAs = BMS.DCM.rfx.bma.mEp.A; meanBs = BMS.DCM.rfx.bma.mEp.B;
% Get rid of self-connections:
meanAsNoDiag = meanAs-diag(diag(meanAs));
meanBsNoDiag = meanBs(:,:,taskCondition)-
diag(diag(meanBs(:,:,taskCondition)));
pvalsNoDiag = ParameterMeansTTest2-diag(diag(ParameterMeansTTest2));

% Have only one scale factor for A and B mtx positive saturation values and
```

```
% another scale factor for negs:
mxA= max(max(meanAsNoDiag)); mxB=max(max(meanBsNoDiag)); mx=max([mxA mxB]);
mnA= min(min(meanAsNoDiag)); mnB=min(min(meanBsNoDiag)); mn=min([mnA mnB]);

% ================================================= (upper block)
% FOR A MATRIX GRAPHIC:
onlyPos = find(meanAsNoDiag>0);
cleanMeanAsNoDiag = zeros(A_dims);
cleanMeanAsNoDiag(onlyPos) = meanAsNoDiag(onlyPos);
posScale = 255/mx; posColorsAmtx = round(cleanMeanAsNoDiag*posScale)

onlyNeg = find(meanAsNoDiag<0);
cleanMeanAsNoDiag = zeros(A_dims);
cleanMeanAsNoDiag(onlyNeg) = meanAsNoDiag(onlyNeg);
negScale = 255/mn; negColorsAmtx = round(cleanMeanAsNoDiag*negScale)

% line widths specified in pixels for graphing.
% "0.5" is fudgeable for aesthetics/viewability:
lineWidthsAmtx = log(1./pvalsNoDiag)*0.5

% ================================================= (lower block)
% FOR B MATRIX GRAPHIC:

% onlyPos = find(meanBsNoDiag>0);
% cleanMeanBsNoDiag = zeros(A_dims);
% cleanMeanBsNoDiag(onlyPos) = meanAsNoDiag(onlyPos);
% posScale = 255/mx; posColorsBmtx = round(cleanMeanBsNoDiag*posScale)
%
% onlyNeg = find(meanAsNoDiag<0);
% cleanMeanBsNoDiag = zeros(A_dims);
% cleanMeanBsNoDiag(onlyNeg) = meanBsNoDiag(onlyNeg);
% negScale = 255/mn; negColorsBmtx = round(cleanMeanBsNoDiag*negScale)
%
% lineWidthsBmtx = log(1./pvalsNoDiag)*0.5
```

Appendix 2

A Protocol for a Two Group DCM Analysis

THE ORDER OF EVENTS FOR A DCM ANALYSIS FOR PATIENT POPULATIONS
by Salvatore Torrisi. UCLA Mood Disorders Research Program. October, 2011
(*italics = a separate script or file to use*, * = wild card):

PRELIMINARIES:

Don't attempt DCM unless you've had some experience with SPM and Matlab.
If you've already performed a PPI analysis that's even better.
Think hard about the network you want to test and the problem you want to test.
Read at least 5 DCM papers and get to know the technique and how it's used.
Do both the 'DCM for fMRI' and 'Bayesian Model Inference' tutorials in the manual, in that order.
Read at least 5 more DCM papers (including "Ten Simple Rules…") after you've done the tutorials in their entirety. It's preferable, by the way, not to just apply DCM to data that's already been collected.
Design/use an experiment for your particular questions. Scan tons of subjects :-)

SPM ANALYSIS:

Make sure the two groups of subjects you start with are gender and age matched.
Set up your directories correctly; see help for *dcm_spm8_batch_fn.m*
Batch preprocess everyone (start w/ slice timing correction if data was acquired interleaved).
Make your 1st levels batch **.m* w/ model estimation, T & F contrasts, and added motion regressors (from *rp_**). Run this file, which will among other things will make 1st level masks for everyone.
Make an everyone-together-mask with Ged's "Masking" toolbox, modify a line in *spm_defaults.m* to make work. Run *messWith*Files.m* which gets rid of SPM.mats to make over-writing easier.
Change the 1st level **.m* using the new mask explicitly and re-run all 1st levels.
Run all 2nd level within and between group contrasts.

DCM ANALYSIS PART 1:

Study 2nd level within and between group results. Continue thinking hard about the network you want to test. Think hard about your model space and if you want to partition it into families.
It's better to use families than to estimate elements of your model sequentially (e.g. doing BMS to compare models which only differ by driving input, then using the winner as a 'backdrop' to test modulations... Better to have a space that BMS can compare families from all at once). Draw little network graphs, number stuff, learn how to 'think matrix', make sure you really know what you're doing.
I recommend specifying a few of your models via the DCM GUI, then mine the a, b and c matrices to see how they're represented that way. Then elaborate on those when building your batched model space. If you wish to permute some matrix connections/modulations but not others you can use *mtxPerm.m*

DETOUR: NODE FINDING AND CONSEQUENCES:

After you've decided on your number of nodes, manually get unique coordinates for each individual's 1st levels. Do this by following *VOI_selection_rules.rtf*. For example, this part took me over 15 hours for 71 subjects x 4 nodes. Discard subjects which don't meet criteria, I was left with 62. Check behavior and motion (run *SummarizeMotion.m*) and double check age & gender again between groups. Perhaps get rid of more subjects if there are significant differences between groups. *This is your final subject pool.* Run all 2nd level within and between group contrasts again (in different folders) and hopefully the main results still stay. For example, I had to run *AlphaSim* (in the REST toolbox) to confirm that my slightly weaker between group results were still fine at that cluster threshold. It is the pics from this analysis that you'll report for the SPM portion of your paper. Export coordinates from *VOI_COORDINATES.xlsx* as tab-delimited .txt with those same columns in that order. Optional: run *mip_maker.m* to plot coordinates for each group for a supplementary figure.

DCM ANALYSIS PART 2:

You should now have 5 files in each group folder:

dcm_AhmadFaces.m
dcm_spm8_batch_fn.m
fillVOIs.m
VOI_COORDINATES.txt
VOIs.mat

Use *fillVOIs.m* to put the coordinates (and contrasts they came from) in *VOI_COORDINATES.txt* into *VOI.mat*.
Delete other workspace variables except VOIs and then save the updated *VOIs.mat.*

Customize and then run *dcm_AhmadFaces.m* for each group separately.
This script will call the function *dcm_spm8_batch_fn.m*, which will:

make a new 'dummy' GLM with a necessary collinear driving stimulus regressor
extract X timeseries, adjusted for effects of interest
specify Y models in their /DCM folder
estimate those models
repeat for each subject

DCM ANALYSIS PART 3:

Specify families by grouping models together in non-overlapping subsets.
Perform either fixed or random effects BMS depending on your assumptions.
If part of your scientific questions, include BMA. Then use *BMA_TTEST.m* to compare parameter values between groups (or *TTEST_withinGroup_bma.m* to look within one group and for figure plotting information).

REFERENCES

Almeida, J.R.C., Mechelli, A., Hassel, S., Versace, A., Kupfer, D.J., Phillips, M.L., 2009a. Abnormally increased effective connectivity between parahippocampal gyrus and ventromedial prefrontal regions during emotion labeling in bipolar disorder. Psychiatry Research Neuroimaging 174, 195–201.

Almeida, J.R.C., Versace, A., Mechelli, A., Hassel, S., Quevedo, K., Kupfer, D.J., Phillips, M.L., 2009b. Abnormal Amygdala-Prefrontal Effective Connectivity to Happy Faces Differentiates Bipolar from Major Depression. BPS 66, 451–459.

Altshuler, L.L., Bookheimer, S.Y., Proenza, M., Townsend, J.D., Sabb, F., Firestine, A., Bartzokis, G., Mintz, J., Mazziotta, J.C., Cohen, M.S., 2005a. Increased Amygdala Activation During Mania: A Functional Magnetic Resonance Imaging Study. American Journal of Psychiatry 162, 1211–1213.

Altshuler, L.L., Bookheimer, S.Y., Townsend, J.D., Proenza, M., Sabb, F., Mintz, J., Cohen, M.S., 2008. Regional brain changes in bipolar I depression: a functional magnetic resonance imaging study. Bipolar Disorders 10, 708–717.

Altshuler, L.L., Bookheimer, S.Y., Townsend, J.D., Proenza, M.A., Eisenberger, N., Sabb, F., Mintz, J., Cohen, M.S., 2005b. Blunted activation in orbitofrontal cortex during mania: a functional magnetic resonance imaging study. BPS 58, 763–769.

Altshuler, L.L., Post, R.M., Leverich, G.S., Mikalauskas, K., Rosoff, A., Ackerman, L., 1995. Antidepressant-induced mania and cycle acceleration: a controversy revisited. Am J Psychiatry 152, 1130–1138.

Amaral, D.G., 1992. *Anatomical organization of the primate amygdaloid complex*. Wiley-Liss, New York.

Amunts, K., Kedo, O., Kindler, M., Pieperhoff, P., Mohlberg, H., Shah, N., Habel, U., Schneider, F., Zilles, K., 2005. Cytoarchitectonic mapping of the human amygdala, hippocampal region and entorhinal cortex: intersubject variability and probability maps. Anatomy and Embryology 210, 343–352.

Anand, A., Li, Y., Wang, Y., Lowe, M.J., Dzemidzic, M., 2009. Resting state corticolimbic connectivity abnormalities in unmedicated bipolar disorder and unipolar depression. Psychiatry Research Neuroimaging 171, 189–198.

Anderson, S.W., Bechara, A., Damasio, H., Tranel, D., Damasio, A.R., 1999. Impairment of social and moral behavior related to early damage in human prefrontal cortex. Nat Neurosci 2, 1032–1037.

Anticevic, A., Van Snellenberg, J.X., Cohen, R.E., Repovs, G., Dowd, E.C., Barch, D.M., 2012. Amygdala Recruitment in Schizophrenia in Response to Aversive Emotional Material: A Meta-analysis of Neuroimaging Studies. Schizophrenia Bulletin 38, 608–621.

Banks, S., Eddy, K., Angstadt, M., Nathan, P., Phan, K., 2007. Amygdala-frontal connectivity during emotion regulation. Social Cognitive and Affective Neuroscience 2, 303–312.

Barnes, A., Bullmore, E.T., Suckling, J., 2009. Endogenous Human Brain Dynamics Recover Slowly Following Cognitive Effort. PLoS ONE 4, e6626.

Baron, R.M., Kenny, D.A., 1986. The Moderator-Mediator Variable Distinction in Social Psychological Research: Conceptual, Strategic, and Statistical Considerations. Journal of Personality and Social Psychology 51, 1173–1182.

Beckmann, C.F., Jenkinson, M., Smith, S.M., 2003. General multilevel linear modeling for group analysis in FMRI. NeuroImage 20, 1052–1063.

Beckmann, M., Johansen-Berg, H., Rushworth, M.F.S., 2009. Connectivity-Based Parcellation of Human Cingulate Cortex and Its Relation to Functional Specialization. journal of neuroscience 29, 1175–1190.

Behzadi, Y., Restom, K., Liau, J., Liu, T.T., 2007. A component based noise correction method (CompCor) for BOLD and perfusion based fMRI. NeuroImage 37, 90–101.

Berkman, E.T., Burklund, L.J., Lieberman, M.D., 2009. Inhibitory spillover: Intentional motor inhibition produces incidental limbic inhibition via right inferior frontal cortex. NeuroImage 47, 705–712.

Berkman, E.T., Lieberman, M.D., 2009. Using Neuroscience to Broaden Emotion Regulation: Theoretical and Methodological Considerations. Social and Personality Psychology Compass 3, 475–493.

Biswal, B.B., Yetkin, F.Z., Haughton, V.M., Hyde, J.S., 1995. Functional connectivity in the motor cortex of resting human brain using echo-planar MRI. Magn Reson Med 34, 537–541.

Bohland, J.W., Bokil, H., Allen, C.B., Mitra, P.P., 2009. The Brain Atlas Concordance Problem: Quantitative Comparison of Anatomical Parcellations. PLoS ONE 4, e7200.

Box, G.E., Draper, N.R., 1987. *Empirical Model-Building and Response Surfaces*. Wiley-Liss.

Bracht, T., Tüscher, O., Schnell, S., Kreher, B., Rüsch, N., Glauche, V., Lieb, K., Ebert, D., Il'yasov, K.A., Hennig, J., Weiller, C., Elst, L.T.V., Saur, D., 2009. Extraction of prefronto-amygdalar pathways by combining probability maps. Psychiatry Research Neuroimaging 174, 217–222.

Brett, M., Anton, J.-L., Valabregue, R., Poline, J.-B.P. (Eds.), n.d. Region of interest analysis using an SPM toolbox. 8th International Conference on Functional Mapping of the Human Brain, June 2-6, 2002, Sendai, Japan. Available on CD-ROM in NeuroImage, Vol 16, No 2.

Brodersen, K.H., Schofield, T.M., Leff, A.P., Ong, C.S., Lomakina, E.I., Buhmann, J.M., Stephan, K.E., 2011. Generative Embedding for Model-Based Classification of fMRI Data. PLoS Comput Biol 7, e1002079.

Buhle, J.T., Silvers, J.A., Wager, T.D., Lopez, R., Onyemekwu, C., Kober, H., Weber, J., Ochsner, K.N., 2013. Cognitive Reappraisal of Emotion: A Meta-Analysis of Human Neuroimaging Studies. Cereb Cortex.

Burklund, L.J., Creswell, J.D., Irwin, M.R., Lieberman, M.D., 2012. The common neural bases of affect labeling and reappraisal.

Carmichael, S., Price, J.L., 1995. Limbic Connections of the Orbital and Medial Prefrontal Cortex in Macaque Monkeys. The Journal of Comparative Neurology 1–27.

Cerullo, M.A., Fleck, D.E., Eliassen, J.C., Smith, M.S., Delbello, M.P., Adler, C.M., Strakowski, S.M., 2012. A longitudinal functional connectivity analysis of the amygdala in bipolar I disorder across mood states. Bipolar Disorders 14, 175–184.

Chai, X.J., Castonon, A.N., Öngür, D., Whitfield-Gabrieli, S., 2011a. Anticorrelations in resting state networks without global signal regression. NeuroImage 1–9.

Chai, X.J., Whitfield-Gabrieli, S., Shinn, A.K., Gabrieli, J.D.E., Castonon, A.N., Mccarthy, J.M., Cohen, B.M., Ongür, D., 2011b. Abnormal Medial Prefrontal Cortex Resting-State Connectivity in Bipolar Disorder and Schizophrenia. Neuropsychopharmacology : official publication of the American College of Neuropsychopharmacology 36, 2009–2017.

Chen, C.-H., Suckling, J., Lennox, B.R., Ooi, C., Bullmore, E.T., 2011. A quantitative meta-analysis of fMRI studies in bipolar disorder. Bipolar Disorders 13, 1–15.

Chepenik, L.G., Raffo, M., Hampson, M., Lacadie, C.M., Wang, F., Jones, M.M., Pittman, B., Skudlarski, P., Blumberg, H.P., 2010. Functional connectivity between ventral prefrontal cortex and amygdala at low frequency in the resting state in bipolar disorder. Psychiatry Research Neuroimaging 182, 207–210.

Chiavaras, M.M., Legoualher, G., Evans, A., Petrides, M., 2001. Three-Dimensional Probabilistic Atlas of the Human Orbitofrontal Sulci in Standardized Stereotaxic Space. NeuroImage 13, 479–496.

Cohen Kadosh, K., Cohen Kadosh, R., Dick, F., Johnson, M.H., 2011. Developmental Changes in Effective Connectivity in the Emerging Core Face Network. Cereb Cortex 21, 1389–1394.

Cohen, J., Berkman, E.T., Lieberman, M.D., 2011. Intentional and Incidental Self-Control in Ventrolateral PFC, in: Stuss, D., Knight, R. (Eds.), Principles of Frontal Lobe Function. pp. 417–440.

Cole, D.M., Smith, S.M., Beckmann, C.F., 2010. Advances and pitfalls in the analysis and interpretation of resting-state FMRI data. Front. Syst. Neurosci. 4, 1–15.

Dapretto, M., Bookheimer, S.Y., 1999. Form and Content: Dissociating Syntax and Semantics in Sentence Comprehension. Neuron 24, 427–432.

Deco, G., Jirsa, V.K., McIntosh, A.R., 2011. Emerging concepts for the dynamical organization of resting-state activity in the brain 1–14.

Descamps, B., Roggeman, C., Vandemaele, P., Achten, E., 2007. Image Acquisition Order and Input Order of BOLD-fMRI Data for Slice Time Correction in fMRI Data Processing Tools. Abstract presented at First Benelux In Vivo MR Methods Symposium.

DeSteno, D., Kubzansky, L., Gross, J.J., n.d. Affective Science and Health: The Importance of Emotion and Emotion Regulation. Health Psychology 32, 474–486.

Diekhof, E.K., Geier, K., Falkai, P., Gruber, O., 2011. Fear is only as deep as the mind allows: A coordinate-based meta-analysis of neuroimaging studies on the regulation of negative affect. NeuroImage 58, 275–285.

Dima, D., Stephan, K.E., Roiser, J.P., Friston, K.J., Frangou, S., 2011. Effective Connectivity during Processing of Facial Affect: Evidence for Multiple Parallel Pathways. journal of neuroscience 31, 14378–14385.

Egner, T., Etkin, A., Gale, S., Hirsch, J., 2008. Dissociable Neural Systems Resolve Conflict from Emotional versus Nonemotional Distracters. Cereb Cortex 18, 1475–1484.

Eickhoff, S.B., Stephan, K.E., Mohlberg, H., Grefkes, C., Fink, G.R., Amunts, K., Zilles, K., 2005. A new SPM toolbox for combining probabilistic cytoarchitectonic maps and functional imaging data. NeuroImage 25, 1325–1335.

Ekman, P., Friesen, W.V., 1976. Pictures of Facial Affect. Consulting Psychologists Press, Palo Alto.

Fairhall, S.L., Ishai, A., 2007. Effective Connectivity within the Distributed Cortical Network for Face Perception. Cereb Cortex 17, 2400–2406.

First, M.B., 2002. DSM_IV_TR Handbook of Differential Diagnosis. American Psychiatric Publishers.

Foland-Ross, L.C., Altshuler, L.L., Bookheimer, S.Y., Eisenberger, N.I., Townsend, J.D., Thompson, P.M., 2008. Evidence for deficient modulation of amygdala response by prefrontal cortex in bipolar mania. Psychiatry Research Neuroimaging 162, 27–37.

Foland-Ross, L.C., Bookheimer, S.Y., Lieberman, M.D., Sugar, C.A., Townsend, J.D., Fischer, J., Torrisi, S.J., Penfold, C., Madsen, S.K., Thompson, P.M., Altshuler, L.L., 2012. Normal amygdala activation but deficient ventrolateral prefrontal activation in adults with bipolar disorder during euthymia. NeuroImage 59, 738–744.

Fornito, A., Harrison, B.J., Zalesky, A., Simons, J.S., 2012. Competitive and cooperative dynamics of large-scale brain functional networks supporting recollection. Proc Natl Acad Sci USA 109, 12788–12793.

Fox, M.D., Greicius, M.D., 2010. Clinical applications of resting state functional connectivity. Front. Syst. Neurosci. 4, 1–13.

Fox, M.D., Raichle, M.E., 2007. Spontaneous fluctuations in brain activity observed with functional magnetic resonance imaging. Nat Rev Neurosci 8, 700–711.

Fox, M.D., Snyder, A.Z., Zacks, J.M., Raichle, M.E., 2006. Coherent spontaneous activity accounts for trial-to-trial variability in human evoked brain responses. Nat Neurosci 9, 23–25.

Friston, K.J., 2011. Functional and Effective Connectivity: A Review. Brain Connectivity 1, 13–36.

Friston, K.J., Buechel, C., Fink, G., Morris, J., Rolls, E., Dolan, R., 1997. Psychophysiological and Modulatory Interactions in Neuroimaging. NeuroImage 6, 218–229.

Friston, K.J., Harrison, L., Penny, W.D., 2003. Dynamic Causal Modelling. NeuroImage 19, 1273–1302.

Friston, K.J., Holmes, A.P., Worsley, K.J., Poline, J.-B.P., Frith, C.D., Frackowiak, R.S., 1995. Statistical parametric maps in functional imaging: a general linear approach. Hum. Brain Mapp. 2, 189–210.

Friston, K.J., Li, B., Daunizeau, J., Stephan, K.E., 2011. Network discovery with DCM. NeuroImage 56, 1202–1221.

Friston, K.J., Price, C.J., 2011. Modules and brain mapping. Cognitive Neuropsychology 28, 241–250.

Friston, K.J., Price, C.J., FLETCHER, P., MOORE, C., Frackowiak, R., Dolan, R., 1996. The Trouble with Cognitive Subtraction. NeuroImage 4, 97–104.

Ghashghaei, H., Barbas, H., 2002. Pathways for emotion: Interactions of prefrontal and anterior temporal pathways in the amygdala of the rhesus monkey. Neuroscience 115, 1261–1279.

Gitelman, D.R., Penny, W.D., Ashburner, J., Friston, K.J., 2003. Modeling regional and psychophysiologic interactions in fMRI: the importance of hemodynamic deconvolution. NeuroImage 19, 200–207.

Goldin, P., Mcrae, K., Ramel, W., Gross, J.J., 2008. The Neural Bases of Emotion Regulation: Reappraisal and Suppression of Negative Emotion. BPS 63, 577–586.

Goodwin, F.K., Jamison, K.R., 2007. Manic-Depressive Illness: Bipolar Disorders and Recurrent Depression, 2nd ed. Oxford University Press.

Green, M., Cahill, C., Malhi, G.S., 2007. The cognitive and neurophysiological basis of emotion dysregulation in bipolar disorder. Journal of Affective Disorders 103, 29–42.

Greicius, M.D., 2008. Resting-state functional connectivity in neuropsychiatric disorders. Current Opinion in Neurology 21, 424–430.

Gross, J.J., 1998. Antecedent- and response-focused emotion regulation: divergent consequences for experience, expression, and physiology. Journal of Personality and Social Psychology 74, 224–237.

Gross, J.J. (Ed.), 2007. Handbook of Emotion Regulation. The Guilford Press, New York.

Gruber, J., Harvey, A.G., Gross, J.J., 2012. When trying is not enough: Emotion regulation and the effort–success gap in bipolar disorder. Emotion 12, 997–1003.

Gyurak, A., Gross, J.J., Etkin, A., 2011. Explicit and implicit emotion regulation: A dual-process framework. Cognition & Emotion 25, 400–412.

Hafeman, D.M., Chang, K.D., Garrett, A.S., Sanders, E.M., Phillips, M.L., 2012. Effects of medication on neuroimaging findings in bipolar disorder: an updated review. Bipolar Disorders 14, 375–410.

Halligan, S.L., Cooper, P.J., Fearon, P., Wheeler, S.L., Crosby, M., Murray, L., 2013. The longitudinal development of emotion regulation capacities in children at risk for externalizing disorders. Develop. Psychopathol. 25, 391–406.

Hamilton, M., 1960. A Rating Scale For Depression. J. Neurol. Neurosurg. Psychiat. 23, 56–62.

Hariri, A.R., Bookheimer, S.Y., Mazziotta, J.C., 2000. Modulating emotional responses: effects of a neocortical network on the limbic system. NeuroReport 11, 43–48.

Haxby, J., Hoffman, E., Gobbini, M., 2000. The distributed human neural system for face perception. Trends in Cognitive Science 4, 223–233.

Henson, R., 2005. What can functional neuroimaging tell the experimental psychologist? The Quarterly Journal of Experimental Psychology Section A 58, 193–233.

Honey, C.J., Thivierge, J.-P., Sporns, O., 2010. Can structure predict function in the human brain? NeuroImage 52, 766–776.

Kalisch, R., 2009. The functional neuroanatomy of reappraisal: Time matters. Neuroscience & Biobehavioral Reviews 33, 1215–1226.

Kalisch, R., Wiech, K., Herrmann, K., Dolan, R.J., 2006. Neural Correlates of Self-distraction from Anxiety and a Process Model of Cognitive Emotion Regulation. Journal of Cognitive Neuroscience 18, 1266–1276.

Kessler, R.C., Berglund, P., Demler, O., Jin, R., Merikangas, K.R., Walters, E.E., 2005. " Lifetime prevalence and age-of-onset distributions of DSM-IV disorders in the National Comorbidity Survey replication": Erratum. Archives of General Psychiatry 62, 593–603.

Kiebel, S.J., Klöppel, S., Weiskopf, N., Friston, K.J., 2007. Dynamic causal modeling: A generative model of slice timing in fMRI. NeuroImage 34, 1487–1496.

Kim, M.J., Gee, D.G., Loucks, R.A., Davis, F.C., Whalen, P.J., 2011. Anxiety Dissociates Dorsal and Ventral Medial Prefrontal Cortex Functional Connectivity with the Amygdala at Rest. Cereb Cortex 21, 1667–1673.

Kircanski, K., Lieberman, M.D., Craske, M.G., 2012. Feelings Into Words: Contributions of Language to Exposure Therapy. Psychol Sci.

Koole, S.L., Rothermund, K., 2011. "I feel better but I don't know why": The psychology of implicit emotion regulation. Cognition & Emotion 25, 389–399.

Lam, D.H., Hayward, P., Watkins, E.R., Wright, K., Sham, P., 2005. Relapse prevention in patients with bipolar disorder: cognitive therapy outcome after 2 years. American Journal of Psychiatry 162, 324–329.

Lang, P., Bradley, M., Cuthbert, B., 1997. International Affective Picture System (IAPS): Technical Manual and Affective Ratings. Gainsville: The Center for Research in Psychophysiology, University of Florida 1–5.

Lazarus, R.S., 1991. Emotion and Adaptation. Oxford University Press, New York, NY.

Leahy, R.L., Tirch, D., Napolitano, L.A., 2011. Emotion Regulation in Psychotherapy: A Practitioner's Guide. The Guilford Press, New York, N.Y.

Leff, A.P., Schofield, T.M., Stephan, K.E., Crinion, J.T., Friston, K.J., Price, C.J., 2008. The Cortical Dynamics of Intelligible Speech. journal of neuroscience 28, 13209–13215.

Levy, B.J., Wagner, A.D., 2011. Cognitive control and right ventrolateral prefrontal cortex: reflexive reorienting, motor inhibition, and action updating. Annals of the New York Academy of Sciences 1224, 40–62.

Li, J., Liu, J., Liang, J., Zhang, H., Zhao, J., Rieth, C.A., Huber, D.E., Li, W., Shi, G., Ai, L., Tian, J., Lee, K., 2010. Effective connectivities of cortical regions for top-down face processing: A Dynamic Causal Modeling study. Brain Research 1340, 40–51.

Lieberman, M.D., Eisenberger, N.I., Crockett, M.J., Tom, S.M., Pfeifer, J.H., Way, B.M., 2007. Putting Feelings Into Words: Affect Labeling Disrupts Amygdala Activity in Response to Affective Stimuli. Psychological Science 18, 421–428.

Lieberman, M.D., Hariri, A.R., Jarcho, J.M., Eisenberger, N.I., Bookheimer, S.Y., 2005. An fMRI investigation of race-related amygdala activity in African-American and Caucasian-American individuals. Nat Neurosci 8, 720–722.

Lieberman, M.D., Inagaki, T.K., Tabibnia, G., Crockett, M.J., 2011. Subjective responses to emotional stimuli during labeling, reappraisal, and distraction. Emotion 11, 468–480.

Mauss, I.B., Evers, C., Wilhelm, F.H., Gross, J.J., 2006. How to Bite Your Tongue Without Blowing Your Top: Implicit Evaluation of Emotion Regulation Predicts Affective Responding to Anger Provocation. Personality and Social Psychology Bulletin 32, 589–602.

McIntosh, A.R., 2004. Contexts and Catalysts *A Resolution of the Localization and Integration of Function in the Brain*. Neuroinformatics 2, 175–182.

Mcrae, K., Ciesielski, B., Gross, J.J., 2012. Unpacking cognitive reappraisal: Goals, tactics, and outcomes. Emotion 12, 250–255.

Mcrae, K., Hughes, B., Chopra, S., Gabrieli, J.D.E., Gross, J.J., Ochsner, K.N., 2009. The Neural Bases of Distraction and Reappraisal. Journal of Cognitive Neuroscience 2, 248–262.

Merikangas, K.R., Jin, R., He, J.-P., Kessler, R.C., Lee, S., Sampson, N.A., Viana, M.C.,

Andrade, L.H., Hu, C., Karam, E.G., 2011. Prevalence and correlates of bipolar spectrum disorder in the world mental health survey initiative. Archives of General Psychiatry 68, 241.

Meyer, M.L., Berkman, E.T., Karremans, J.C., Lieberman, M.D., 2011. Incidental regulation of attraction: The neural basis of the derogation of attractive alternatives in romantic relationships. Cognition & Emotion 25, 490–505.

Minkel, J.D., McNealy, K., Gianaros, P.J., Drabant, E.M., Gross, J.J., Manuck, S.B., Hariri, A.R., 2012. Minkel2012. Biology of Mood & Anxiety Disorders 2, 1–1.

Monti, M.M., 2011. Statistical Analysis of fMRI Time-Series: A Critical Review of the GLM Approach. Front. Hum. Neurosci. 5, 1–13.

Morgan, M.A., LeDoux, J.E., 1995. Differential contribution of dorsal and ventral medial prefrontal cortex to the acquisition and extinction of conditioned fear in rats. Behav Neurosci 109, 681–688.

Mumford, J.A., 2013. Re: GLM design problem [WWW Document]. FSL LISTSERV Archives. URL https://www.jiscmail.ac.uk/cgi-bin/webadmin?A2=ind1302&L=fsl&D=0&P=108075 (accessed 8.13.13).

Murphy, K., Birn, R.M., Handwerker, D.A., Jones, T.B., Bandettini, P.A., 2009. The impact of global signal regression on resting state correlations: Are anti-correlated networks introduced? NeuroImage 44, 893–905.

Noesselt, T., Driver, J., Hans-Jochen, H., Ray, D., 2005. Asymmetrical Activation in the Human Brain during Processing of Fearful Faces. Current Biology 15, 424–429.

Noesselt, T., Shah, N., Jäncke, L., 2003. Top-down and bottom-up modulation of language related areas – An fMRI Study. BMC Neurosci 4, 12.

Ochsner, K.N., Gross, J.J., 2005. The cognitive control of emotion. Trends in Cognitive Science 9, 242–249.

Ochsner, K.N., Ray, R., Cooper, J., Robertson, E., Chopra, S., Gabrieli, J.D.E., Gross, J.J., 2004. For better or for worse: neural systems supporting the cognitive down- and up-regulation of negative emotion. NeuroImage 23, 483–499.

Ochsner, K.N., Silvers, J.A., Buhle, J.T., 2012. Functional imaging studies of emotion regulation: a synthetic review and evolving model of the cognitive control of emotion. Annals of the New York Academy of Sciences 1251, E1–E24.

Oishi, K., Faria, A., van Zijl, P.C., Mori, S., 2011. MRI Atlas of Human White Matter, 2nd ed. Elsevier.

Palaniyappan, L., Cousins, D.A., 2010. Brain networks: Foundations and futures in bipolar disorder. J Ment Health 19, 157–167.

Paret, C., Brenninkmeyer, J., Meyer, B., Yuen, K.S.L., Gartmann, N., Mechias, M.-L., Kalisch, R., 2011. A test for the implementation-maintenance model of reappraisal. Front Psychol 2,

216.

Payer, D.E., Baicy, K., Lieberman, M.D., London, E.D., 2012. Overlapping neural substrates between intentional and incidental down-regulation of negative emotions. Emotion 12, 229–235.

Penny, W.D., 2012. Comparing Dynamic Causal Models using AIC, BIC and Free Energy. NeuroImage 59, 319–330.

Penny, W.D., Stephan, K.E., Daunizeau, J., Rosa, M.J., Friston, K.J., Schofield, T.M., Leff, A.P., 2010. Comparing families of dynamic causal models. PLoS Comput Biol 6, e1000709.

Penny, W.D., Stephan, K.E., Mechelli, A., Friston, K.J., 2004. Comparing dynamic causal models. NeuroImage 22, 1157–1172.

Pessoa, L., Adolphs, R., 2010. Emotion processing and the amygdala: from a 'low road' to “many roads” of evaluating biological significance. Nat Rev Neurosci 11, 773–783.

Phillips, M.L., Ladouceur, C.D., Drevets, W.C., 2008a. A neural model of voluntary and automatic emotion regulation: implications for understanding the pathophysiology and neurodevelopment of bipolar disorder. Mol Psychiatry 13, 833–857.

Phillips, M.L., Travis, M.J., Fagiolini, A., Kupfer, D.J., 2008b. Medication Effects in Neuroimaging Studies of Bipolar Disorder. Am J Psychiatry 165, 313–320.

Poline, J.-B.P., Brett, M., 2012. The general linear model and fMRI: Does love last forever? NeuroImage 62, 871–880.

Pompei, F., Dima, D., Rubia, K., Kumari, V., Frangou, S., 2011. Dissociable functional connectivity changes during the Stroop task relating to risk, resilience and disease expression in bipolar disorder. NeuroImage 57, 576–582.

Power, J.D., Barnes, K.A., Snyder, A.Z., Schlaggar, B.L., Petersen, S.E., 2011. Spurious but systematic correlations in functional connectivity MRI networks arise from subject motion. NeuroImage 1–13.

Price, C.J., 2012. A review and synthesis of the first 20years of PET and fMRI studies of heard speech, spoken language and reading. NeuroImage 62, 816–847.

Price, J.L., Drevets, W.C., 2009. Neurocircuitry of Mood Disorders. Neuropsychopharmacology Reviews 1–25.

Quirk, G.J., Likhtik, E., Pelletier, J.G., Pare, D., 2003. Stimulation of Medial Prefrontal Cortex Decreases the Responsiveness of Central Amygdala Output Neurons. journal of neuroscience 23, 8800–8807.

Raichle, M.E., 2011. The Restless Brain. Brain Connectivity 1, 3–12.

Ramnani, N., Behrens, T.E.J., Penny, W.D., Matthews, P.M., 2004. New approaches for exploring anatomical and functional connectivity in the human brain. BPS 56, 613–619.

Rehme, A.K., Eickhoff, S.B., Grefkes, C., 2013. State-dependent differences between functional and effective connectivity of the human cortical motor system. NeuroImage 67, 237–246.

Richardson, F.M., Seghier, M.L., Leff, A.P., Thomas, M.S.C., Price, C.J., 2011. Multiple Routes from Occipital to Temporal Cortices during Reading. journal of neuroscience 31, 8239–8247.

Ridgway, G.R., Omar, R., Ourselin, S., Hill, D.L.G., Warren, J.D., Fox, N.C., 2009. Issues with threshold masking in voxel-based morphometry of atrophied brains. NeuroImage 44, 99–111.

Ritter, P., Schirner, M., McIntosh, A.R., Jirsa, V.K., 2013. The Virtual Brain Integrates Computational Modeling and Multimodal Neuroimaging. Brain Connectivity 3, 121–145.

Rogerson, P.A., 2001. Statistical Methods for Geography. Sage Publications, London.

Rowe, J.B., 2010. Connectivity analysis is essential to understand neurological disorders. Front. Syst. Neurosci. 4, 1–13.

Rowe, J.B., Hughes, L.E., Barker, R.A., Owen, A.M., 2010. Dynamic causal modelling of effective connectivity from fMRI: Are results reproducible and sensitive to Parkinson's disease and its treatment? NeuroImage 52, 1015–1026.

Roy, A.K., Shehzad, Z., Margulies, D.S., Kelly, A.C., Uddin, L.Q., Gotimer, K., Biswal, B.B., Castellanos, F.X., Milham, M.P., 2009. Functional Connectivity of the Human Amygdala using Resting State fMRI. NeuroImage 45, 614–626.

Schofield, T.M., Penny, W.D., Stephan, K.E., Crinion, J.T., Thompson, A.J., Price, C.J., Leff, A.P., 2012. Changes in Auditory Feedback Connections Determine the Severity of Speech Processing Deficits after Stroke. journal of neuroscience 32, 4260–4270.

Schuyler, B., Ollinger, J.M., Oakes, T.R., Johnstone, T., Davidson, R.J., 2010. Dynamic Causal Modeling applied to fMRI data shows high reliability. NeuroImage 49, 603–611.

Seghier, M.L., Zeidman, P., Neufeld, N.H., Leff, A.P., Price, C.J., 2010. Identifying abnormal connectivity in patients using dynamic causal modeling of FMRI responses. Front. Syst. Neurosci. 4.

Sheppes, G., Gross, J.J., 2011. Is Timing Everything? Temporal Considerations in Emotion Regulation. Personality and Social Psychology Review 15, 319–331.

Smith, S.M., 2012. The future of FMRI connectivity. NeuroImage 1–10.

Smith, S.M., Fox, P.T., Miller, K.L., Glahn, D.C., Fox, P.M., Mackay, C.E., Filippini, N., Watkins, K.E., Toro, R., Laird, A.R., Beckmann, C.F., 2009. Correspondence of the brain's functional architecture during activation and rest. Proc Natl Acad Sci USA 106, 13040–13045.

Stein, J.L., Wiedholz, Bassett, D., Weinberger, D., Zink, C., Mattay, V., Meyer-Lindenberg, A., 2007. A validated network of effective amygdala connectivity. NeuroImage 36, 736–745.

Stephan, K.E., Penny, W.D., Moran, R.J., Ouden, den, H.E.M., Daunizeau, J., Friston, K.J., 2010. Ten simple rules for dynamic causal modeling. NeuroImage 49, 3099–3109.

Strakowski, S.M. (Ed.), 2012. The Bipolar Brain: Integrating Neuroimaging and Genetics. Oxford University Press, New York, NY.

Tabibnia, G., Lieberman, M.D., Craske, M.G., 2008. The lasting effect of words on feelings: Words may facilitate exposure effects to threatening images. Emotion 8, 307–317.

Torrisi, S.J., Lieberman, M.D., Bookheimer, S.Y., Altshuler, L.L., 2013. Advancing understanding of affect labeling with dynamic causal modeling. NeuroImage 82, 481–488.

Townsend, J.D., Altshuler, L.L., 2012. Emotion processing and regulation in bipolar disorder: a review. Bipolar Disorders 14, 326–339.

Townsend, J.D., Bookheimer, S.Y., Foland-Ross, L.C., Sugar, C.A., Altshuler, L.L., 2010. fMRI abnormalities in dorsolateral prefrontal cortex during a working memory task in manic, euthymic and depressed bipolar subjects. Psychiatry Research Neuroimaging 22–29.

Townsend, J.D., Torrisi, S.J., Lieberman, M.D., Sugar, C.A., Bookheimer, S.Y., Altshuler, L.L., 2013. Frontal-Amygdala Connectivity Alterations During Emotion Downregulation in Bipolar I Disorder. BPS 73, 127–135.

Urry, H.L., 2009. Using reappraisal to regulate unpleasant emotional episodes: Goals and timing matter. Emotion 9, 782–797.

Van Dijk, K.R.A., Hedden, T., Venkataraman, A., Evans, K.C., Lazar, S.W., Buckner, R.L., 2010. Intrinsic Functional Connectivity As a Tool For Human Connectomics: Theory, Properties, and Optimization. Journal of Neurophysiology 103, 297–321.

Versace, A., Thompson, W.K., Zhou, D., Almeida, J.R.C., Hassel, S., Klein, C.R., Kupfer, D.J., Phillips, M.L., 2010. Abnormal Left and Right Amygdala-Orbitofrontal Cortical Functional Connectivity to Emotional Faces: State Versus Trait Vulnerability Markers of Depression in Bipolar Disorder. BPS 67, 422–431.

Vizueta, N., Patrick, C.J., Jiang, Y., Thomas, K.M., He, S., 2012a. Dispositional fear, negative affectivity, and neuroimaging response to visually suppressed emotional faces. NeuroImage 59, 761–771.

Vizueta, N., Rudie, J.D., Townsend, J.D., Torrisi, S.J., Moody, T., Bookheimer, S.Y., Altshuler, L.L., 2012b. Regional fMRI Hypoactivation and Altered Functional Connectivity During Emotion Processing in Nonmedicated Depressed Patients With Bipolar II Disorder. American Journal of Psychiatry 1–10.

Volokhov, R.N., Demaree, H.A., 2010. Spontaneous emotion regulation to positive and negative stimuli. Brain and Cognition 73, 1–6.

Wager, T.D., Davidson, M.L., Hughes, B.L., Lindquist, M.A., Ochsner, K.N., 2008. Prefrontal-Subcortical Pathways Mediating Successful Emotion Regulation. Neuron 59, 1037–1050.

Wang, F., Kalmar, J.H., He, Y., Jackowski, M., Chepenik, L.G., Edmiston, E.E., Tie, K., Gong, G., Shah, M.P., Jones, M., Uderman, J., Constable, R.T., Blumberg, H.P., 2009. Functional and structural connectivity between the perigenual anterior cingulate and amygdala in bipolar disorder. BPS 66, 516–521.

Wehr, T.A., Goodwin, F.K., 1987. Can antidepressants cause mania and worsen the course of affective illness? American Journal of Psychiatry 144, 1403–1411.

Whitfield-Gabrieli, S., Nieto-Castanon, A., 2012. Conn: A Functional Connectivity Toolbox for Correlated and Anticorrelated Brain Networks. Brain Connectivity 2, 125–141.

Whitfield-Gabrieli, S., Thermenos, H.W., Milanovic, S., Tsuang, M.T., Faraone, S.V., McCarley, R., Shenton, M., Green, A., Nieto-Castanon, A., LaViolette, P., Wojcik, J., Gabrieli, J.D.E., Seidman, L., 2009. Hyperactivity and hyperconnectivity of the default network in schizophrenia and in first-degree relatives of persons with schizophrenia. PNAS 106, 1279–1284.

Wilke, M., 2012. An alternative approach towards assessing and accounting for individual motion in fMRI timeseries. NeuroImage 59, 2062–2072.

Wittenberg, D., Possin, K.L., Rascovsky, K., Rankin, K.P., Miller, B.M., Kramer, J.H., 2008. The Early Neuropsychological and Behavioral Characteristics of Frontotemporal Dementia. Neuropsychological Review 18, 91–102.

Young, R., Biggs, J., Ziegler, V., Meyer, D., 1978. A Rating Scale for Mania: Reliability, Validity and Sensitivity. British Journal of Psychiatry 133, 429–435.

Zorumski, C., Rubin, E., 2011. Psychiatry and Clinical Neuroscience: A Primer. Oxford University Press, New York, NY.